

Corrections and additional comments made to the rebuttals submitted to *Climate of the Past* in March 2018 are indicated with red ink and italic.

Answer to Reviewer 1 for the interactive comment on “Late Oligocene obliquity-paced contourite sedimentation in the Wilkes Land margin of East Antarctica: implications for paleoceanographic and ice sheet configurations” by A. Salabarnada et al.

We apologize for the late response but I have been embarked on a research cruise in Antarctica. We would like to thank anonymous Reviewer 1 for his/her comments and constructive suggestions, which will help to improve the manuscript. Below are our answers to the comments in black ink and italic.

Does the manuscript represent a substantial contribution to scientific progress within the scope of *Climate of the Past* (substantial new concepts, ideas, methods, or data)?

Good

Scientific quality:

Are the scientific approach and applied methods valid? Are the results discussed in an appropriate and balanced way (consideration of related work, including appropriate references)?

Good

Presentation quality:

Are the scientific results and conclusions presented in a clear, concise, and well-structured way (number and quality of figures/tables, appropriate use of English language)?

Good/Excellent

Does the paper address relevant scientific questions within the scope of CP?

Yes it does.

Does the paper present novel concepts, ideas, tools, or data?

Yes.

Are substantial conclusions reached?

Yes. Though, partially due to the nature of the data/research, many conclusions remain largely speculative.

Are the scientific methods and assumptions valid and clearly outlined?

Partially. I think that such a wide variety of data is presented, that integrating all lines of evidence is very complex. I think that the authors can improve on this point. Especially, by better outlining/introducing their approach (why each data set is presented and what it shows) and in their summary/conclusions (How the argument (largely sedimentological in nature) is constructed). The paleoclimatic and paleoceanographic conclusions are speculative.

The high recovery of late Oligocene sediments during Expedition 318 provided an

unique opportunity to study the environmental conditions at this site that is close to the Antarctic margin. No single indicator provides a clear picture of these past high-CO2 world environments but the multiproxy approach used here helps in testing out some of the environmental signals. The conclusions reached are by the nature of this study speculative since they are reached with data from a single site. However, the paleoclimatic and paleoceanographic conclusions are not so speculative as they may appear when we take into account that the paleoclimatic conditions are supported by the Sea Surface paleotemperatures reported by the companion paper submitted to Climate of the Past by Hartman et al.; and the paleoceanographic conditions by the paper by Bijl et al. It is unfortunate that the reviewers did not have access to these other two papers.

In the Methods and Discussion sections, we have added an introduction to the information provided by each of the proxies used for this study to better understand depositional settings in past climates at this poorly studied margin of Antarctica. We note that these proxies have been sparsely applied in the Antarctic region and thus, our subjective (rather than speculative) interpretations will of course be subject to further refinement with improved spatial coverage of this time periods in Antarctica, and future development of proxies to test the hypotheses developed in this paper. Lines 210, 237, 482, 492, 730.

Are the results sufficient to support the interpretations and conclusions?

Yes, I think so. However this research comes with large limitations of course.

Is the description of experiments and calculations sufficiently complete and precise to allow their reproduction by fellow scientists (traceability of results)?

Yes.

Do the authors give proper credit to related work and clearly indicate their own new/original contribution?

Yes.

Does the title clearly reflect the contents of the paper?

Yes. I think so. Though perhaps be more careful with the orbital interpretations. Good age control in these sediments is difficult to achieve. Perhaps replace “obliquity” with “astronomical”? Given the moderate recovery (many gaps), 1 million year length of the record, and relatively poor absolute&relative age control, I wonder if the generalization of the presumed obliquity pacing for the (entire?) Late Oligocene (as the title could suggest) is too much.

We concur with the comment by the reviewer and will substitute obliquity with astronomical in title. We also changed “implications” with “insights”.

Title has been changed.

Also, I wonder if contourite is the correct sedimentological description of these sediments. I realise that this argument is explored in great detail in this manuscript, however I am no sedimentologist and I wonder how these contourites compare to those from, for example, the Iberian margin. Levy et al. PNAS 2016 present 5 motives for a very proximal site. Could the lithological alterations at Wilkes Land not be linked to these motives as well? And are we still speaking of contourites then?

*We appreciate the candid comment of the Reviewer indicating that he is not a sedimentologist. Contourites in any setting and location refer to sediments deposited or significantly affected by the action of bottom currents, despite their origin. In the Wilkes Land Site U1356, the sediments deposited during glacial and interglacial cycles, which are dominantly gravity flows and hemipelagites, respectively, are reworked by bottom currents resulting in the sediments recovered at this site. Contourites from the Iberian margin are also the result of reworking of downslope and hemipelagic sedimentation. Contrary to turbidite deposits, contourites do not exhibit a “type contourite facies association model or motif” but contourite facies/structures (i.e., laminated vs bioturbated, etc) are common to all bottom current deposits (see for example the review paper by Rebesco et al., 2014). Levy et al., PNAS 2016, shows a stacking patterns of different motifs recovered from the McMurdo Sound coastal sector of the Ross Sea by the ANDRILL2A. Levy et al., interpret the sedimentary cycles represented by the motifs in terms of advances and retreats of the ice sheet grounding line forced by eccentricity. Therefore, the motifs in the Levy et al paper result from sedimentary processes associated with the **direct influence of grounding line advances and retreats in a coastal setting**. Our record is a **distal marine record**. Therefore, our site receives sediment input from the continent (which provides an indirect record for continental glaciation) and the rain of hemipelagic materials that are then reworked by ocean currents. In both Levy’s et al. paper and ours, we interpret the alternation in motifs and facies to be astronomically forced.*

Does the abstract provide a concise and complete summary?

Improvements can be made. Please see below.

Abstract has been modified in order to make it more clear, concise and shorter.

Is the overall presentation well structured and clear?

In general it is a very long paper with many (complex) lines of evidence. I feel that this could be outlined (signposted throughout the manuscript) a bit better. Perhaps introduce when new datasets are presented and why these data are important for this study. What questions will they help answering?

We understand the multiproxy approach used in this study can make it hard to follow the different lines of evidence. At present, each of the indicators used for this study and their relevance is explained in the Material and Methods section. However, to address this concern of Reviewer 1, we will introduce a brief outline of the relevance of the indicators used in each of the subsections in the Results.

Combined with earlier comment, we tried to clarify and better structure our text.

Changes have been made all through the text.

Lines 210, 237, 482, 492, 730.

Is the language fluent and precise?

Yes.

Are mathematical formulae, symbols, abbreviations, and units correctly defined and used?

Yes.

Should any parts of the paper (text, formulae, figures, tables) be clarified, reduced,

combined, or eliminated?

I think that making the manuscript more concise/focussed would help with getting the main points across.

We will work to make the revised version of this manuscript more concise.

We hope the revised version of this manuscript is now more concise.

Are the number and quality of references appropriate?

Yes. Perhaps add Levy et al. 2016 PNAS.

In our paper, we have established comparisons with the environmental setting between the Wilkes Land and the Ross Sea. We have focussed on coeval records to those we are studying, both coastal (CPR, Barrett, 2007) and distal (DSDP Site 270, Kemp and Barrett, 1975) sites. We will introduce the reference to Levy et al 2016 in the "4.2 Ice sheet configuration during the warm late Oligocene" chapter, in line 553, by adding "Also, a dynamic ice sheet is described for the early Miocene coastal section of AND-2A with glacial and interglacial advances and retreats of the EAIS (Levy et al., 2016), that could have a similar paleotopographic configuration to that for the Oligocene."

Reference has been introduced in Line 675.

Is the amount and quality of supplementary material appropriate?

I have not been able to find the supplementary data online. I have not reviewed this.

It is unfortunate that if appears that the Reviewer did not have access to the Supplementary material when these were available online as they were submitted with the manuscript.

Further comments:

L43: I think that the link between the data presented in this paper and ice sheet configuration is speculative at best. I would not start the abstract with such a bold claim. Delete, or move to the final line of the abstract and say something like: "we speculate on the ice sheet configurations of the Wilkes Land Basin from between 25 and 26 million years ago.

We will proceed in the revision as advised by the Reviewer. However, our claim on the retreated ice sheet is reinforced by several lines of evidence: (1) How the late Oligocene interval studies compares to the rest of the Oligocene and early Miocene sediments (presented in the supplementary materials to which the Reviewer unfortunately did not have access). Earlier Oligocene and Miocene sections contain Ice Rafted Debris, suggesting an extended ice sheet. No IRD was found in the studied interval and we argue this could be indicative of less extensive ice sheets. (2) As referred in the paper and more extensively covered in the companion paper to this one by Bijl et al., dyncocists indicate that during the studied interval there is no evidence for sea ice suggesting a warmer setting and reduced ice sheets during the studied late Oligocene interval. Sea ice species are however present in other Oligocene and Miocene intervals from U1356 core. (3) High Sea Surface Temperature reconstructions as shown in the companion paper to this one by Hartmann et al. that

support the sea ice free scenario. (4) Reconstructions derived from fossil pollen in Site U1356 suggesting high terrestrial temperatures (Salzmann et al., 2016; Strother et al, in prep).

We have made changes to clarify that our interpretations are based in several lines of evidence. All geological studies are interpretative, with various degrees of uncertainties. Speculative however implies we do not have clear evidence, which is not the case as outlined above in our rebuttal.

Line 40.

L46: Physical properties are only magnetic susceptibility. I would just say that. I would also be more precise about what geochemical techniques are presented. Key paleoceanographic/ice sheet indicators, such as fish tooth and detrital Nd are not presented. Make that clear in the abstract.

We will follow the suggestion by the Reviewer. For the physical properties however, in addition to the magnetic susceptibility, we also use density.

L. 45

L51-54: Not a sentence. I would first present a short summary of the sedimentological result. Then say how these are interpreted. Best not to mix these up.

We will follow the advise of the Reviewer

L. 52

L58: Why lowlands? Why not topographic highs? Could your data not support both options?

We see the confusion caused by the way the sentence is written. Of course the ice caps and glaciers occupied as well topographic highs. We wanted to mainly emphasize the different topography of the Wilkes subglacial Basin compared to today, which in the Oligocene was not yet over-deepened. We will try to clarify this by rephrasing the sentence to indicate "These observations, supported by elevated sea surface paleotemperatures and the absence of sea-ice, suggest that between 26 and 25 Ma open water conditions prevailed and therefore glaciers or ice caps occupied the topographic highs and lowlands of the now over-deepened Wilkes Land subglacial Basin."

L. 62 changed as follows: "...these evidences suggest that glaciers or ice caps likely occupied the topographic highs and lowlands of the now marine Wilkes Subglacial Basin (WSB)."

L64-65: The line about spectral analysis is stuck on the end of the abstract. A strange place to present new results/interpretations. I would advice to end the abstract with the biggest (although perhaps speculative) conclusions. Not new information about the sedimentological/statistical description.

We will rewrite following the advise of the Reviewer.

Moved at Line 55.

L137: Just say magnetic susceptibility of the bulk sediment.

We will rewrite as advised.

Line 150

L184: Cite individual chapters of the Gradstein volume. In this case Vandenberghe et al. (the Paleogene chapter).

We will cite as advised.

Line 205

L191: I have not been able to find supplementary information online. Did I miss anything?

It is unfortunate that the supplementary materials were not found since they are online and were submitted at the same time as the rest of the manuscript. The Supplementary information provides more detail regarding the spectral analysis applied to our datasets and also explains in more detail the sedimentary section from the early Oligocene to the early Miocene.

First appearance Line 216 inside Facies Analysis section

L205: Which lab was used for this analysis?

CT-scans were done at the Kochi Core Center (KCC) lab (Japan). It was stated in the text (L201) but we clarified it.

Line 227

L235: Al counts are often very sensitive to coring disturbances. I think this should be mentioned and that the authors should be careful with the interpretation of Al counts from heavily disturbed sediments.

We agree with the reviewer. Although we don't have core disturbances all along our studied section, we detected that Al and Si elements collected by the continuous X-Ray Fluorescence (XRF) scanner present more than one order of magnitude gains although the sediments were not deformed, and therefore they were not used. To overcome this problem, XRF analyses in discrete samples from non-deformed intervals were also conducted and are the ones used in our research. We clarified in the text that the interval for which we collected XRF data did not show core disturbances (L233).

Line 258. We added, "Data points from disturbed intervals in the core face (i.e., slight fractures and cracks) were removed."

L256: Crucial point. How was the data anchored (tuned) to obliquity? This point needs to be described and explored in much more detail. What assumptions are underlying the tuning? The readers need to know how certain the authors are about the age model/tuning etc. What is the room for improvement?

The information requested by the reviewer is contained in the supplementary materials to which, unfortunately, the reviewer did not get access. To avoid further confusions, we also will add a sentence in the main text of the manuscript to provide

information about anchoring the time series. For the main research we used the Evolutive Average Spectral Misfit method (Meyers, 2014) for the astrochronologic testing, that was evaluated using ETP (eccentricity, obliquity and precession) target from La04 (Laskar et al., 2004). Afterwards, an astronomical tuning is done by using the Frequency domain minimal tuning (Meyers et al., 2014) where spatial frequencies are afterwards converted to sedimentation rates using the average period of 41 Kyr/obliquity. Time series is afterwards anchored to our paleomagnetic tie points. We added a sentence in methods section and also in the result section.

In the supplementary data, there is also another tuning done for initial evaluation of the time series, where we tested with AnalyseSeries method (Paillard et al., 1996) by filtering our data in depth scale and comparing it to the Obliquity solution of La04 (Laskar et al., 2004).

Clarification added in Line 293 in methods section and in Line 468 in results section.

L256 and L260/261 mention two different tuning targets. One based on obliquity, the other on eccentricity, obliquity and precession. Please clarify.

Related and answered with the previous comment.

L270: Please clarify how your sedimentological descriptions are better than the shipboard description. How did you improve?

Shipboard, sedimentologists describe the sections as cores are opened. Shipboard descriptions, although thorough, are preliminary since there is no time to look at the cores in the detail and the context is often lost because of changing work shifts and describers. Shipboard descriptions interpreted deposition during the studies interval to be dominated by hemipelagic and turbidity flows/bottom current processes. Post-cruise, we had a chance to re-describe all core sections in detail and by the same group of people, which included experts in turbidite and contourite deposits (not always easy to differentiate). This resulted in the very detailed lithological log presented in this paper. In addition, the integration of the detailed lithological log with magnetic susceptibility (collected shipboard), continuous/discrete XRF data, high-resolution images and CT-Scans and SEM images (obtained in the frame of this study), allowed us to further characterise the facies.

Line 215, 307, we clarified that the new lithologic log was constructed by re-describing the cores at mm to cm-scale resolution in comparison with the low-resolution descriptions conducted shipboard.

L435: Perhaps compare to Levy et al?

In this part of the discussion we focus our comparisons to facies from different settings that are similar to site U1356, mainly around East Antarctic margin. AND-2 from Levy et al., obtained sediments from a coastal site.

We cited Levy et al., 2016 in Line 675.

L520: Could there be other reasons why there is no IRD at your site? (Absence of evidence is not necessarily evidence of absence)

We agree with the reviewer that the absence of IRD cannot be directly linked to a

retreated ice sheet. However, as mentioned earlier, our interpretations regarding the lack of an extended ice-sheet similar to the one existing in the earlier Oligocene is not only based on the absence of IRD's but in several lines of evidence, as mentioned before, which include: (1) How the late Oligocene interval studies compares to the rest of the Oligocene and early Miocene sections (presented in the supplementary materials to which the Reviewer unfortunately did not have access). Earlier Oligocene and Miocene sections contain Ice Rafted Debris, suggesting an extended ice sheet. No IRD was found in the studied interval and we argue this could be indicative of less extensive ice sheets. (2) No evidence for sea ice indicated by dinocists and reported in detail in the companion paper to this one by Bijl et al., suggesting a warmer setting and reduced ice sheets. Sea ice species are however present in other Oligocene and Miocene intervals. (3) High Sea Surface Temperature reconstructions reported in the companion paper to this one by Hartmann et al. that support the sea ice free scenario. (4) Reconstructions derived from fossil pollen in Site U1356 suggesting high terrestrial temperatures (Salzmann et al., 2016; Strother et al, in prep). In addition, we compare the environmental setting during the studied late Oligocene interval to iceberg modelling studies conducted in Pliocene sediments from the Wilkes Land margin by Cook et al (2014). The modelling shows that despite the high sea surface temperatures during warmer climate periods of the Pliocene, iceberg armadas were able to travel as far as to the continental rise sites in this margin.

We restructured the "Ice sheet configuration during the warm late Oligocene" subsection (Line 589-675) in order to clarify that the interpretations reached are not only based on the absence of evidence of IRDs but is also supported by other lines of evidence as outlined in the rebuttal.

L580: I do not understand how the authors conclude that ice was present in the lowlands. Are topographic highs not a much more likely location of land ice?

We agree with the Reviewer. ice sheets and/or glaciers would occupy both high- and lowlands. This agrees with the pollen assemblages in sediments from this interval (Ulrich Salzmann personal communication). Although what we wanted to note is that ice would be occupying the non-overdeepened Wilkes subglacial basin. We will rephrase this in the revised version to make sure it is clear.

Line 655. We rephrased the paragraph. We changed it in the abstract and conclusions too.

Line 63, 625, 869.

L603: do the authors mean that the palynomorphs are partially oxidized/poorly preserved? Please clarify if that is the case.

We will address the text in order to make clear that Palynomorphs have good preservation, and that don't show notable changes in their preservation between F1 and F2 (companion paper to this by Bijl et al.,).

Included "good preservation" in Line 699.

L681: What is the evidence that northern component waters were reaching this site that is located so far south in the modern and in the Oligocene? The evidence for NCW in the Oligocene needs to be better explained/this point needs to be presented/supported in

a much better way.

We will improve our discussion regarding this point in the text. We consider that as Circumpolar Deep Water is a mixture of AABW and also the NADW and the northern component waters (NCW), we interpret that during warmer times, and also due to the influence of the shifted Polar Fronts to the South during interglacials, NCW would have a higher influence on the proto-CDW, and thus, shifting the chemical characteristics towards a carbonate friendly environment. The presence of preserved coccoliths in such southernmost positions in Antarctica, and in the continental rise is rare, as many studies correlate coccoliths with the presence of a carbonated and warmer water mass shifting south, being the NCW or the NADW in the actual configuration of the ocean.

We rephrased our manuscript in order to make clearer the argument as follows: "Circumpolar Deep Water (CDW) is a mixing of abyssal, deep, and intermediate water masses, that includes AABW and NADW nowadays (Johnson, 2008). During warmer interglacials, the influence of more northern-sourced water masses into the proto-CDW, relative to Antarctic-sourced, could enable carbonate productivity as seen in the interglacial facies with coccolithosphere remains (Fig. 7c)."

We restructured the whole paragraph of the discussion and added some references to clarify our interpretations about the influence of North Component Waters at the site.

Line 730-808.

L689: Noise and gaps in time series are two different things. Please correct.

This will be corrected on the revised version of the manuscript.

We added "discontinuous due to gaps" in Line 828.

L697: Why would precession suggest a dynamic ice sheet? Are there other mechanisms that could be thought of to explain a potential precession beat in your data?

We agree with the Reviewer that precession can have different interpretations in our record. Although highly speculative, as our record captures the precession frequencies, we suggested that high latitude summer insolation during late Oligocene had an influence on the continental terrigenous fraction suggesting ice melt and rapid ice-sheet volume changes as Patterson et al., (2014) also suggested for core U1361 in Wilkes Land during the Pliocene. However, given that this interpretation does not add to any of the relevant point of the manuscript and is highly speculative, we will remove it.

This was stated in addition to Obliquity. We have reworded to highlight it is responded dynamically to orbital forcing at a range of frequencies.

We rephrased.

Line 835: "In addition to obliquity precession is also present, which implies a dynamic response of the EAIS and offshore oceanic water masses to orbital forcing."

L711: More caution needs to be taken when interpreting tuned records. Many assumptions are implicit.

We agree with the reviewer, and in no way are our results dependent on the tuning

applied. Line 711 refers to a previous study by Palike et al., which highlight an obliquity “heartbeat” to the climate system in the Oligocene from deep sea sediments in the Pacific. We support this observation with evidence directly from the Antarctic margin, and in no way is this dependent on tuning. We use distinct tie points and extensive statistical tests to identify the orbital periods (sup info – ASM method)

L744: Nd evidence is needed before this can be suggested with any level of confidence. This is just speculation in my opinion. Please rephrase.

We agree with the reviewer that Nd isotopes are a good evidence of distinct water masses. However, no fish teeth were recovered from this interval to conduct these studies. The chemistry of the water mass influences the elemental concentrations and also can give paleoceanographic information. For example, bottom waters chemistry affects the preservation of carbonates in sediments. Here, we postulate that the presence of nannofossils in site U1356 is enhanced due to more carbonated and warmer waters, less corrosive to carbonate, as are the warmer north component waters (NADW-like), that are entrained and mixed within the circumpolar deep waters (proto-CDW), that bath the basins of Antarctica.

L749: Add “in the Wilkes Land Basin”

Corrected.

Line 897.

L753: how is this conclusion supported by the data? No ice volume estimates are presented.

We agree with the reviewer. We left that there is a retreat of the ice sheet in the Wilkes Land Basin but we took out the processes that control the melting of the ice sheet.

We took out the conclusion. And we added a part of the paragraph to the discussions section in Line 806.

Despite my (hopefully) constructive criticism, I am very supportive of this paper. I hope to see it published soon in *Climate of the Past* and wish to congratulate the authors on a very nice study.

References:

- Barrett, P.J., 2007. Cenozoic Climate and Sea Level History from Glacimarine Strata off the Victoria Land Coast, Cape Roberts Project, Antarctica, in: *Glacial Sedimentary Processes and Products*. pp. 259–287.
- Bijl, P.K., Houben, A.J.P., Hartman, J.D., Pross, J., Salabarnada, A., Escutia, C., Sangiorgi, F., 2017. Oligocene–Miocene paleoceanography off the Wilkes Land Margin (East Antarctica) based on organic-walled dinoflagellate cysts. *Clim. Past Discuss.* 2017, 1–43.

- Cook, C.P., Hill, D.J., van de Flierdt, T., Williams, T., Hemming, S.R., Dolan, A.M., Pierce, E.L., Escutia, C., Harwood, D., Cortese, G., Gonzales, J.J., 2014. Sea surface temperature control on the distribution of far-traveled Southern Ocean ice-rafted detritus during the Pliocene. *Paleoceanography* 29, 533–548.
- Hartman, J.D., Sangiorgi, F., Salabarnada, A., Peterse, F., Houben, A.J.P., Schouten, S., Escutia, C., Bijl, P.K., 2017. Oligocene TEX86-derived seawater temperatures from offshore Wilkes Land (East Antarctica). *Clim. Past Discuss.* 2017, 1–31.
- Johnson, G.C., 2008. Quantifying Antarctic Bottom Water and North Atlantic Deep Water volumes. *J. Geophys. Res. Ocean.* 113, 1–13.
- Kemp, E.M., Barrett, P.J., 1975. Antarctic glaciation and early Tertiary vegetation. *Nature* 258, 507–508.
- Laskar, J., Robutel, P., Joutel, F., Gastineau, M., Correia, a. C.M., Levrard, B., 2004. A long-term numerical solution for the insolation quantities of the Earth. *Astron. Astrophys.* 428, 261–285.
- Levy, R., Harwood, D., Florindo, F., Sangiorgi, F., Tripathi, R., von Eynatten, H., Gasson, E., Kuhn, G., Tripathi, A., DeConto, R., Fielding, C., Field, B., Golledge, N., McKay, R., Naish, T., Olney, M., Pollard, D., Schouten, S., Talarico, F., Warny, S., Willmott, V., Acton, G., Panter, K., Paulsen, T., Taviani, M., 2016. Antarctic ice sheet sensitivity to atmospheric CO₂ variations in the early to mid-Miocene. *Proc. Natl. Acad. Sci.* 201516030.
- Meyers, S.R., 2014. Astrochron: An R Package for Astrochronology. <http://cran.r-project.org/package=astrochron>.
- Paillard, D., Labeyrie, L., Yiou, P., 1996. Macintosh Program performs time-series analysis. *Eos, Trans. Am. Geophys. Union* 77, 379–379.
- Patterson, M.O., McKay, R., Naish, T., Escutia, C., Jimenez-Espejo, F.J., Raymo, M.E., Meyers, S.R., Tauxe, L., Brinkhuis, H., Klaus, a., Fehr, a., Bendle, J. a. P., Bijl, P.K., Bohaty, S.M., Carr, S. a., Dunbar, R.B., Flores, J. a., Gonzalez, J.J., Hayden, T.G., Iwai, M., Katsuki, K., Kong, G.S., Nakai, M., Olney, M.P., Passchier, S., Pekar, S.F., Pross, J., Riesselman, C.R., Röhl, U., Sakai, T., Shrivastava, P.K., Stickley, C.E., Sugasaki, S., Tuo, S., van de Flierdt, T., Welsh, K., Williams, T., Yamane, M., 2014. Orbital forcing of the East Antarctic ice sheet during the Pliocene and Early Pleistocene. *Nat. Geosci.* 7, 841–847.
- Rebesco, M., Hernández-Molina, F.J., Van Rooij, D., Wåhlin, A., 2014. Contourites and associated sediments controlled by deep-water circulation processes: State-of-the-art and future considerations. *Mar. Geol.* 352, 111–154.
- Salzmann, U., Strother, S., Sangiorgi, F., Bijl, P., Pross, J., Woodward, J., Escutia, C., Brinkhuis, H., 2016. Oligocene to Miocene terrestrial climate change and the demise of forests on Wilkes Land, East Antarctica, in: EGU General Assembly Conference Abstracts, EGU General Assembly Conference Abstracts. p. EPSC2016-2717.
- Tauxe, L., Stickley, C.E., Sugasaki, S., Bijl, P.K., Bohaty, S.M., Brinkhuis, H., Escutia, C., Flores, J. a., Houben, a. J.P., Iwai, M., Jimenez-Espejo, F., McKay, R., Passchier, S., Pross, J., Riesselman, C.R., Röhl, U., Sangiorgi, F., Welsh, K., Klaus, A., Fehr, A., Bendle, J. a. P., Dunbar, R., Gonzalez, J., Hayden, T., Katsuki, K., Olney, M.P., Pekar, S.F., Shrivastava, P.K., van de Flierdt, T., Williams, T., Yamane, M., 2012. Chronostratigraphic framework for the IODP Expedition 318 cores from the Wilkes Land Margin: Constraints for paleoceanographic reconstruction. *Paleoceanography* 27, 19.
- Vandenbergh, N., Hilgen, F.J., Speijer, R.P., Ogg, J.G., Gradstein, F.M., Hammer, O., Hollis, C.J., Hooker, J.J., 2012. The Paleogene Period, in: *The Geologic Time Scale*. Elsevier, pp. 855–921.

Corrections and additional comments made to the rebuttals submitted to *Climate of the Past* in March 2018 are indicated with red ink and italic.

Answer to Referee Dr. S. Pekar for the interactive comment on “Late Oligocene obliquity-paced contourite sedimentation in the Wilkes Land margin of East Antarctica: implications for paleoceanographic and ice sheet configurations” by A. Salabarnada et al.

We apologize for the late response but I have been embarked on a research cruise in Antarctica with very limited internet connection. Firstly, we would like to thank the reviewer, Dr. Steve Pekar, for his comments and constructive suggestions, which will improve the manuscript. Below, we address the main concerns of Dr. Pekar in cursive font:

Concern 1: “...major concern with the manuscript was it stating about the lack of IRD in their studied interval is taken to indicate the relative absence of marine-terminating ice sheets at the nearby margin. I have to differ with this important result as in another study by D. Hauptvogel, identified IRD’s in the same interval at Site U1356. He did this by counting grains larger than 150 microns in many samples within this interval. In approximately 25% of his samples within the same interval used in this manuscript contained significant numbers of >150 micron grains usually between 2 and 5%. In addition, the sand percent for the Late Oligocene is not much less than what is seen in the early Oligocene from Site U1356. I remember that Dr. Hauptvogel spoke with the lead author back in 2016 and he sent her his sand percentage data as well as visually showed her the work he had done on the sand fraction. While there could be an argument that bottom currents could move fine sand size grains, medium size grain sized grains were also identified. So I am not sure if grains larger than 150 microns could easily be moved from the Mertz Shear Fracture (source of the grains based on Ar/Ar dating) to Site U1356 only by bottom water currents. At the very least, the authors need to discuss and explain this point far better.”

We agree with the reviewer that the absence of IRD in our studied interval is not to be taken as the sole evidence for (the relative) lack of marine terminating ice sheets in the Wilkes Land margin. We first want to point out that we reach this conclusion not only based on the relative absence of IRDs but also other supporting evidence such as: (1) the lack of sea ice indicated by the dinocists (Bijl et al companion paper to this one in CP); (2) elevated sea surface temperature (Hartmann et al. companion paper to this one in CP); and (3) palynomorph data (Salzmann et al 2016).

We like to note that the grains interpreted as IRD in Dr. Hauptvogel’s thesis are, as Dr. Pekar indicates in his review, those that have a grain-size >150 microns. This is not a commonly accepted cut-off for IRD, which is 250 microns (at a minimum; See Patterson et al., and references therein) – and thus the high percentage cited are skewed by this very fine grained cut-off values. Hauptvogel do not provide detailed grain size frequency distribution to prove that these >150 microns are outliers within the grain size population. Although it is possible there is some background IRD in our

record, we argue it is minimal compared to elsewhere in the core – and thus represents a likely minima state in ice sheet extent relative to the periods before and after. We also note that in Dr. Hauptvogel thesis, assumes that sand grains >150microns can only be delivered to the continental rise site U1356 by icebergs (as also stated in page 48 from Hauptvogel 2015, PhD Thesis). However, globally, sand and gravels can be transported to deep areas of the basins by multiple processes such as are Mass Transport Deposits (MTDs), turbidity currents, hyperpycnal flows, etc. MTDs are clearly present in the U1356 core (455 to 575 mbsf), directly contradicting this assumption. In addition, moderately-to-well sorted, sandy granule-pebble sediments grading upwards into well-sorted fine, crudely stratified sands were recovered from Site U1355 at 3729 m water depth at the mouth on one of the submarine channels (Escutia et al., 2011). Also on the Wilkes Land, a sample collected by the USNS Eltanin from one of the Wilkes Land continental rise channels, has high-content in sand and rock fragments (Payne and Conolly 1972; Escutia et al., 2000). These findings point to delivery of very coarse material from the continental shelf to the continental rise by gravitational processes.

Also, note that in our manuscript, we do not claim the sand to be delivered by bottom currents as implied in Dr. Pekar’s review. Instead, our facies analyses points to sediments delivered to where site U1356 is located on the continental rise, dominantly by gravity flows (bringing coarse material) and hemipelagic sedimentation, which are then reworked by bottom currents. However, we concede there may be some background IRD, but it is minimal relative to other parts of the core.

*In the Sedimentary Facies subsection of the Results, we provide evidences backed with references of coarse-grained sediments being delivered to Site U1356 and other sites on the Wilkes margin by gravity flow processes (Mass Transport Deposits and turbidity currents). We have also included a paragraph in the Site Description subsection of the Methods regarding the depositional setting of Site U1356 during the late Oligocene on an incipient levee, which received overbank sediments from the turbidity flows traveling through the adjacent submarine channel. In addition, we have noted in Line 360 that “Although maybe some background IRD is present, it is minimal relative to other parts of the core”. Changes are found in the following lines:
Line 175, 350-361, 539, 589-609.*

Concern 2: “I also have some concerns with the age model, as there is only one good tie point for the late Oligocene, which is at 26.1 Ma. The spectral analysis looks good in figure 6 until 25.8 Ma but looks far more uncertain above, probably because the age model is not well resolved”.

We use the three paleomagnetic chrons by Tauxe et al. 2012. Using the two different statistical approaches provided in the manuscript and the Supplementary, we arrived to a well-resolved age model that considers two strong tie points: one in the top of the studied core interval and another one at the bottom (Chron C8n.1n (o), 25.260 Ma, at 643.37 mbsf; and C8n.2n (o), 25.900 Ma, at 678.98 mbsf). We will clarify in the revision that the age control, although reliable is of low-resolution.

We make it clear at Line 468.

Concern 3: “I think that the statement about ice in the lowlands versus the coast or versus the highlands is a bit speculative. Especially since there are no data that estimates ice volume in this manuscript as well as that there are grains larger than 150 microns that C2 occur throughout the late Oligocene section at Site U1356.

Our data can not provide ice volume estimates. We see the confusion caused by the way the sentence is written. Of course, the ice caps and glaciers occupied lowlands as well topographic highs. In our sentence, we mainly wanted to emphasize the different topography of the Wilkes subglacial Basin, which in the Oligocene was not yet over-deepened. We will try to clarify this by rephrasing the sentence to “These observations, supported by elevated sea surface paleotemperatures and the absence of sea-ice, suggest that between 26 and 25 Ma open water conditions prevailed and therefore glaciers or ice caps occupied the topographic highs and lowlands of the now over-deepened Wilkes Land subglacial Basin.”

*We rephrased the statements all around the manuscript as specified.
Line 63, 625, 869.*

Concern 4: “The evidence of NCW to explain the glacial /interglacial changes seen here are a bit thin. The papers cited are explaining long term trends not at Milankovitch timescales. I would suggest that this be discussed in a better way.

We like to clarify that we do not use NCW to explain glacial/interglacial cyclicity. The cyclicity in our record is explained by the alternation of facies, which we find are astronomically forced, at 40Kyr. Based on the unusual presence of calcareous coccolithospheres in some of the intervals in our record (at <60° S latitude), we hypothesise that during higher than normal interglacials a proto-CDW may have been influenced by warmer NCW as the Polar Front was displaced to the south. Similar interpretations are provided in other studies in sediments of Pliocene-Pleistocene age around the Southern Ocean recording the striking presence of calcareous nannofossils (Kuhn and Diekmann, 2002; Cowan et al., 2008; Villa et al., 2012)

*We restructured the whole paragraph of the discussion and make it clear towards our working hypothesis about the North Component Waters adding more details and evidences.
Line 730-808*

Concern 5: “ I don’t understand how precession suggests a dynamic ice sheet.”

This was stated in addition to Obliquity. We have reworded to highlight it is responded dynamically to orbital forcing at a range of frequencies.

We rephrased.

Line 835: “In addition to obliquity precession is also present, which implies a dynamic response of the EAIS and offshore oceanic water masses to orbital forcing.”

Concern 6: “The last paragraph of the conclusions is speculative as there is little data to support it.”

We agree with the reviewer. We reformulated the paragraph in order to be more precise and expose only the data where we are confident.

Line 900.

References:

- Bijl, P.K., Houben, A.J.P., Hartman, J.D., Pross, J., Salabarnada, A., Escutia, C., Sangiorgi, F., 2017. Oligocene-Miocene paleoceanography off the Wilkes Land Margin (East Antarctica) based on organic-walled dinoflagellate cysts. *Clim. Past Discuss.* 2017, 1–43.
- Cowan, E.A., Hillenbrand, C.D., Hassler, L.E., Ake, M.T., 2008. Coarse-grained terrigenous sediment deposition on continental rise drifts: A record of Plio-Pleistocene glaciation on the Antarctic Peninsula. *Palaeogeogr. Palaeoclimatol. Palaeoecol.* 265, 275–291.
- Escutia, C., Brinkhuis, H., Klaus, A., Scientists, I.E. 318, 2011. Expedition 318 summary, in: *Proceedings of the Integrated Ocean Drilling Program, Volume 318.*
- Escutia, C., Eitrem, S.L., Cooper, K., Nelson, C.H., 2000. Morphology and acoustic character of the antarctic Wilkes Land turbidite systems: Ice-sheet-sourced versus river-sourced fans. *J. Sediment. Res.* 70, 84–93.
- Hartman, J.D., Sangiorgi, F., Salabarnada, A., Peterse, F., Houben, A.J.P., Schouten, S., Escutia, C., Bijl, P.K., 2017. Oligocene TEX86-derived seawater temperatures from offshore Wilkes Land (East Antarctica). *Clim. Past Discuss.* 2017, 1–31.
- Hauptvogel, D.W., 2015. *The State Of The Oligocene Icehouse World : Sedimentology , Provenance , And Stable Isotopes Of Marine Sediments From The Antarctic Continental Margin.* PhD Dissertation. The City University Of New York.
- Kuhn, G., Diekmann, B., 2002. Late Quaternary variability of ocean circulation in the southeastern South Atlantic inferred from the terrigenous sediment record of a drift deposit in the southern Cape Basin (ODP Site 1089). *Palaeogeogr. Palaeoclimatol. Palaeoecol.* 182, 287–303.
- Patterson, M.O., McKay, R., Naish, T., Escutia, C., Jimenez-Espejo, F.J., Raymo, M.E., Meyers, S.R., Tauxe, L., Brinkhuis, H., Klaus, a., Fehr, a., Bendle, J. a. P., Bijl, P.K., Bohaty, S.M., Carr, S. a., Dunbar, R.B., Flores, J. a., Gonzalez, J.J., Hayden, T.G., Iwai, M., Katsuki, K., Kong, G.S., Nakai, M., Olney, M.P., Passchier, S., Pekar, S.F., Pross, J., Riesselman, C.R., Röhl, U., Sakai, T., Shrivastava, P.K., Stickley, C.E., Sugasaki, S., Tuo, S., van de Flierdt, T., Welsh, K., Williams, T., Yamane, M., 2014. Orbital forcing of the East Antarctic ice sheet during the Pliocene and Early Pleistocene. *Nat. Geosci.* 7, 841–847.
- Payne, R.R., Conolly, J.R., Aabbott, W.H., 1972. Turbidite Muds within Diatom Ooze off Antarctica: Pleistocene Sediment Variation Defined by Closely Spaced Piston Cores. *GSA Bull.* 83, 481–486.
- Salzmann, U., Strother, S., Sangiorgi, F., Bijl, P., Pross, J., Woodward, J., Escutia, C., Brinkhuis, H., 2016. Oligocene to Miocene terrestrial climate change and the demise of forests on Wilkes Land, East Antarctica, in: *EGU General Assembly Conference Abstracts, EGU General Assembly Conference Abstracts.* p. EPSC2016-2717.
- Villa, G., Persico, D., Wise, S.W., Gadaleta, A., 2012. Calcareous nannofossil evidence for Marine Isotope Stage 31 (1Ma) in Core AND-1B, ANDRILL McMurdo Ice Shelf Project (Antarctica). *Glob. Planet. Change* 96–97, 75–86.

Late Oligocene ~~obliquity-paced~~ astronomically paced contourite sedimentation in the Wilkes Land margin of East Antarctica: ~~implications~~ insights for ~~into~~ paleoceanographic and ice sheet configurations

5 Keywords:

Late Oligocene

Paleoceanography

Antarctic Ice sheet

Contourites

10 **Obliquity**

Ariadna Salabarnada¹, Carlota Escutia¹, Ursula Röhl², C. Hans Nelson¹, Robert McKay³, Francisco J. Jiménez-Espejo⁴, Peter K. Bijl⁵, Julian D. Hartman⁵, Stephanie L. Strother⁶, Ulrich Salzmann⁶, Dimitris Evangelinos¹, Adrián López-Quirós¹, José Abel Flores⁷, Francesca Sangiorgi⁵, Minoru Ikehara⁸, Henk
15 Brinkhuis^{5,9}

¹Instituto Andaluz de Ciencias de la Tierra, CSIC-Univ. de Granada, Armilla, 18100, Spain

²MARUM - Center for Marine Environmental Sciences, University of Bremen, Leobener Strasse 8, 28359 Bremen, Germany

20 ³Antarctic Research Centre, Victoria University of Wellington, Wellington, 6140, New Zealand

⁴Department of Biogeochemistry, Japan Agency for Marine-Earth Science and Technology, Yokosuka, Kanagawa, 237-0061, Japan

⁵Department of Earth Sciences, Marine Palynology and Palaeoceanography, Faculty of Geosciences, Laboratory of Palaeobotany and Palynology, Utrecht University, Princetonlaan 8a, 3584 CB Utrecht, The Netherlands

25 ⁶Department of Geography and Environmental Sciences, Faculty of Engineering and Environment, Northumbria University, Newcastle upon Tyne NE1 8ST, UK

⁷Department of Geology, University of Salamanca, Salamanca, 37008, Spain

⁸Center for Advanced Marine Core research, Kochi University, Nankoku, Kochi, 783-8502, Japan

30 ⁹NIOZ, Royal Netherlands Institute for Sea Research, and Utrecht University, Landsdiep 4, 1797SZ 't Horntje, Texel, The Netherlands

Correspondence to: Ariadna Salabarnada (a.salabarnada@csic.es)

Abstract

~~The late Oligocene experienced atmospheric concentrations of CO₂ between 400 and 750 ppm, which are within the IPCC projections for this century, assuming unabated CO₂ emissions. However, Antarctic ice sheet and Southern Ocean paleoceanographic configurations during the late Oligocene are not well resolved. These are however, but are important to understand the influence of high-latitude Southern Hemisphere feedbacks on global climate under such CO₂ scenarios (between 400 and 750 ppm) such as those The late Oligocene experienced atmospheric concentrations of CO₂ between 400 and 750 ppm, which are within the projected by the IPCC for projections for this century, assuming unabated CO₂ emissions (between 400 and 750 ppm). Sediments recovered by the Integrated Ocean Drilling Program (IODP) at Site U1356, offshore of the Wilkes Land margin in East Antarctica, provide an opportunity to study ice sheet and paleoceanographic configurations during the late Oligocene (26-25 Ma). Here, we present late Oligocene (26-25 Ma) ice sheet and paleoceanographic reconstructions scenarios recorded in sediments recovered by IODP Site U1356, offshore of the Wilkes Land margin in East Antarctica. Our study, based on a combination of sediment facies analysis, physical properties (physical properties magnetic susceptibility, NGR) density, and XRF inorganic X-Ray Fluorescence geochemical data, geochemical parameters, shows that glacial and interglacial sediments are continuously reworked by bottom-currents, with maximum velocities occurring during the interglacial periods. Glacial sediments record poorly ventilated, low-oxygenation bottom water conditions, interpreted to represent result from a northward shift of westerly winds and surface oceanic fronts. During interglacial times sediments record, more oxygenated and ventilated bottom water conditions and strong current velocities with enhanced current velocities, prevailed, which suggests enhanced mixing of the water masses as a result of a southward shift of the Polar Front with enhanced current velocities. Intervals Levels with preserved carbonated nannofossils Mieritic limestone intervals within some of the interglacial facies are interpreted to represent form under warmer paleoclimatic conditions when less corrosive warmer northern component water (e.g. North Atlantic sourced deep water) had a greater influence on the site Site. Spectral analysis on the late Oligocene sediment intervals from the eastern Wilkes Land margin show that the glacial-interglacial cyclicity and resulting lateral displacements of the Southern Ocean frontal systems between 26-25 Ma were forced mainly by obliquity. The lack paucity of iceberg rafted debris (IRD) throughout the studied interval contrasts with earlier Oligocene and post-Oligocene Miocene Climate Optimum sections from Site U1356 and with late Oligocene strata from the Ross Sea (CRP and DSDP 270), which contain IRD and evidence for coastal glaciers and sea ice and glaciers. These observations, supported by elevated sea surface paleotemperatures, and the absence of sea-ice, suggest that and reconstructions of fossil pollen between 26 and 25 Ma at Site U1356, suggest that open ocean water conditions prevailed. Combined, these evidences suggest and therefore at reduced glaciers or ice caps likely occupied the terrestrial lowland topographic highs and lowlands of the now marine over-deepened Wilkes Land Land Subglacial Basin (WSB) margin. Unlike today, the continental shelf was not over-deepened, and thus marine-based ice sheet expansion was likely limited to coastal regions. Combined, these data suggest that ice sheets in the Wilkes Subglacial Basin WSB were likely largely land-based and marine-based ice sheet expansion was likely limited to coastal regions.~~

~~, and therefore retreated as a consequence of surface melt during the warm late Oligocene, rather than direct ocean forcing and marine ice sheet instability processes as it did in younger past warm intervals. Spectral analysis on late Oligocene sediments from the eastern Wilkes Land margin show that the~~

1. Introduction

Today, ice sheets on Antarctica contain about 26.5 million cubic kilometres of ice, which has the potential for raising global average sea level by 58 m, with the East Antarctic Ice Sheet constituting 53.3 m of this sea level equivalent (Fretwell et al., 2013). Satellite observations indicate significant rates of change in most of the West Antarctic Ice Sheet (WAIS) and some sectors of the East Antarctic Ice Sheet (EAIS). These include thinning at their seaward margins (Pritchard et al., 2012) and accelerating ice shelves basal melt rates (Rignot et al., 2013; [Shen et al., 2018](#)). Given the uncertainties in projections of future ice sheet melt, there has been a growing number of studies of sedimentary sections from the surrounding margins of Antarctica targeting records of past warm intervals (i.e., high-CO₂ and elevated temperature climates) in order to better understand ice sheets and Southern Ocean configurations under these conditions. For example, the early Pliocene (5–3 Ma) has been targeted because atmospheric CO₂ concentrations were similar to today's 400 ppmv concentrations (Foster and Rohling, 2013; Zhang et al., 2013). These studies have shown that early Pliocene Southern Ocean surface waters were warmer (i.e., between 2.5– > 4 °C) than present and that the summer sea ice cover was greatly reduced, or even absent (Bohaty and Hardwood, 1998; Whitehead and Bohaty, 2003; Escutia et al., 2009; Cook et al., 2013). They also record the periodic collapse of both the WAIS and EAIS marine-based margins (Naish et al., 2009; Pollard and DeConto, 2009; Cook et al., 2013; Reinardy et al., 2015; DeConto and Pollard, 2016). Foster and Rohling (2013) ~~demonstrated~~ provide a sigmoidal relationship between eustatic sea-level and atmospheric CO₂ levels whereby sea levels stabilise at ~22 +/-12 m above present-day level, between about 400 ppm and 650 ppm, suggesting loss of the Greenland Ice Sheet (6–7 m s.l.e.) and the marine-based West Antarctic Ice Sheet (+7–11 m s.l.e.). This implies that continental EAIS volumes remained relatively stable during these times, but experienced mass loss of some (or all) its marine-based margins (-19 m s.l.e.), relative to the present day. With CO₂ concentrations at > 650 ppm they infer further increases in sea level, suggesting this as a threshold for initiating retreat of the terrestrial margins of EAIS. With sustained warming, CO₂ concentrations of more than 650 ppmv are within the projections for this century (Solomon, 2007; ~~IPCC~~ [Field et al., 2014](#)). The last time the atmosphere is thought to have experienced CO₂ concentrations above 650 ppmv was during the Oligocene (23.03–33.9 Ma), when CO₂ values remained between 400 to ~750–800 ppm (Pagani et al., 2005; Beerling and Royer, 2011; Zhang et al., 2013).

Geological records of heavy isotope values ~ 2.5 ‰ and far field sea level records from passive margins during the Oligocene suggest that, following the continental-wide expansion of ice during the Eocene-Oligocene transition that culminated at the Oi-1 event (33.6 Ma), the Antarctic ice cover was at least ~ 50 % of the current volume (e.g., Kominz and Pekar, 2001; Zachos et al., 2001; Coxall et al., 2005; Pekar et al., 2006; Liebrand et al., 2011, 2017; Mudelsee et al., 2014). The early part of the Oligocene records a significant $\delta^{18}\text{O}$ decreasing slope with high-latitude sites exhibiting a strong deglaciation/warming that persisted until ~ 32 Ma (Mudelsee et al., 2014). This was followed by seemingly stable conditions on Antarctica as evidenced by minimal $\delta^{18}\text{O}$ and Mg/Ca changes (Billups and Schrag, 2003; Lear et al., 2004; Mudelsee et al., 2014). A slight glaciation/cooling is recorded before ~~~ 27 to 28~~ ~ 27 Ma, which was followed by an up to 1 ‰ long-term decrease in the $\delta^{18}\text{O}$ isotope records that was interpreted to result from the deglaciation of large parts of the Antarctic ice sheets during a significant warming trend in the late Oligocene (27-26 Ma) (Zachos et al., 2001a). Nevertheless, there are marked differences between the late Oligocene low $\delta^{18}\text{O}$ values recorded in Pacific, Indian and Atlantic Ocean sites (e.g., Pälike et al., 2006; Cramer et al., 2009; Liebrand et al., 2011; Mudelsee et al., 2014; Hauptvogel et al., 2017), and the sustained high $\delta^{18}\text{O}$ values recorded in Southern Ocean sites (Pekar et al., 2006; Mudelsee et al., 2014). High $\delta^{18}\text{O}$ values in the Southern Ocean sediments are in agreement with the ice proximal record recovered by the Cape Roberts Project (CRP) in the Ross Sea, which show the existence of glaciers/ice sheets at sea level (Barrett et al., 2007; Hauptvogel et al., 2017). Based on the study of the isotopic record in sediments from the Atlantic, the Indian and the equatorial Pacific, Pekar et al. (2006) explained ~~this~~ conundrum of a glaciated Antarctica, and varying intrabasinal $\delta^{18}\text{O}$ values with the coeval existence of two deep-water masses, one sourced from Antarctica and another, warmer bottom-water, sourced from lower latitudes. Superimposed on the above long-term swings in the $\delta^{18}\text{O}$ Oligocene record, fluctuations on timescales shorter than several Myr were identified in the high-resolution benthic $\delta^{13}\text{C}$ record from ODP 1218 (Pälike et al., 2006). These fluctuations in periods of 405 kyr and 1.2 Myr are related to Earth's orbital variations in eccentricity and obliquity, respectively and have been referred as the short-term "heartbeat" of the Oligocene climate (Pälike et al., 2006). Oligocene records close to Antarctica are needed to better resolve Antarctic ice sheet and paleoceanographic configurations at different time scales and under scenarios of increasing atmospheric CO_2 values that can be related to global records concentrations. ~~Oligocene records close to Antarctica are needed to better resolve Antarctic ice sheet and paleoceanographic configurations and variations at different timescales and under scenarios of increasing atmospheric CO_2 values and $\delta^{18}\text{O}$ records, which imply a climatic warming and/or ice volume loss.~~

Integrated Ocean Drilling Program (IODP) Expedition 318 drilled a transect of sites across the eastern Wilkes Land margin at the seaward termination of the Wilkes Subglacial Basin (WSB) (Escutia et al., 2011; Escutia et al., 2014) (Fig. 1). Relatively good recovery (78.2 %) of late Oligocene (26-25 Ma) sediments from Site U1356 between 689.4 and 641.4 meters below sea floor (mbsf) provides an opportunity to study ice-sheet and ocean configurations during the late Oligocene and to relate them with other Antarctic and global records. In this paper, we present a new glacial-interglacial sedimentation and paleoceanographic model for the distal glacio-marine record of the Wilkes Land margin constructed on the basis of sedimentological data (visual core description, facies analysis, computed tomography images, and high-resolution scanning electron microscopy images), physical properties (i.e., magnetic susceptibility of the bulk sediment and grain density)~~selected physical properties data (magnetic susceptibility)~~, and X-ray fluorescence data (XRF). We also provide insights into the configuration of the ice sheet in this sector of the east Antarctic margin and evidence for orbital forcing of the glaciomarine glacial-interglacial sedimentation at Site U1356.

2. Materials and Methods

2.1 Site U1356 description

Site U1356 (63° 18.6138'S, 135° 59.9376'E) is located at 3992 m water depth in front of the glaciated margin of the eastern Wilkes Land Coast of East Antarctica, and penetrated 1006 meters into the flank of a levee deposit in the transition between the lower continental rise and the abyssal plain (Escutia et al., 2011; Fig. 1). Overall recovery was 35% with sediments dated between the early Eocene and Pliocene, but several intervals provide good stratigraphic control (Escutia et al., 2011; Tauxe et al., 2012). The Oligocene section was recovered between 895 and 430.8 mbsf, Cores U1356-95R-3 83 cm to U1356-46R. Our study focuses on the relatively high-recovery (78.2 %) interval within the late Oligocene, which spans from 689.4 to 641.4 mbsf (Cores U1356-72R to -68R). The sediments from this interval are part of shipboard lithostratigraphic Unit V, which is characterized by light greenish-grey, strongly bioturbated claystones and micritic limestones interbedded with dark brown, sparsely bioturbated, parallel- and ripple-laminated claystones with minor cross-laminated interbeds (Escutia et al., 2011). The bioturbated and calcareous claystones and limestones were broadly interpreted to represent pelagic sedimentation superimposed on the background hemipelagic sedimentary input (Escutia et al., 2011). The laminated claystones and ripple cross-laminated sandstones were interpreted to likely result from variations in bottom current strength and fine-grained terrigenous supply (Escutia et al., 2011). In addition, a notable absence of Ice Rafted Debris (IRD) (>250µm) in this interval relative to underlying and overlying strata was also recorded.

175 ~~The late Oligocene depositional setting of Site U1356 during the late Oligocene was however different~~
~~to today's~~ to that of today. The stratigraphic evolution of the region testifies ~~to the~~ the progradation of the
continental shelf taking place after continental ice sheet build-up during the Eocene-Oligocene
Transition (EOT, 33.6 Ma; Eittrheim et al., 1995; Escutia et al., 1997, 2005; ~~Escutia et al., 2014~~), which
180 resulted in: 1) seismic and sedimentary facies on the continental rise becoming more proximal up-
section (Hayes and Frakes, 1975; Escutia et al., 2000; ~~Escutia et al., 2005~~; ~~Escutia et al., 2014~~), and 2)
high sedimentation rates during the Oligocene (Escutia et al., 2011; Tauxe et al., 2012). In this context,
the studied late Oligocene sediments from Site U1356 record distal continental rise deposition in an
incipient/low-relief levee of a submarine channel. As progradation continued, a complex network of
well-developed channels and high-relief levee systems developed on the continental rise (Escutia et al.,
185 2000) from the latest Oligocene onwards.

Today, Site U1356 lies close to the Southern Boundary of the Antarctic Circumpolar Current, near the
Antarctic Divergence at ~63°S (Orsi, 1995; Bindoff, 2000) (Fig. 1). However, the paleolatitude of Site
U1356 was around 58.5±2.5°S (van Hinsbergen et al., 2015) during the late Oligocene, more northerly
190 than today. Scher et al. (2008, 2015) reconstructed the position of the early Oligocene Antarctic
Divergence to be located around 60°S (Fig. 1), based on the distribution of terrigenous and biogenic
(calcareous and siliceous microfossils) sedimentation, Nd isotopes, and Al/Ti ratios through a core
transect across Australian-Antarctic basin in the Southern Ocean. According to these interpretations Site
U1356 lay far to the north of the Antarctic Divergence zone, and was closer to the Polar Front, during
195 the Oligocene.

2.2 Age Model

The age model for Site U1356 was established on the basis of the magnetostratigraphic datums
constrained by marine diatom, radiolaria, calcareous nannoplankton and dinocyst biostratigraphic
200 control (Escutia et al., 2011; Tauxe et al., 2012; Bijl et al., ~~in press~~2018). The late Oligocene interval
contains three magnetostratigraphic datums (Table 1): 1) Chron C8n.1n (o) between 643.70 and 643.65
mbsf (U1356-68R-2); 2) C8n.2n (y) between 652.60 and 652.55 mbsf (U1356-69R-2), and 3) C8n.2n
(o) between 679.90 and 678.06 mbsf (U1356-71R). For this study, the age model by Tauxe et al.
(2012), which was calibrated to the Gradstein 2004 Geological Time Scale, has been updated using the
205 GPTS 2012 Astronomic Age Model (to the Geological Time Scale of Gradstein-Vanderberghe et al.
(2012). Based on this calibration, the age of sediments between 678.98 and 643.37 mbsf is 25.99 and
25.26 Ma, respectively (Fig. 2; Table 1).

2.3 Facies Analyses

210 Detailed facies analyses provide a stratigraphic framework on which we base our sedimentary processes and paleoenvironmental interpretations. Lithofacies are determined on the basis of detailed visual logging of the core during a visit to the IODP-Gulf Coast Repository (GCR), expanding on the lower resolution preliminary descriptions in Escutia et al. (2011). ~~For this analysis, w~~We logged the lithology, sedimentary texture (i.e., shape, size and distribution of particles) and structures with a focus on the contacts between the beds and on bioturbation at a mm to cm-scale resolution in cores expanding from 896 to ~~392-95.4~~ mbsf (Cores U1356-95R to ~~-42R11R~~) (see Supplementary material S1 Fig. S1, S2). Physical properties data were measured during IODP Exp. 318 using the Whole-Round Multisensor Logger. Magnetic susceptibility measurements were taken at 2.5 cm intervals, and Natural gamma radiation (NGR) was measured every 10 cm (Escutia et al., 2011). In this paper, we focus on the interval between 689.4 and 641.4 mbsf that comprise cores 72R to 68-R (Fig. 2).

X-ray Computed Tomography scans (CT-scans) measure changes in density and allow for analysis of fine-scale stratigraphic changes and internal structures of sedimentary deposits in a non-destructive manner (e.g., Dulu, 1999; St-Onge and Long, 2009; Van Daele et al., 2014; Fouinat et al., 2017). To further characterize the different facies in our cores, selected intervals of Core U1356-71R-6 (678.11 to 676.91 mbsf) and Core U1356-71R-2 (672.8 to 671.35 mbsf) were CT-scanned at the Kochi Core Center (KCC) (Japan), ~~with. For this, we used the the~~ GE Medical systems LightSpeed Ultra 16. 2D scout (shooting conditions at 120Kv with 100mA, and 3D Helical image with 120Kv and 100mA and FOV=22.0). Image spatial resolution consisted of 0.42 mm/pixel with 0.625 mm of slice thickness (voxel spatial resolution of 0.42 x 0.42 x 0.625 mm).

The type and composition of biogenic and terrigenous particles, particle size, and morphology of each lithofacies was characterized with a high-resolution scanning electron microscope (HR-SEM) at the Centro de Instrumentación Científica (University of Granada, Spain).

2.4 X-Ray Fluorescence (XRF) analyses

Detailed bulk-chemical composition records acquired by ~~X-Ray Fluorescence (XRF)~~ core scanning allows accurate determination of sedimentological changes as well as and the assessment of the contribution of the various components in the biogenic and lithogenic fraction of the marine sediments (Croudace et al., 2006). This non-destructive method yields element intensities on the surface of split sediment cores and provides statistically significant data for major and minor elements (Richter

et al., 2006; O'Regan et al. 2010, Wilhelms-Dick et al., 2012). The data are given as element intensities in total counts.

245 ~~Non-destructive X-ray fluorescence (XRF)~~ core scanning measurements were collected every 2 cm down-core over a 1 cm² area with split size of 10 mm, a current of 0.2 mA (Al - Fe) and 1.5 mA (all other elements) respectively, and a sampling time of 20 seconds, directly at the split core surface of the archive half with XRF Core Scanner III at the MARUM – Center for Marine Environmental Sciences, University of Bremen, Germany. Prior to the scanning, cores were thermally equilibrated to room
250 temperature, the surface was cleaned, flattened, and covered with 4 µm thin SPEXCerti Prep Ultralene1 foil to protect the sensor and prevent contamination during the scanning procedure. Scans were collected during three separate runs using generator settings of 10 kV for the elements Al, Si, S, K, Ca, Ti, Mn, Fe; 30 kV for elements such as Br, Rb, Zr, Mo, Pb; and 50 kV for Ba. The here reported data have been acquired by a Canberra X-PIPS Silicon Drift Detector (SDD; Model SXD 15C-150-500) with
255 150eV X-ray resolution, the Canberra Digital Spectrum Analyzer DAS 1000 and an Oxford Instruments 100W Neptune X-ray tube with rhodium (Rh) target material. Raw data spectra were processed by the Analysis of X-ray spectra by Iterative Least square software (WIN AXIL) package from Canberra Eurisys. Data points from disturbed intervals in the core face (i.e., slight fractures and cracks) were removed.

260 ~~This non-destructive method yields element intensities on the surface of split sediment cores and provides statistically significant data for major and minor elements (Richter et al., 2006; O'Regan et al. 2010, Wilhelms-Dick et al., 2012). Detailed bulk chemical composition records acquired by XRF core scanning allows accurate determination of sedimentological changes as well as assessment of the contribution of the various components in the biogenic and lithogenic fraction of the marine sediments (Croudace et al., 2006). The data are given as element intensities in total counts.~~ The light elements Al, Si, and K show large element variations (intra-element variations of 1 order of magnitude or more, Fig. 2). Core disturbances are not present in the core as sediments are mostly lithified, data points from cores with fractures and crack zones where removed. Similar variations have been previously described in
270 sediment cores to indicate substantial analytical deviations due to physical sedimentary properties (i.e. Tjallingii and Röhl et al., 2007; Hennekam and de Lange 2012). Accordingly, for this study we have discarded the continuous records of Al, Si, and K and concentrated our interpretations on Al, Si and K values from the XRF analyses in discrete samples (see below). As Titanium (Ti) is restricted to the terrigenous phase in sediments and is inert to diagenetic processes (Calvert and Pedersen, 2007), we
275 utilized Ti to normalize other chemical elements for the terrigenous fraction. Linear correlation (r Pearson) above standardised values has been done in order to find statistical relationships among the variables.

In addition, we conducted measurements of a total of 50 major and minor trace elements in 25 discrete sediment samples collected at 0.4 and 1 m spacing to determine their chemical composition. For this, we used a Pioneer-Bruker X-Ray Fluorescence (XRF) spectrometer S4 at the Instituto Andaluz de Ciencias de la Tierra (CSIC-UGR) in Spain, equipped with a Rh tube (60 kV, 150 mA) using internal standards. The samples were prepared in a Vulcan 4Mfusion machine and the analyses performed using a standard-less spectrum sweep with the Spectraplus software.

2.5 Spectral Analyses

We selected key environmental indicators from XRF core scanner data and elemental ratios (i.e., Zr/Ba, Ba, Zr/Ti, Ca/Ti, MS) to conduct spectral analyses on the data from the interval between 689.4 to 641.4 mbsf (Cores U1356-72R to 68R). We performed evolutionary spectral and harmonic analysis on each dataset using Astrochron toolkit on the R software (Meyers, 2014). Detailed methodology is provided as supplementary information following the Astrochron code of Wanlu Fu et al. (2016). This method allows the detection of non-stationary spectra variability within the time series. The time series were analysed ~~in-on~~ the depth scale and then, ~~anchored to the obliquity solution (Laskar 2004)~~ applying the Frequency domain minimal tuning (Meyers et al., 2001), we converted spatial frequencies to sedimentation rates using an average period of 41 Kyr, to transform them to an age scale, with the basis of the already resolved age model. The Evolutionary Average Spectral Misfit method was then used to resolve unevenly sampled series and changing sedimentation rates (Meyers et al., 2012). This method is used to test a range of plausible timescales and simultaneously evaluate the reliability of the presence of astronomical cycles ~~The eccentricity, obliquity and precession target periods were determined from La04 (Laskar et al., 2004) using the interval from 25.0–26.4 Ma~~ (Supplemental material S2).

3. Results

3.1 Sedimentary facies

The revised Oligocene facies log (Fig S1, S2), includes the high-recovery interval between 689.4 and 641.4 mbsf (Fig. 2). The integration of our lithofacies analyses, with physical properties (MS), CT-sans and HR-SEM analyses characterize an alternation between two main facies (Facies 1 and 2) (Figs. 2, 3, 4). ~~Although these two facies were already visually identified shipboard, but the interpretation of these facies was limited. Consequently, our analyses allow us to a more detailed characterization and interpretation comprehensively characterize the facies, and to provide a more rigorous additional~~

310 ~~interpretation about of~~ the depositional environments and the processes involved in their development. ~~not considered before.~~

315 Facies 1 (F1) consists of slightly bioturbated greenish claystones with sparse (Fig. 3a) to common laminations (Figs. 2, 3a-f; Table 2). Laminae, as described on shipboard, vary from 0.1 to 1 cm thick and, based on non-quantitative smear slide observations, are composed of well-sorted silt to fine sand size quartz grains (Escutia et al., 2011). Laminations can be planar, wavy, with ripple-cross lamination structures (Escutia et al., 2011), and show faint internal truncation surfaces, mud offshoots, and internal erosional surfaces (Fig. 3a-f). HR-SEM analyses of the claystones show that the matrix is composed of clay-size particles and clay minerals (Fig. 3g, i). In addition, they show rare calcareous nannofossils that are partially dissolved (Fig. 3g, i). Authigenic carbonate crystals are also identified (Fig. 3i). Bioturbation in F1 is scarce, ichnofossils in the sediments are dominated mainly by *Chondrites* Fig. 3d). CT-scans also show the presence of *Skolithos*, with their vertical thin tubes filled with high-density material suggesting they are pyritized (Fig. 3b). Pyrite was also observed in shipboard smear slides in small abundances from the laminated facies in the studied interval (Escutia et al., 2011). Magnetic susceptibility values within the laminated facies are low, between 40-70 MS instrumental units (iu), with higher values when silt laminations are more abundant (Figs. 2, 4). Natural Gamma Ray (NGR) is anti-correlated with MS, with high values in F1 varying between 50 - 65 counts per second (cps) (Fig. 2).

330 Facies 2 (F2) is composed by light greenish grey strongly bioturbated claystones and silty claystones (Figs, 2, 3; Table 2) with variable carbonate content varying between 5-16% based on our XRF analyses. No primary structures are preserved due to the pervasive bioturbation (Fig. 3a-c). Burrows are backfilled with homogeneous coarse material (silt/fine sand). Different types of ichnofossils are present with *Planolites* and *Zoophycos* being the most abundant (Fig. 3a, b). HR-SEM images show: 1) silt-size grains containing quartz grains with conchoidal fractures in the corners and impact marks on the crystal faces, indicative of high-energy environments; and 2) biogenic carbonate consisting of moderately to poorly preserved coccoliths, which exhibit dissolution of their borders, and to a minor degree detrital carbonate grains (Fig. 3h - j). A total of 13 carbonate-rich layers have been observed within the studied interval F2, and they range in thickness from 10 to 110 cm. **Facies 2** CT-scans images show an increase in density (i.e., gradation towards lighter colours in the scan) towards the top of each bioturbated interval (Fig. 3b). MS values are higher in F2 compared to F1. Values vary from 50-150 instrumental units (iu) and exhibit an inverse grading or a bigradational-like morphology (Fig. 2, 4), while NGR is inversely correlated with minimum values occurring in F2 (between 35-55 cps) (Fig. 2).

345 Contacts between the two facies are sharp and apparently non-erosive, with minimal omission surfaces or lags (Figs. 3,4). However, when bioturbation is present, gradual contacts in the transition from F1 to F2 also occur (Fig. 3b). Both sharp and transitional contacts are well imaged on the MS plots (Fig. 2).

In addition, where available, the CT-scan images confirm the shipboard and our own visual
350 observations regarding the absence of outsized clasts and coarse sands grains in F1 and F2. Hauptvogel (2015) however, reports grains that are >150µm in size (fine sand fraction) as IRD. He argues that grains of that size could only reach Site U1356 through ice rafting given the distance of the site to shore, unless they were delivered by gravity flows. Thick and coarse-grained Mass Transport Deposits (MTDs) during the latest Oligocene at site U1356 (Escutia et al., 2011), argue for coarse material being
355 delivered to the site by gravity flows. In addition, fine sand grains to gravel size clasts have been reported from channels on the lower continental rise off the Wilkes Land margin transported by gravity flows, including turbidity flows (Payne and Conolly, 1972; Escutia et al., 2000; Busetti et al., 2003). Given that during the late Oligocene, Site U1356 is located on a low-relief levee of a submarine channel, one can expect delivery of fine-grained sand and even coarser sediment to the site. In any case,
360 even if some background IRD is present in our record, we argue it is minimal compared to elsewhere in the core.

3.2 Geochemistry

Down-core changes in the log ratios of various elements have been plotted against the facies log (Figs.
365 2, 4). In addition, in order to determine geochemical element associations we performed a Pearson correlation coefficient analysis of major elements on the whole XRF-scanner dataset (Table 3). This analysis highlights two main groups that are used as proxies for terrigenous (i.e., Zr, Ti, Rb, Ba) vs biogenic (i.e., Ca = carbonate) sedimentation.

370 Titanium (Ti), Zirconium (Zr), and Rubidium (Rb) are primarily derived from terrigenous sources, where Ti represents the background terrigenous input. During sediment transport Zr, Rb and Ti tend to become concentrated in particular grain-size fractions due to the varying resistance of the minerals in which these elements principally occur. Zr tends to become more concentrated in fine sand and coarse silt fractions, Ti in somewhat finer fractions and Rb principally in the clay-sized fraction (Veldkamp and Kroonenberg 1993; Dypvik and Harris 2001). The lack of correlation between Zr and Ti (Fig. 2;
375 Table 3) implies that they are settled in different minerals and processes. The Zr/Rb ratio has been applied as a sediment grain-size proxy in marine records (Schneider, et al., 1997; Dypvik and Harris 2001; Croudace et al., 2006; Campagne et al., 2015). Zr/Al has been interpreted as an indicator for the accumulation of heavy minerals due to bottom currents (Bahr et al., 2014). In our cores, Zr/Rb and

380 Zr/Ti ratios have a near identical variability downcore (Fig. 2). We utilize the high-amplitude Zr/Ti
signal in our records as indicator for larger grain-size and current velocity (Fig. 2). The Zr/Ti ratio
varies between 0.1 and 1 and exhibits maximum values within F2 showing an increasing upwards or
bigradational patterns (Fig. 2). Although minimum Zr values (cps) are found in F1, laminations with
coarser-grained sediment within this claystone facies are also characterized by elevated Zr values
385 similar to those in F2 (Figs. 3, 4; Table 3). The Zr/Ti pattern is positively correlated with magnetic
susceptibility throughout the studied interval (Fig. 2).

The Zr/Ti, Zr/Rb and Zr/Ba ratios co-vary characterizing the laminations within F1 and the alternation
between F1 and F2 by defining the contacts between them (Figs. 2, 4). They also mark the coarsening
390 upwards or bigradational tendency in F2 (Fig. 4). Of the three ratios, the Zr/Ba ratio is the one that
highlights these patterns best (Figs. 2, 4).

Barium (Ba) is present in marine sediments mainly in detrital plagioclase crystals and in the form of
barite (BaSO₄; Tribovillard et al., 2006). In the studied sediments, Ba and Ti have a correlation factor of
395 $r^2=0.66$ (Table 3), which is taken to indicate that Barium is predominantly present as a constituent of the
continental terrigenous fraction and/or that biogenic barite was sorted by bottom currents. Ba has
maximum values (10,000 total counts) at the base of F1 and decreases upwards in a saw-tooth pattern,
reaching minimum concentrations within F2 (5,000 total counts) (Fig. 2; Table 3). The detrital fraction
of Ba in the open ocean has been used in other studies as a tracer of shelf waters (Moore and Dymond,
400 1991; Abrahamsen et al., 2009; Roeske, 2011) and Ba record also is affected by current intensity in
other depositional contourite systems (Bahr et al., 2014) preventing his use as paleoproductivity proxy
in environments dominated by contour currents.

Variations in Ca, Mn, and Sr are strongly intercorrelated (Fig. 2) with $r^2>0.87$ (Table 3). Biogenic
405 calcite precipitated by coccoliths and foraminifera have greater Sr concentration than inorganically
precipitated calcite or dolomite (Hodell et al., 2008). The positive Ca and Sr correlation could therefore
potentially be used to differentiate between terrigenous Ca sources (e.g. feldspars and clays) and
biogenic carbonates (e.g. Richter et al., 2006, Foubert and Henriot, 2009, Rothwell and Croudace,
2015). Based on these observations, we interpret that Ca in our sediments is mainly of biogenic origin
410 (CaCO₃). This interpretation is supported by HR-SEM images taken from carbonate-rich intervals of
F2, which show abundant coccoliths (Fig. 3d). Peaks in Ca in our record (Fig. 2) coincide with the
carbonate-rich layers listed in the previous section. Additional peaks in the record may indicate
carbonate-rich layers that we have been unable to identify visually.

415 In order to estimate the CaCO₃ content continuously throughout the studied interval we use a calibration
($r^2_{U1356}=0.81$) between natural logarithm (ln) of Ca/Ti ratio (ln(Ca/Ti)) from the XRF core scanner data
and the XRF discrete CaCO₃ measurements (weight %) from Site U1356 as applied in other studies
(Zachos et al., 2004; Liebrand et al., 2016) (Fig. 5). “CaCO₃ est.” is used throughout the text to refer to
carbonate content estimated by ln(Ca/Ti) ratio. CaCO₃ est. concentrations are generally low (between 0-
420 16%). Carbonates are mostly present in F2, varying between 5-16 %, although small contents (from 0 to
5 %) can be seen in the intervals of F1 with scarce laminations (Fig. 4). CaCO₃ est. peaks in some
intervals have a particular morphology producing a double peak in the beginning and/or the end of
bioturbated F2 (Figs. 2, 4).

425 Mn(II) is soluble under anoxic conditions and precipitates as Mn(IV) oxyhydroxides under oxidising
conditions (Tribovillard et al., 2006). Manganese is frequently remobilized to the sedimentary pore
fluids under reducing conditions. Dissolved Mn can thus migrate in the sedimentary column and
(re)precipitate when oxic conditions are encountered (Calvert and Pedersen, 1996). As such, large Mn
enrichments primarily reflect changing oxygen levels at the sediment–water interface (Jaccard et al.,
430 2016). The strong-correlated peaks of Mn and Ca (Fig. 2; Table 3) suggest that at least some of the Mn
is present in the studied interval as Mn carbonates and/or Mn oxyhydroxides under oxic sediment-water
interphase (Calvert and Pedersen, 1996; Calvert and Pedersen 2007; Tribovillard et al., 2006).

Br/Ti has been previously used as an indicator of organic matter in sediments (e.g., Agnihotri et al.,
435 2008; Ziegler et al., 2008; Bahr et al., 2014). Br/Ti in our record shows generally low values (Fig. 2)
most likely as the organic matter content in both facies types is relatively low (<0.5 %, Escutia et al.,
2011). However, it exhibits some variability (0.01 to 0.05 Br/Ti ratio) within the two facies with higher
ratio values in F1. Darker coloured sediments in F1 are in agreement with these higher Br/Ti values
inside F1.

440 In addition to the elemental analyses of the XRF-scanned data, we use the detrital Al/Ti ratio in discrete
XRF bulk sediment samples to reflect changes in terrigenous provenance (Kuhn and Diekmann, 2002;
Scher et al., 2015). Al/Ti ratio varies between 17-21, with the highest values found within F1 and the
lowest in F2 (Fig. 2).

445

3.4 Spectral analysis

To detect periodical signals, spectral analysis of time series was performed on the Zr/Ba and other
elemental proxies (i.e., Ba, Zr/Ti, CaCO₃, Magnetic Susceptibility) using Astrochron R software
(Meyers, 2014; Figs. 6; S3-10).

Multiple-taper spectral analysis (MTM) in Zr/Ba show a clear and statistically significant (>90%) cyclicity every 2m (0.5 cycles/m), and at 4.67m (0.21 cycles/m), and less significant one (>80%) at 1m (0.94 cycles/m) (Fig. S3). On the basis of a linearly calculated sedimentation rate between the two extreme tie-points (Table 1), we obtained a sedimentation rate of approximately 5 cm/kyr. Within this sedimentation rate, the 0.5 cycles/m peak corresponds to the 41-kyr obliquity frequency; and the 0.21 and 0.94 cycles/m to the 95 and 21-kyr shorter eccentricity periods and precession frequencies, respectively.

After initial analysis, we ran an Evolutive Harmonic Analysis (EHA) (Astrochron (Meyers, 2014)) with 3 data tapers for the untuned Zr/Ba in depth domain with 2 cm resolution (Fig. S3). The statistical significance of spectral peaks was tested relative to the null hypothesis of a robust red noise background, AR(1) modelling of median smoothing, at a confidence level of 95% (Mann and Lees, 1996). Despite a short core gap in the middle of the time series, obliquity (41 kyr) dominates throughout the time series (Fig. 6). The sedimentation rates obtained by this method vary between 4.6 and 5.4 cm/kyr for the studied section, similar to those obtained with linearly calculated sedimentation rates. Additionally, the Nyquist frequency for Zr/Ba data is 1 m^{-1} (0.5 kyr), which implies the site is sampled sufficiently to resolve precessional scale variations however, core gaps prevent identification of long eccentricity cycles (Fig. S6). ~~The time series is afterwards~~ Time-anchored series were anchored to the more robust paleomagnetic tie point ~~from the U1356 age model (where 606.226 from the time scale is equivalent to 678.78 m or,~~ which is 25.99 Ma at 678.78 mbsf (Fig. S7).

Apart from obliquity, spectral analyses of the tuned age model reveal an alignment of the eccentricity and precession bands (Fig. 6, S8). For example, a marked cyclicity at the obliquity periods of 41 Kyr is seen at Ba and Zr/Ti (99% confidence) and also eccentricity at 100 kyr, and precession at 20kyr (95% confidence) (Fig. S9). We also observe coherent power above the 90% significance level at ~54 and ~29 ky periods, which are secondary components of obliquity. The anchored age model provides an unprecedented 500 yr resolution (2.5 cm sampling) of the data during the Late Oligocene. Orbital frequencies were tested in each core section individually in the Zr/Ba dataset in the depth scale in order to assure that cyclicity is not an artefact related to the gaps in the series (Fig. S10).

4. Discussion

Based on the integration of the facies characterized on the basis of sedimentological data (visual core description, facies analysis, CT-scans, HR-SEM), physical properties (magnetic susceptibility, NGR),

485 and geochemical data (XRF), we provide for the late Oligocene interval (26 to 25 Ma): 1) a new glacial-
interglacial sedimentation model for the distal glaciomarine record in the Wilkes Land margin
dominated by bottom-current reworking of both, glacial and interglacial deposits; 2) insights into the
configuration of the ice sheet in this sector of the east Antarctic margin; 3) changes in the
paleoceanographic glacial-interglacial configuration; and 4) evidence for orbital forcing of the
glaciomarine glacial-interglacial sedimentation at Site U1356.

4.1 Glacial and interglacial contourite sedimentation off Wilkes Land

490 Laminated claystones (F1) from Site U1356 were originally interpreted by the shipboard science team
to have formed during glacial times relating to variations in bottom current strength and fine-grained
terrigenous supply. Conversely, the bioturbated claystones and micritic limestones (F2) were interpreted
495 to result from mostly hemipelagic sedimentation during interglacial times (Escutia et al., 2011).
Alternations between laminated glacial deposits and bioturbated hemipelagic deposits, similar to those
in F1 and F2, have been previously reported to characterize Pleistocene and Pliocene glacial-interglacial
continental rise sedimentation, respectively, on this sector of the Wilkes Land margin (Escutia et al.,
2003; Patterson et al., 2014). Gravity flows, mainly turbidity flows are the dominant process during
500 glacial times resulting in laminated deposits. Interglacial sedimentation is dominated by hemipelagic
deposition with higher opal and biogenic content (Escutia et al., 2003, Buseti et al., 2003). Erosion and
re-deposition of fine-grained sediment by bottom contour currents has also been reported as another
important process during Pleistocene and Plio-Quaternary interglacials (Escutia et al., 2002; Escutia et
al., 2003, Buseti et al., 2003).

505 ~~The depositional setting on the continental rise was however different during the late Oligocene. The
stratigraphic evolution of the region testifies the progradation of the continental shelf taking place after
continental ice sheet build-up during the Eocene-Oligocene Transition (EOT, 34 Ma) (Eittrheim et al.,
1995; Escutia et al., 1997; Escutia et al., 2005), which resulted in: 1) seismic and sedimentary facies
becoming more proximal up-section (Hayes and Frakes, 1975; Escutia et al., 2000; Escutia et al., 2005;
510 Escutia et al., 2014), and 2) high sedimentation rates during the Oligocene (Escutia et al., 2011; Tauxe
et al., 2012). In this context, the late Oligocene sediments from Site U1356 record distal continental rise
deposition in an incipient/low-relief levee of a channel-levee complex. As progradation continued, a
complex network of well-developed channels and high-relief levee systems developed on the
continental rise (Escutia et al., 2000) from the latest Oligocene onwards.~~

515 ~~Laminated claystones (F1) from Site U1356 were originally interpreted by the shipboard science team
to have formed during glacial times relating to variations in bottom current strength and fine-grained
terrigenous supply. Conversely, the bioturbated claystones and micritic limestones (F2) were interpreted~~

520 to result from mostly hemipelagic sedimentation during interglacial times (Eseutia et al., 2011). In this study, we have further characterized these facies on the basis of sedimentological data (visual core description, facies analysis, CT-scans, HRSEM), physical properties (magnetic susceptibility, NGR); and geochemical data (X-ray Fluorescence XRF), which allow us to construct a sedimentation model for the depositional setting of Site U1356 during the late Oligocene that is dominated by bottom-current reworking of both, glacial and interglacial deposits.

525 ~~Laminated, fossil barren, glaciogenic deposits consistent with those of Facies F1 have been observed on younger sedimentary sections from other polar margins and interpreted as contour current modified turbidite deposits and as muddy contourites (Anderson et al., 1979; Mackensen et al., 1989; Grobe and Mackensen, 1992; Pudsey, 1992; Gilbert et al., 1998; Pudsey and Howe, 1998; Pudsey and Camerlenghi, 1998; Anderson, 1999; Williams and Handwerker, 2005; Lucchi and Rebesco, 2007; Eseutia et al., 2009). This particular type of glaciogenic contourite facies is associated with glaciomarine deposition during glacial times, and has been interpreted to result from unusual, climate related, environmental conditions of suppressed primary productivity and oxygen-poor deep waters (Lucchi and Rebesco, 2007).~~ Despite being sparse, the occurrence of bioturbation in our laminated sediments in F1, 530 which slightly affects both claystones and silt laminations, indicates slow and continuous sedimentation. This, ~~which~~ is not consistent with instantaneous turbidite deposition, which would be expected at the Site U1356 located on the left low-relief levee of a contiguous channel during the late Oligocene. It is however consistent with fine-grained turbidite overbank deposits being consequently entrained by bottom currents. ~~distal overbank fine-grained sediments being entrained by bottom currents.~~ Silt layer 540 sedimentary structures similar to those described by Rebesco et al. (2008, 2014) indicate that there is current reworking of the sediments. For example, silt layers can be continuous or discontinuous with wavy and irregular morphologies, and within layers, sedimentary structures such as cross-laminations are common (Fig. 3c-f). Within the cross laminae, mud offshoots and internal erosional surfaces are distinctive features of fluctuating currents where successive traction and suspension events are super- 545 imposed, indicating bottom-currents sedimentation as the principal process for the F1 laminated claystones (Shanmugam et al., 1993; Stow et al., 2002). Based on these observations, we interpret F1 as glacial laminated muddy contourites following the classification of Stow and Faugères (2008). The F1 sedimentary structures suggest bottom-currents with fluctuating intensities, that result in laminations and internal structures forming during peak current velocities (Lucchi and Rebesco, 2007; Martín-Chivelet et al. 2008; Rebesco et al., 2014). Laminated, fossil-barren, glaciogenic deposits, consistent with those of Facies F1, have been observed on younger sedimentary sections in glaciated ~~from other~~ polar margins and interpreted as contour current modified turbidite deposits and as muddy contourites (Anderson et al., 1979; Mackensen et al., 1989; Grobe and Mackensen, 1992; Pudsey, 1992; Gilbert et al., 1998; Pudsey and Howe, 1998; Pudsey and Camerlenghi, 1998; Anderson, 1999; Williams and

555 Handwerger, 2005; Lucchi and Rebesco, 2007, Escutia et al., 2009). This particular type of glaciogenic
contourite facies is associated with glaciomarine deposition during glacial-times of glacial advance, and
has been interpreted to result from unusual, climate-related, environmental conditions of suppressed
primary productivity and oxygen-poor deep-waters (Lucchi and Rebesco, 2007).

560 Bioturbated sediments in F2 were previously interpreted as interglacial hemipelagic deposits (Escutia et
al., 2011). In this study, we interpret F2 as hemipelagic and overbank deposits reworked by bottom-
currents. The coarser grain-size in F2 compared to F1 (silty-clay matrix as seen in HR-SEM Fig. 3g-j),
the distribution of heavy minerals as indicated by the Zr/Ba, and the elevated values of the magnetic
susceptibility record with a bigradational pattern within the facies (Figs. 2,4), support the notion that
565 interglacial sediments of F2 have been heavily modified by bottom currents. Hemipelagic sediments are
expected to be homogeneous in terms of grain-size and grading is not expected. Current winnowing of
hemipelagic deposits and removal of the fine-grained fraction can produce the higher accumulation of
heavy (indicated by the Zr) and ferromagnetic (indicated by MS) minerals observed in F2 compared to
F1 (Fig. 2; Table 2). High MS values result from stronger bottom currents deposition and/or increased
570 terrigenous input (e.g., Pudsey et al., 2000; Hepp et al., 2007). Also, bi-gradational trends have been
previously described in contourite sediments and interpreted to record an increase followed by a
decrease in the current velocities (e.g., Martín-Chivelet et al., 2008). The bi-gradational patterns in the
Zr/Ba and MS plots (Figs. 2,4) are therefore interpreted to depict a constant and smooth increase
followed by a decrease in current velocity with little gradual changes in flow strength. In addition, the
575 presence of grains of quartz with conchoidal fractures and reworked coccolitospheres with signs of
dissolution (Fig., 3h,j) support the reworking of background hemipelagic and turbidite overbank
sediments by bottom currents in a high-energy environment (Damiani et al., 2006). Following the
classification by Stow and Faugères (2008), we interpret that F2 has more silty massive contourites
resulting from higher and more constant bottom current velocity compared to F1.

580 Transitions between the F1 and F2 facies are characterized by glacial-to-interglacial contacts that may
be sharp or diffuse due to bioturbation, and characterized by a gradual change in physical and
geochemical sediment parameters (Figs., 3, 4; Table 3). Interglacial-to-glacial contacts (F2 to F1), on
the other hand, are characterized by an apparently non-erosional sharp lithological boundary. The sharp
585 lithological boundaries between interglacial to glacial transitions can be explained by maximum current
intensities achieved at the end of the interglacials (Shanmugam, 2008; Rebesco et al., 2014).

4.2. Ice sheet configuration during the warm late Oligocene

590 Early Oligocene ~~and post-Oligocene~~ Mid Miocene climate transition sediments from Site U1356 contain ~~granule and larger outsized~~-clasts (>2mm) interpreted as ice rafted debris (IRD₂) (Escutia et al., 2011; Sangiorgi et al., 2018; Fig. S1). In addition, dinocyst assemblages indicate the presence of sea ice (Houben et al., 2013). Based on this, ~~the site should have been one could expect the site to be~~ within the reach of icebergs calving from an expanded ice sheet grounded at the coast or beyond in the late Oligocene. This is supported by Pliocene-Pleistocene sedimentary sections in adjacent continental rise sites containing IRD (Escutia et al., 2011; Patterson et al., 2014). ~~In addition to the paucity of IRD in our studied interval, - Thus, the lack of IRD in our studied interval is taken to indicate the relative absence of marine terminating ice sheets at the nearby margin.~~

600 ~~The interpretation of smaller ice sheets and partly ice-free margins is in agreement with~~ the absence of sea ice-loving species *Selenopemphix antarctica* and common to abundant gonyaulacoid phototrophic dinocysts, ~~which~~ suggest warm-temperate surface waters (Bijl et al., submitted, this volume). ~~A sea ice-free scenario during the late Oligocene~~ Overall is also supported by elevated sea surface temperatures (i.e., ~~average summer temperatures are ~19°C~~ 10–15 °C) based on biomarker sea surface temperatures (TEX₈₆ data in Hartman et al., submitted, this volume) ~~support a sea ice free scenario during the late~~ Oligocene. Furthermore, the presence of *in situ* terrestrial palynomorphs suggests that during the late Oligocene margins nearby were in part free of ice sheets and covered by a cool-temperate vegetation with trees and shrubs (Salzmann et al., 2016, Strother et al., 2017). ~~All these observations, suggest a reduced ice sheet and partly ice-free margins in the Wilkes margin during the late Oligocene.~~

610 These observations are consistent with the iceberg survivability modelling in the Southern Ocean ~~during~~ for the warm Pliocene intervals, which shows the distance that icebergs could travel before melting was significantly reduced (Cook et al., 2014). Warm Pliocene ~~seasonal~~-summer sea surface temperatures up to 6°C warmer than today during interglacials and prolonged Pliocene warm intervals have been reported in the Ross Sea (e.g., Naish et al., 2009; McKay et al., 2012) and other locations around Antarctica (Whitehead and Bohaty, 2003; Whitehead et al., 2005; Escutia et al., 2009; Bart and Iwai, 615 2012). Contrary to what we observe in our late Oligocene record ~~and in the Miocene Climatic Optimum (Sangiorgi et al., 2018), during the warm Pliocene~~ abundant IRD were delivered to ~~adjacent~~ continental rise sites ~~adjacent to Site U1356 during the warm Pliocene~~ (Escutia et al., 2011; Patterson et al., 2014). This was interpreted by Cook et al. (2017) to suggest that a considerable number of icebergs (iceberg 620 armadas) had to be produced in order to reach the site under these warm Pliocene conditions. We argue that the lack of IRD delivery to site U1356 during the ~~studied warm~~ late Oligocene interval ~~can likely results result from~~ the different ~~Wilkes Subglacial Basin (WSB) late Oligocene~~ paleotopographic

625 setting. ~~between the Oligocene and compared to the Pliocene.~~ Paleotopographic reconstructions from 34
Ma ago (Wilson et al., 2012) and the early Miocene (Gasson et al., 2016), show the ~~Wilkes Subglacial~~
~~Basin (WSB)~~ to be an area of lowlands and shallow seas in contrast to the over-deepened marine basin
that it is today (Fretwell et al., 2013). ~~This paleotopographic configuration would have precluded~~
~~widespread marine ice sheet instability- during the Oligocene.~~ This difference is important, as an ice
sheet grounded on an overdeepened continental shelf can experience marine ice sheet instability, a
runaway process relating to ice sheet retreat across a reverse slope continental shelf (Weertman 1974),
630 which is proposed to be a driver for ~~Pliocene collapse-retreat~~ of ~~the EAIS in~~ the WSB ~~during the warm~~
~~Pliocene~~ (Cook et al., 2013). ~~This paleotopographic configuration would have precluded widespread~~
~~marine ice sheet instability during the Oligocene.~~ Conversely, a shallower continental shelf allows for
the potential expansion of grounded ice sheets into the marine margin during warmer-than-present
climates (Wilson et al. 2012), and thus direct records are required to assess the climate threshold for
635 such an advance.

~~Thus, the lack of IRD in our studied interval is taken to indicate the relative absence of marine-~~
~~terminating ice sheets at the nearby margin.~~

In ~~contrast-comparison~~ to the distal U1356 Wilkes Land margin record, the Ross Sea Embayment ice
640 proximal sediments obtained by the Cape Roberts Project (CRP) contain Oligocene to Early Miocene
palynomorphs, foraminifera and clay assemblages that point to a progressive decrease in fresh
meltwater, cooling and intensifying glacial conditions (Leckie and Webb, 1983; Hannah et al., 2000;
2001; Raine and Askin, 2001; Thorn, 2001; Ehrmann et al., 2005; Barrett, 2007). Therefore, the coastal
CRP sediment record does not support a significant loss of ice or warming during the late Oligocene
645 (Barrett, 2007), ~~as has been suggested by compilations of deep-sea benthic $\delta^{18}\text{O}$ data (Zachos et al.,~~
~~2001).~~ ~~The high sedimentation rates during the late Oligocene-early Miocene recorded at Deep Sea~~
~~Drilling Project (DSDP) Site 270 were interpreted to reflect turbid plumes of glaciomarine sediments~~
~~derived from polythermal-style glaciers or ice sheets that were calving into an open Ross Sea, without~~
~~an ice shelf (Kemp and Barrett, 1975).~~ In addition, seismic data indicate that during the late-mid
650 ~~Oligocene widespread expansion of a marine-based ice sheet onto the outer Ross Sea shelf did not take~~
~~place but instead glaciers and ice caps drained from local highs and advanced only into shallow marine~~
~~areas, rather than whole-scale marine ice sheet advance (Brancolini et al., 1995; De Santis et al., 1995;~~
~~Bart and De Santis, 2012).~~

Moreover, ~~sediments recovered at Deep Sea Drilling Project (DSDP) Site 270 on the mid-continental~~
655 ~~shelf of the Ross Sea contain IRD and pollen assemblages that provide evidence for the coexistence of~~
~~ice masses and vegetation through the Oligocene (Kemp and Barrett, 1975).~~ ~~The high sedimentation~~
~~rates during the late Oligocene-early Miocene at Site 270 were interpreted to reflect turbid plumes of~~
~~glaciomarine sediments derived from polythermal style glaciers or ice sheets that were calving into an~~

660 ~~open Ross Sea, without an ice shelf (Kemp and Barrett, 1975). In addition, seismic data indicate that during the late mid Oligocene widespread expansion of a marine based ice sheet onto the outer Ross Sea shelf did not take place but instead glaciers and ice caps drained from local highs and advanced only into shallow marine areas, rather than whole scale marine ice sheet advance (Draneolini et al., 1995; DeSantis et al., 1995; Bart and De Santis, 2012).~~

665 Combined, ~~this~~ these evidences suggest that during the late Oligocene marine-terminating glaciers, ice caps ~~or ice sheets~~ and glaciers persisted along the Transantarctic Mountain front ~~in the~~ reaching the Ross Sea coastal areas, but ~~not in~~ may have been more confined within a warmer the eastern Wilkes Land WSB margin. ~~This suggests an ice sheet with a similar configuration as modelled for Miocene topographies with CO₂ scenarios of 500-840 ppm (Gasson et al., 2016) (Fig. 7).~~ This is also supported by vegetation reconstructions derived from fossil pollen from both margins, which indicate for the middle Miocene and Late Oligocene higher terrestrial temperatures and more tree taxa at Wilkes Land (Salzmann et al., 2016; Sangiorgi et al., 2018) than the Ross Sea (Askin and Raine, 2000; Prebble et al., 2006). This is consistent with the ice sheet modelled configuration for Miocene topographies with CO₂ scenarios of 500-840 ppm (Gasson et al., 2016; Levy et al 2016; Fig. 7).

4.3 Paleocceanographic implications

680 Sediment physical properties and geochemical signatures of F1 and F2 are here related to changes in bottom water-sediment interphase oxygenation/ventilation during successive glacial and interglacial periods (Table 2). ~~These changes~~ We hypothesize ~~interpret that these changes~~ are linked to shifts in water-masses driven by a north-south displacement of the position of the westerlies, and associated changes in the intensity of frontal mixing or location of the Polar Front and Antarctic Divergence (Fig. 7). Based on ~~these~~ our observations, we propose a model to explain the interpreted changes in bottom-water conditions at Site U1356 during successive glacial and interglacial times (Fig. 7).

4.3.1. Glacial paleocceanographic configuration

690 The *Chondrites*-like bioturbation with pyrite infilling the tubes of *Skolithos* within F1 (Fig. 3b, d) has previously been reported to characterize low-oxygen conditions at the water-sediment interphase (Bromley and Ekdale, 1984). In addition, pyritized diatoms are present throughout the Oligocene section of this site, but are found preferentially inside F1. The presence of pyritized diatoms was interpreted during Expedition 318 to indicate a prolific production and syn-sedimentary diagenesis in a restricted circulation (low oxygen) environment, mainly during glacial periods (Escutia et al., 2011).

Reducing conditions in the sediment also help to preserve primary sedimentary structures of the silt layers in F1 because bioturbation is limited. Higher amounts of organic matter in F1 compared to F2 are suggested by increased values of the Br/Ti ratio (Fig. 2). ~~This-The~~ higher organic content most likely ~~results-produces from oxygen depletion in the water-sediment interphase, which creates~~ a poorly ventilated environment with near reducing conditions at the water-sediment interphase, where pyrite ~~has been able to~~ can precipitate (Tribovillard et al., 2006). In spite of this, ~~no~~ total oxygen depletion did not is observed, and is occurs as indicated supported by ~~the~~ palynomorphs good preservation ~~inside-within~~ F1 (Bijl et al., submitted, this volume).

~~In our record, low MS values are found in F1 (Fig.4; Table 2).~~ Low MS values such as those recorded within F1 (Fig.4; Table 2) ~~around Antarctica~~ have been reported around Antarctica and attributed to MS magnetic minerals dissolution caused by dilution and/or primary diagenesis effects on the sediments due to the higher concentration in organic matter or to changing redox conditions (Korff et al., 2016). Several authors have postulated that oxygen-depleted Antarctic Bottom Water (AABW) occupying the abyssal zones of the oceans can change the redox conditions in the sediment, trapping and preserving dissolved and particulate organic matter and, consequently reducing and dissolving both, biogenic and detrital magnetite (Florindo et al., 2003; Hepp et al., 2009; Korff et al., 2016). At present, Site U1356 is influenced by AABW forming in the adjacent Wilkes Land shelf (Orsi et al., 1999; Fukamachi et al., 2000) and in the Ross Sea spilling over to the Wilkes Land continental shelf (Fukamachi et al., 2010) (Fig. 1). Our records ~~indicate-suggest~~ a reduced continental ice-sheet in the eastern Wilkes Land margin ~~, likely not reaching the coastline,~~ and reduced sea ice presence compared to today (Bijl et al., submitted, this volume). Under these conditions, bottom water formation and downwelling can still occur (with or without presence of sea ice) as a result of density contrasts related to seasonal changes in surface water temperature and salinity (Huber and Sloan, 2001; Otto-Bliesner et al., 2002). Moreover, stable Nd isotopic composition in Eocene-Oligocene sediments from Site U1356 is consistent with modern day formation of bottom water from Adélie Land, as reported by Huck et al (2017).

Our evidence above points to deposition of F1 during glacial cycles under poorly-ventilated, low-oxygenation conditions at the water-sediment interface (Fig. 7a). We postulate, that during glacial periods, westerly winds and surface oceanic fronts migrate towards the equator, generating a more stratified ocean and reduced upwelling closer to the margin, with sporadic and fluctuating currents (Fig. 7a). Records of the Last Glacial Maximum show that this northward migration results in a weakening of the upwelling of the Circumpolar Deep Water (CDW) (Govin et al., 2009), increasing stratification and reduced mixing of water masses also due to an enhanced sea ice formation, not seen during the late Oligocene.

4.3.2. Interglacial paleoceanographic configurations

730 ~~We differentiate two different interglacial paleoceanographic configurations based on the presence of~~
~~some intervals of micritic limestone with calcareous nannofossils.~~

~~The~~ ~~In general, the~~ higher degree of bioturbation in F2 with no primary structures preserved and the
735 ichnofacies association (i.e., *Planolites* and *Zoophycos*), suggest a more oxygenated environment in
comparison with F1. This is supported by the covariance of Mn and CaCO₃ est. (Fig 4) where Mn
enrichments ~~can be interpreted as redox changes variations indicate the redox state conditions at the~~
~~sediment-water interface~~ (Calvert and Pedersen, 2007; Jaccard et al., 2016). More oxygenated
conditions during interglacial periods can be achieved under a more ventilated and mixed water masses,
with enhanced current velocities. ~~Enhanced currents are interpreted during deposition of~~ ~~We interpret~~
740 ~~that~~ ~~F2 are interpreted had enhanced current velocities~~ based on coarser grain size, and the increased
accumulation of heavy and ferromagnetic minerals as indicated by the high values of the Zr/Ti ratio and
MS within F2 (Figs. 2,4). The bigradational pattern of the Zr/Ba and the MS (Fig. 4) is also interpreted
to record an increase followed by a decrease in current velocities within F2. ~~The intervals of micritic~~
~~limestone within F2 have calcareous nannofossils preserved (Fig 3d). The productivity of calcareous~~
745 ~~nannofossils and the later preservation of these coccoliths in the sediment indicate specific geochemical~~
~~conditions enabling carbonate deposition and preservation. Although today nannoplankton is abundant~~
~~in surface waters at the Antarctic Divergence (Eynaud et al., 1999), these rarely deposit on the deep~~
~~ocean floor because of corrosive bottom waters, which dissolve calcareous rain. A number of studies in~~
~~other areas of the Antarctic margin have correlated the presence of calcareous nannofossils during the~~
750 ~~Oligocene with the presence of temperate north component water masses (NADW like) that intrude~~
~~close to the Antarctic continent and influences the Southern Ocean during the late Oligocene (e.g.,~~
~~Nelson & and Cook, 2001; Pekar et al., 2006; Villa and Persico, 2006; Scher and Martin, 2008) and~~
~~during more recent times such as the Quaternary (Diekman, 2007, Villa et al., 2012 Kemp et al., 2010;~~
~~DeCesare et al., 2013).~~ In addition, Pleistocene sedimentary records of past warm interglacial events in
755 ~~Antarctica also have reported enhanced NADW production (e.g. interglacial event MIS11 from M. S.~~
~~Poli et al., 2000, Kemp et al., 2010; DeCesare et al., 2013).~~

~~During interglacials, our records point to more oxygenated and ventilated conditions suggesting~~
~~enhanced mixing of the water masses (Fig. 7b-c). We postulate that during interglacials westerly winds~~
760 ~~and the Polar Front are shifted south and become more aligned. Under these conditions, upwelling of~~
~~deep waters is promoted, facilitating the mixing and oxygenation of surface waters that form the~~
~~precursor to bottom water. Such a process would also generate increased geostrophic current velocities~~

~~of bottom water mass as evinced by the coarser grain size and heavy mineral concentrations in the bioturbated F2 facies.~~

765 The intervals of micritic limestone within F2 have calcareous nannofossils preserved (Fig 3d). The productivity of calcareous nannofossils and the later preservation of these coccoliths in the sediment indicate specific geochemical conditions enabling carbonate deposition and preservation. Although today nannoplankton is abundant in surface waters at the Antarctic Divergence (Eynaud et al., 1999), these rarely deposit on the deep ocean floor because of corrosive bottom waters, which dissolve calcareous rain. A number of studies in other areas of the Antarctic margin and the Southern Ocean have correlated the presence of calcareous nannofossils with the presence of temperate north component water masses (North Atlantic Deep Water-like, NADW) that intrude close to the Antarctic continent and influence the Southern Ocean during the late Oligocene (e.g., Nelson and Cooke, 2001; Pekar et al., 2006; Villa and Persico, 2006; Scher and Martin, 2008), the Miocene (DeCesare et al., 2013; Sangiorgi et al., 2018), and during more recent times such as the Quaternary (Diekman, 2007; Kemp et al., 2010; Villa et al., 2012).

780 The more oxygenated and ventilated conditions in our records suggests enhanced mixing of the water masses (Fig. 7b-c). We postulate that during interglacials westerly winds and the Polar Front are shifted south and become more aligned. Under these conditions, upwelling of deep waters is likely promoted, facilitating the mixing and oxygenation of surface waters that form the precursor to bottom water. Similar process has been reported for the Holocene by Peck et al. (2015). Such a process would also generate increased geostrophic current velocities of the bottom water mass, supported by the coarser grain size and heavy mineral concentrations in the bioturbated F2 facies.

785 Similar to what is occurring under the present warming, bottom water formation during interglacials is likely fresher and less dense due to enhanced freshwater runoff from surface and subglacial melt of the continental ice sheet (Wijk and Rintoul, 2014). Today, a reduction in the volume of the AABW is compensated by the expansion of the Circumpolar Deep Water (CDW) (Wijk and Rintoul, 2014), which forms by mixing of abyssal, deep, and intermediate water masses, including the AABW and the NADW (Johnson, 2008). During interglacials, bottom water formation is likely warmer and less saline due to enhanced freshwater runoff from surface and subglacial melt of the continental ice sheet. This may allow this less dense water mass to occupy shallower depths in abyssal to intermediate ocean, and promote more vigorous mixing with oxygenated CDW (Fig. 7b). Circumpolar Deep Water (CDW) is a mixing of abyssal, deep, and intermediate water masses, that includes AABW and NADW nowadays (Johnson, 2008). We hypothesize, that during -warmer interglacials, the influence of more northern-sourced water masses into the proto-CDW, relative to Antarctic-sourced (Fig. 7c), could enable carbonate productivity and preservation of as seen in the interglacial facies with coccolithosphere

800 remains, seen at least 13 occasions in our record. (Fig. 7e). These data are also in agreement with the $\delta^{13}\text{C}$ global isotopes oscillations between 26 and 25 Ma (Cramer et al., 2009; Liebrand et al., 2017), that suggest low values for an AABW and high $\delta^{13}\text{C}$ values for a NADW, that may represent the different oceanic primary production and ventilation rates, as proposed in this work. In addition, $\delta^{13}\text{C}$ records in the Atlantic show systematic offsets to lower values toward a North Atlantic signal for most of the late Oligocene to early Miocene. These data suggest the influence of two distinct deep-water sources: cooler southern component water and warmer northern component water (Billups et al., 2002; Pekar et al., 2006; Liebrand et al., 2011). In addition, the increased presence of North Component Deep waters influencing this sector of the eastern Wilkes Land margin could be related with a slowdown of the southern limb of the overturning circulation.

810 This is also reinforced by several interpretations that document a late Oligocene increase in the influence of North Component Water (e.g. NADW-like) in the Southern Ocean (Billups et al., 2002; Pekar et al., 2006; Villa and Persico, 2006; Scher and Martin, 2008; Liebrand et al., 2011).

815 ~~These data are also in agreement with the $\delta^{13}\text{C}$ global isotopes oscillations between 26 and 25 Ma (Cramer et al., 2009), that suggest low values for an AABW and high $\delta^{13}\text{C}$ values for a NADW, that may represent the different oceanic primary production and ventilation rates, as proposed in this work. In addition, $\delta^{13}\text{C}$ records on the Atlantic show systematic offsets to lower values toward a North Atlantic signal for most of the late Oligocene to early Miocene. These data suggest the influence of two distinct deep-water sources: cooler southern component water and warmer northern component water (Billups et al., 2002; Pekar et al., 2006; Liebrand et al., 2011). The observed preserved coccolithospheres in the carbonate rich facies suggest an increased influence of warmer northern component waters to the proto-CDW over the site at least in 13 occasions between 26 and 25 Ma.~~

4.4 Orbital forcing and Glacial and Interglacial cyclicity

825 The first spectral analysis on late Oligocene sediments from the eastern Wilkes Land margin at Site U1356 shows that glacial-interglacial cycles, resulting in changes in the oceanic configuration off Wilkes Land, are paced with variations in Earth's orbit and seasonal insolation. Although the data is somewhat ~~noisy-discontinuous~~ due to gaps in our record, it clearly shows that the glacial-interglacial cyclicity (every 2 m or 41 kyr) discussed above has a persistent obliquity pacing throughout the studied late Oligocene interval (26-25 Ma) in the Wilkes Land. Consequently, this obliquity-paced cyclicity modulates the amount of deep-water production in the Southern Ocean, and exerts a major control on oceanic configuration and current strength. Bottom current velocity fluctuations and ventilation of

bottom sediments respond to the forcings applied by the strength of the Southern Hemisphere westerlies, the position of the PF respect to the site, and consequently by the water mass occupying the bottom of the basin at each time. In addition to obliquity, ~~our record captures de precession frequencies, suggesting a late Oligocene dynamic ice sheet.~~ precession is also present, which implies a dynamic response of the EAIS and offshore oceanic water masses to orbital forcing.

East Antarctic ice volume fluctuations at orbital periodicities in the obliquity band in the Wilkes Land margin have been previously reported from early warm Pliocene (3-5 Ma) sediments obtained from Site U1361 (Patterson et al., 2014). In the Ross Sea, cyclicity in sediments collected by the CRP from the late Oligocene, the late Miocene and the early warm Pliocene period was also paced by obliquity (Naish et al., 2001; McKay et al., 2009; Naish et al., 2009). Similar orbital variability in the deep-water circulation patterns have also been inferred to have occurred with the growth of the EAIS during the middle Miocene between 15.5 to 12.5 Ma (Hall et al., 2003). In addition, other studies have linked changes in Atlantic meridional overturning (Lisiecki et al., 2008; Scher et al., 2015) and Antarctic circumpolar ocean circulation (Toggweiler et al., 2008) to obliquity forcing. An interglacial mechanism has been proposed whereby the southward expansion of westerly winds and associated Ekman transport is compensated for by enhanced upwelling of warmer, CO₂-rich CDW (Toggweiler et al., 2008), which also promotes atmospheric warming. In the equatorial Pacific, Pälike et al. (2006) also report strong obliquity in the benthic $\delta^{13}\text{C}$ isotopic record between 26-25 Myr, implying that changes in the carbon cycle (pacing glacial /interglacial periods) are triggered in the high southern latitudes and transferred to the global deep-ocean through the bottom water masses.

5. Conclusions

Our study provides new insights regarding Antarctic ice sheet and paleoceanographic configurations that prevailed in the eastern Wilkes Land margin between 26 and 25 Ma. Sediments at IODP Site U1356 during this interval are characterized by the alternation between two main facies (F1 and F2), that are dominated by reworking by bottom-currents with varying intensities of glacial-interglacial gravity flows and hemipelagic deposits ~~by bottom-currents with varying intensities~~. Claystones with silty laminations (F1) are interpreted to represent fluctuating bottom current intensities during glacial periods. Massive bioturbated silty clays and micritic limestones with coccoliths (F2) are interpreted as interglacial deposits and record maximum velocities of bottom-currents at this site. The lack of iceberg rafted debris (IRD), ~~the absence of and sea ice, and warm sea surface temperatures~~ elevated sea surface temperatures -indicators throughout the studied interval, and reconstructions derived from fossil pollen in Site U1356 suggesting high terrestrial temperatures of cool-temperate vegetation suggest ~~contrasts with early Oligocene and younger sections from Site U1356 and with late Oligocene sediments from the~~

~~Ross Sea (CRP and DSDP 270), which contain IRD and evidence for sea ice and ice at or near the coast. Based on these observations, we postulate that reduced glaciers or ice caps occupied the topographic highs and lowlands of the now overdeepened Wilkes Subglacial Basin between 26 and 25~~
870 ~~Ma and that iceberg calving was only a background process during this time due to the lack of marine terminating ice sheets and open water conditions prevailed, with ablation of the ice sheet was largely controlled by melt processes rather than iceberg calving.~~

875 Glacial sediments record poorly ventilated, low-oxygenation conditions at the water-sediment interface that we postulate result when westerly winds and surface oceanic fronts migrate towards the equator and overturning ~~was is~~ reduced near the Antarctic margin. During interglacial times, more oxygenated and better ~~_~~ventilated conditions are inferred to have prevailed which would act to enhance mixing of the water masses with increased current velocities. We postulate that during interglacials, westerly
880 winds shifted south and became more aligned with the Antarctic Divergence and Polar Fronts, which promoted upwelling of deep waters and facilitated the mixing and oxygenation of bottom waters. Micritic limestone intervals within interglacial F2, record warmer paleoclimatic conditions when ~~a the~~ influence of more northern-sourced water masses into the proto-CDW, relative to Antarctic-sourced (Fig. 7c), could enable carbonate productivity and preservation of ~~with~~ coccolithosphere remains. ~~greater~~
885 ~~relative proportion of warm north component waters reached the site allowing the preservation of carbonate.~~ Preservation of carbonate in some F2 intervals supports previous paleoceanographic studies that consider at least a two-layer ocean with an Antarctic Bottom Water (undersaturated with respect to calcium carbonate), and a proto-CDW with influences of a greater influence of warmer Northern Component Water mass (NADW-like) to reconcile intra-~~_~~basinal differences in $\delta^{18}\text{O}$ values (Pekar et
890 al., 2006). Based on the number of carbonate-rich layers, warmer NADW-like waters reached the site at least 13 times during the studied interval.

Spectral analysis on late Oligocene sediments from the eastern Wilkes Land margin reveal that glacial-interglacial paleoceanographic changes during the late Oligocene are regulated primarily by obliquity,
895 although frequencies in the eccentricity and precession band are also recorded. However, as we do not have a measure of ice dynamics during this time (e.g. ice rafted debris), the orbital response of terrestrial ice in the Wilkes Land Basin remains ambiguous, beyond what is inferred from the deep-sea isotope record.

900 ~~Our record shows that during under the high CO₂ values of the late Oligocene (i.e., from ~750 ppm to 400 ppm), ice sheets had retreated to their terrestrial margins, with ice sheet mass loss dominated by surface melt processes. It also indicates a slowdown of the southern limb of overturning circulation,~~

~~with the increased presence of North Component Deep waters influencing the preservation of carbonate in this sector of the eastern Wilkes Land margin.~~

905

Acknowledgements

This research used samples and data provided by the Integrated Ocean Drilling Program, ~~now the International Ocean Discovery Program (IODP)~~(IODP). ~~The IODP is sponsored by the US National Science Foundation (NSF) and participating countries under the management of Joint Oceanographic Institutions, Inc. Funding for this research is provided by the Spanish Ministerio de Economía y Competitividad (Grant CTM 2011-24079 and CTM2014-60451-C2-1-P) co-funded by the European Union through FEDER funds and the Deutsche Forschungsgemeinschaft (DFG) (RO 1113/6 to UR).~~ We thank the staff onboard IODP Exp. 318; ~~and at the Gulf Coast, the Bremen and the Kochi IODP Core Repositories CR and BCR~~ for assistance in core ~~handling and shipping~~~~and handling~~, ~~and~~. We thank Vera Lukies (MARUM) for technical support with XRF core scanning ~~and Shizu Yanagimoto (KOCHI) for technical support with CT-scans.~~ We also thank the constructive ~~comments of an anonymous reviewer and Dr. Steven Pekar that have helped to improve this manuscript.~~ Funding for this ~~research is provided by the Spanish Ministerio de Economía y Competitividad (Grants CTM 2011-24079 and CTM2014-60451-C2-1-P) co-funded by the European Union through FEDER funds. UR thanks —and—the Deutsche Forschungsgemeinschaft (DFG) (RO 1113/6 to UR).~~ PKB, FS and JDH acknowledges funding through NWO polar programme grant no 866.10.110; PKB acknowledges funding through NWO-VENI grant no 863.13.002. US acknowledges funding received from the Natural Environment Research Council (NERC grant NE/H000984/1).

910

915

920

Author contributions

CE and AS designed the research. PKB, JH, FS and HB, provided insights regarding biomarker-based sea surface temperatures and sea ice conditions based on dinocysts. UR provided XRF core-scanning data. FJJE and UR provided geochemical input. CHN and RM provided input with sedimentary and facies interpretations. MI provided the CT-Scans data. JAF provided input in the paleoceanographic interpretations. DE and ALQ provided Antarctic overview and petrographic input. SR and US provided palynology insights. AS and CE wrote the paper with input from all co-authors.

925

930

6. References

- Abrahamsen, E.P., Meredith, M.P., Falkner, K.K., Torres-Valdes, S., Leng, M.J., Alkire, M.B., Bacon, S., Laxon, S.W., Polyakov, I., Ivanov, V., 2009. Tracer-derived freshwater composition of the Siberian continental shelf and slope following the extreme Arctic summer of 2007. *Geophys. Res. Lett.* 36, 5.
- Agnihotri, R., Altabet, M.A., Herbert, T.D., Tierney, J.E., 2008. Subdecadally resolved paleoceanography of the Peru margin during the last two millennia. *Geochemistry, Geophys. Geosystems* 9.
- Anderson, J., 1999. *Antarctic marine geology*. Cambridge University Press.
- Anderson, J., Kurtz, D., Weaver, F., 1979. Sedimentation on the Antarctic continental slope. *SEPM Spec. Publ.* 27, 265–283.

935

940

- Askin, R.A., Raine, J.I., 2000. Oligocene and Early Miocene Terrestrial Palynology of the Cape Roberts Drillhole CRP-2/2A, Victoria Land Basin, Antarctica. *Terra Antarct.* 7, 493–501.
- Bahr, A., Jiménez-Espejo, F.J., Kolasinac, N., Grunert, P., Hernández-Molina, F.J., Röhl, U., Voelker, A.H.L., Escutia, C., Stow, D.A. V., Hodell, D., Alvarez-Zarikian, C.A., 2014. Deciphering bottom current velocity and paleoclimate signals from contourite deposits in the Gulf of Cádiz during the last 140 kyr: An inorganic geochemical approach. *Geochemistry, Geophys. Geosystems* 15, 3145–3160.
- Barrett, P.J., 2007. Cenozoic Climate and Sea Level History from Glacimarine Strata off the Victoria Land Coast, Cape Roberts Project, Antarctica, in: *Glacial Sedimentary Processes and Products*. pp. 259–287.
- Bart, P.J., Iwai, M., 2012. The overdeepening hypothesis: How erosional modification of the marine-scape during the early Pliocene altered glacial dynamics on the Antarctic Peninsula's Pacific margin. *Palaeogeogr. Palaeoclimatol. Palaeoecol.* 335–336, 42–51.
- Bart, P., De Santis, L., 2012. Glacial Intensification During the Neogene: A Review of Seismic Stratigraphic Evidence from the Ross Sea, Antarctica, Continental Shelf. *Oceanography* 25, 166–183.
- Beerling, D.J., Royer, D.L., 2011. Convergent Cenozoic CO₂ history. *Nat. Geosci.* 4, 418–420.
- 945 Bijl, P.K., Houben, A.J.P., Bruls, A., Pross, J., Sangiorgi, F., 2018. Stratigraphic calibration of Oligocene–Miocene organic-walled dinoflagellate cysts from offshore Wilkes Land, East Antarctica, and a zonation proposal. *J. Micropalaeontology* 37, 105–138.
- Billups, K., Channell, J.E.T., Zachos, J., 2002. Late Oligocene to early Miocene geochronology and paleoceanography from the subantarctic South Atlantic. *Paleoceanography* 17, 4-1-4–11.
- 960 Billups, K., Schrag, D.P., 2003. Application of benthic foraminiferal Mg/Ca ratios to questions of Cenozoic climate change. *Earth Planet. Sci. Lett.* 209, 181–195.
- Bindoff, N.L., Rosenberg, M. a., Warner, M.J., 2000. On the circulation and water masses over the Antarctic continental slope and rise between 80 and 150°E. *Deep Sea Res. Part II Top. Stud. Oceanogr.* 47, 2299–2326.
- 965 Bohaty, S.M., Harwood, D.M., 1998. Southern Ocean pliocene paleotemperature variation from high-resolution silicoflagellate biostratigraphy. *Mar. Micropaleontol.* 33, 241–272.
- Brancolini, G., Cooper, A.K., Coren, F., 1995. Seismic Facies and Glacial History in the Western Ross Sea (Antarctica). *Geol. Seism. Stratigr. Antarct. Margin, AGU Antarct. Res. Ser.* 68, 209–233.
- Bromley, R.G., Ekdale, A.A., 1984. Chondrites: a trace fossil indicator of anoxia in sediments. *Science (80-)*. 224, 872–875.
- 970 Buseti, M., Caburlotto, a., Armand, L., Damiani, D., Giorgetti, G., Lucchi, R.G., Quilty, P.G., Villa, G., 2003. Plio-Quaternary sedimentation on the Wilkes land continental rise: preliminary results. *Deep Sea Res. Part II Top. Stud. Oceanogr.* 50, 1529–1562.
- Calvert, S.E., Pedersen, T.F., 1996. Sedimentary geochemistry of manganese; implications for the environment of formation of manganiferous black shales. *Econ. Geol.* 91.
- 975 Calvert, S.E., Pedersen, T.F., 2007. Chapter Fourteen Elemental Proxies for Palaeoclimatic and Palaeoceanographic Variability in Marine Sediments: Interpretation and Application, in: *Developments in Marine Geology*. pp. 567–644.
- Campagne, P., Crosta, X., Houssais, M.N., Swingedouw, D., Schmidt, S., Martin, A., Devred, E., Capo, S., Marieu, V., Closset, I., Massé, G., 2015. Glacial ice and atmospheric forcing on the Mertz Glacier Polynya over the past 250 years. *Nat. Commun.* 6, 6642.
- 980 Cook, C.P., Hemming, S.R., van de Fliertdt, T., Pierce Davis, E.L., Williams, T., Galindo, A.L., Jiménez-Espejo, F.J., Escutia, C., 2017. Glacial erosion of East Antarctica in the Pliocene: A comparative study of multiple marine sediment provenance tracers. *Chem. Geol.* 466, 199–218.
- 985 Cook, C.P., Hill, D.J., van de Fliertdt, T., Williams, T., Hemming, S.R., Dolan, A.M., Pierce, E.L., Escutia, C., Harwood, D., Cortese, G., Gonzales, J.J., 2014. Sea surface temperature control on the distribution of far-traveled Southern Ocean ice-rafted detritus during the Pliocene. *Paleoceanography* 29, 533–548.
- Cook, C.P., van de Fliertdt, T., Williams, T., Hemming, S.R., Iwai, M., Kobayashi, M., Jimenez-Espejo, F.J., Escutia, C., González, J.J., Khim, B.-K., McKay, R.M., Passchier, S., Bohaty, S.M., Riesselman, C.R., Tauxe, L., Sugisaki, S., Galindo, A.L., Patterson, M.O., Sangiorgi, F., Pierce, E.L., Brinkhuis, H., Klaus, A., Fehr, A., Bendle, J. a. P., Bijl, P.K., Carr, S. a., Dunbar, R.B., Flores, J.A., Hayden, T.G., Katsuki, K., Kong, G.S., Nakai, M., Olney, M.P., Pekar, S.F., Pross, J., Röhl, U., Sakai, T., Shrivastava, P.K., Stickley, C.E., Tuo, S., Welsh, K., Yamane, M., 2013. Dynamic behaviour of the East Antarctic ice sheet during Pliocene warmth. *Nat. Geosci.* 6, 765–769.
- 990 Coxall, H.K., Wilson, P.A., Pälike, H., Lear, C.H., Backman, J., 2005. Rapid stepwise onset of Antarctic glaciation and deeper calcite compensation in the Pacific Ocean. *Nature* 433, 53–57.
- Cramer, B.S., Toggweiler, J.R., Wright, J.D., Katz, M.E., Miller, K.G., 2009. Ocean overturning since the Late Cretaceous: Inferences from a new benthic foraminiferal isotope compilation. *Paleoceanography* 24.

- 000 Croudace, I.W., Rindby, A., Rothwell, R.G., 2006. ITRAX: description and evaluation of a new multi-function X-ray core scanner. *Geol. Soc. London, Spec. Publ.* 267.
- Damiani, D., Giorgetti, G., Turbanti, I.M., 2006. Clay mineral fluctuations and surface textural analysis of quartz grains in Pliocene–Quaternary marine sediments from Wilkes Land continental rise (East-Antarctica): Paleoenvironmental significance. *Mar. Geol.* 226, 281–295.
- 005 De Santis, L., Anderson, J.B., Brancolini, G., Zayatz, I., 1995. Seismic Record of Late Oligocene Through Miocene Glaciation on the Central and Eastern Continental Shelf of the Ross Sea, in: *Geology and Seismic Stratigraphy of the Antarctic Margin*. Antarctic Research Series. pp. 235–260.
- DeCesare, M., Pekar, S.F., DeCesare, 2013. Investigating a Middle to Late Miocene Carbonate Preservation Event in the Southern Ocean. *Am. Geophys. Union, Fall Meet. 2013, Abstr. #PP43A-2072* 12–13.
- 010 DeConto, R.M., Pollard, D., 2016. Contribution of Antarctica to past and future sea-level rise. *Nature* 531, 591–597.
- Diekmann, B., 2007. Sedimentary patterns in the late Quaternary Southern Ocean. *Deep Sea Res. Part II Top. Stud. Oceanogr.* 54, 2350–2366.
- Duliu, O.G., 1999. Computer axial tomography in geosciences: An overview. *Earth Sci. Rev.*
- 015 Dypvik, H., Harris, N.B., 2001. Geochemical facies analysis of fine-grained siliciclastics using Th/U, Zr/Rb and (Zr + Rb)/Sr ratios. *Chem. Geol.* 181, 131–146.
- Ehrmann, W., Setti, M., Marinoni, L., 2005. Clay minerals in Cenozoic sediments off Cape Roberts (McMurdo Sound, Antarctica) reveal palaeoclimatic history. *Palaeogeogr. Palaeoclimatol.*
- Eittrheim, S.L., Cooper, A.K., Wannesson, J., 1995. Seismic stratigraphic evidence of ice-sheet advances on the Wilkes Land margin of Antarctica. *Sediment. Geol.* 96, 131–156.
- 020 Escutia, C., Eittrheim, S.L., Cooper, A.K., NELSON, C.H., 1997. Cenozoic sedimentation on the Wilkes Land continental rise, Antarctica, in: *The Antarctic Region: Geological Evolution and Processes*. Proc. Int. Symp. Antarct. Earth Sci. pp. 791–795.
- Escutia, C., Eittrheim, S.L., Cooper, a K., Nelson, C.H., 2000. Morphology and acoustic character of the antarctic Wilkes Land turbidite systems: Ice-sheet-sourced versus river-sourced fans. *J. Sediment. Res.* 70, 84–93.
- 025 Escutia, C., Bárcena, M.A., Lucchi, R.G., Romero, O., Ballegeer, A.M., Gonzalez, J.J., Harwood, D.M., 2009. Circum-Antarctic warming events between 4 and 3.5Ma recorded in marine sediments from the Prydz Bay (ODP Leg 188) and the Antarctic Peninsula (ODP Leg 178) margins. *Glob. Planet. Change* 69, 170–184.
- Escutia, C., Brinkhuis, H., Klaus, A., 2011. Site U1356, in: *Proceeding of the Integrated Ocean Drilling Program*.
- 030 Escutia, C., De Santis, L., Donda, F., Dunbar, R.B., Cooper, A.K., Brancolini, G., Eittrheim, S.L., 2005. Cenozoic ice sheet history from East Antarctic Wilkes Land continental margin sediments. *Glob. Planet. Change* 45, 51–81.
- Escutia, C., Nelson, C.H., Acton, G.D., Eittrheim, S.L., Cooper, a K., Warnke, D. a., Jaramillo, J.M., 2002. Current controlled deposition on the Wilkes Land continental rise, Antarctica. *Geol. Soc. London, Mem.* 22, 373–384.
- 035 Escutia, C., Warnke, D., Acton, G., Barcena, A., Burckle, L., Canals, M., Frazee, C., 2003. Sediment distribution and sedimentary processes across the Antarctic Wilkes Land margin during the Quaternary. *Deep Sea Res. Part II Top. Stud. Oceanogr.* 50, 1481–1508.
- Escutia, C., Brinkhuis, H., 2014. From Greenhouse to Icehouse at the Wilkes Land Antarctic Margin: IODP Expedition 318 Synthesis of Results, in: *Developments in Marine Geology*. Elsevier, pp. 295–328.
- 040 Escutia, C., Brinkhuis, H., Klaus, A., Scientists, I.E. 318, 2011. Expedition 318 summary, in: *Proceedings of the Integrated Ocean Drilling Program, Volume 318*.
- Eynaud, F., Giraudeau, J., Pichon, J.J., Pudsey, C.J., 1999. Sea-surface distribution of coccolithophores, diatoms, silicoflagellates and dinoflagellates in the South Atlantic Ocean during the late austral summer 1995. *Deep. Res. Part I Oceanogr. Res. Pap.* 46, 451–482.
- 045 Field, C.B., Barros, V.R., Dokken, D.J., Mach, K.J., Mastrandrea, M.D., Bilir, T.E., Chatterjee, M., Ebi, K.L., Estrada, Y.O., Genova, R.C., 2014. IPCC, 2014: Climate Change 2014: Impacts, Adaptation, and Vulnerability. Part A: Global and Sectoral Aspects. Contribution of Working Group II to the Fifth Assessment Report of the Intergovernmental Panel on Climate Change.
- Florindo, F., Roberts, A.P., Palmer, M.R., 2003. Magnetite dissolution in siliceous sediments. *Geochemistry, Geophys. Geosystems* 4, 1–13.
- 050 Foster, G.L., Rohling, E.J., 2013. Relationship between sea level and climate forcing by CO₂ on geological timescales. *Proc. Natl. Acad. Sci. U. S. A.* 110, 1209–14.
- Foubert, A., Henriot, J.-P., 2009. Nature and significance of the recent carbonate mound record: the Mound Challenger code. Springer.
- 055 Fouinat, L., Sabatier, P., Poulencard, J., Reyss, J.-L., Montet, X., Arnaud, F., 2017. A new CT scan methodology to characterize a small aggregation gravel clast contained in a soft sediment matrix. *Earth Surf. Dyn.* 5, 199–209.

- 060 Fretwell, P., Pritchard, H.D., Vaughan, D.G., Bamber, J.L., Barrand, N.E., Bell, R., Bianchi, C., Bingham, R.G.,
Blankenship, D.D., Casassa, G., Catania, G., Callens, D., Conway, H., Cook, a. J., Corr, H.F.J., Damaske,
D., Damm, V., Ferraccioli, F., Forsberg, R., Fujita, S., Gim, Y., Gogineni, P., Griggs, J. a., Hindmarsh, R.C.
a., Holmlund, P., Holt, J.W., Jacobel, R.W., Jenkins, A., Jokat, W., Jordan, T., King, E.C., Kohler, J.,
065 Krabill, W., Riger-Kusk, M., Langley, K. a., Leitchenkov, G., Leuschen, C., Luyendyk, B.P., Matsuoka, K.,
Mouginot, J., Nitsche, F.O., Nogi, Y., Nost, O. a., Popov, S. V., Rignot, E., Rippin, D.M., Rivera, A.,
Roberts, J., Ross, N., Siegert, M.J., Smith, a. M., Steinhage, D., Studinger, M., Sun, B., Tinto, B.K., Welch,
070 B.C., Wilson, D., Young, D. a., Xiangbin, C., Zirizzotti, A., 2013. Bedmap2: improved ice bed, surface and
thickness datasets for Antarctica. *Cryosph.* 7, 375–393.
- Fukamachi, Y., Rintoul, S.R., Church, J.A., Aoki, S., Sokolov, S., Rosenberg, M.A., Wakatsuchi, M., 2010.
Strong export of Antarctic Bottom Water east of the Kerguelen plateau. *Nat. Geosci.* 3, 327–331.
- Fukamachi, Y., Wakatsuchi, M., Taira, K., Kitagawa, S., Furukawa, T., Fukuchi, M., 2000. Seasonal variability
075 of bottom water properties off Adlie Land , Antarctica 105, 6531–6540.
- Gasson, E., DeConto, R.M., Pollard, D., Levy, R.H., 2016. Dynamic Antarctic ice sheet during the early to mid-
Miocene. *Proc. Natl. Acad. Sci.* 113, 3459–3464.
- Gilbert, R., Nielsen, N., Desloges, J., Rasch, M., 1998. Contrasting glacial marine sedimentary environments of two
arctic fiords on Disko, West Greenland. *Mar. Geol.*
- 075 Govin, A., Michel, E., Labeyrie, L., Waelbroeck, C., Dewilde, F., Jansen, E., 2009. Evidence for northward
expansion of Antarctic Bottom Water mass in the Southern Ocean during the last glacial inception.
Paleoceanography 24.
- Grobe, H., Mackensen, A., 1992. Late Quaternary climatic cycles as recorded in sediments from the Antarctic
continental margin, in: *The Antarctic Paleoenvironment: A Perspective on Global Change: Part One.* pp.
080 349–376.
- Hall, I.R., McCave, I.N., Zahn, R., Carter, L., Knutz, P.C., Weedon, G.P., 2003. Paleocurrent reconstruction of
the deep Pacific inflow during the middle Miocene: Reflections of East Antarctic Ice Sheet growth.
Paleoceanography 18, n/a-n/a.
- Hannah, M.J., Wilson, G.J., Wrenn, J.H., 2000. Oligocene and miocene marine palynomorphs from CRP-2/2A,
085 Victoria Land Basin, Antarctica. *Terra Antarct.* 7, 503–511.
- Hannah, M.J., Wrenn, J., Wilson, G., 2001. Preliminary report on early Oligocene and latest Eocene marine
palynomorphs from CRP-3 drillhole, Victoria Land Basin, Antarctica. *Terra Antart.*
- Hartman, J.D., Sangiorgi, F., Salabarnada, A., Peterse, F., Houben, A.J.P., Schouten, S., Escutia, C., Bijl, P.K.,
2017. Oligocene TEX86-derived seawater temperatures from offshore Wilkes Land (East Antarctica). *Clim.*
090 *Past Discuss.* 2017, 1–31.
- Hauptvogel, D.W., Pekar, S.F., Pincay, V., 2017. Evidence for a heavily glaciated Antarctica during the late
Oligocene ?warming? (27.8-24.5?Ma): Stable isotope records from ODP Site 690. *Paleoceanography* 32,
384–396.
- Hauptvogel, D.W., 2015. *The State Of The Oligocene Icehouse World : Sedimentology , Provenance , And
095 Stable Isotopes Of Marine Sediments From The Antarctic Continental Margin.* PhD Dissertation. The City
University Of New York.
- Hayes, D.E., Frakes, L.A., Barrett, P.J., Burns, D.A., Chen, P.-H., Ford, A.B., Kaneps, A.G., Kemp, E.M.,
McCollum, D.W., Piper, D.J.W., Wall, R.E., Webb, P.N., 1975. Site 264, in: *Initial Reports of the Deep Sea
Drilling Program, Volume 28.* pp. 19–48.
- 100 Hennekam, R., de Lange, G., 2012. X-ray fluorescence core scanning of wet marine sediments: methods to
improve quality and reproducibility of high-resolution paleoenvironmental records. *Limnol. Oceanogr.*
Methods 10, 991–1003.
- Hepp, D.A., 2007. *Late Miocene-Pliocene glacial cyclicity in a deep-sea sediment drift on the Antarctic
Peninsula continental margin : Sedimentary and diagenetic processes,* Ph.D Thesis. Bremen.
- 105 Hepp, D.A., Mörz, T., Hensen, C., Frederichs, T., Kasten, S., Riedinger, N., Hay, W.W., 2009. A late Miocene–
early Pliocene Antarctic deepwater record of repeated iron reduction events. *Mar. Geol.* 266, 198–211.
- Hodell, D.A., Channell, J.E.T., Curtis, J.H., Romero, O.E., Röhl, U., 2008. Onset of “Hudson Strait” Heinrich
events in the eastern North Atlantic at the end of the middle Pleistocene transition (~640 ka)?
Paleoceanography 23.
- 110 Houben, A.J.P., Bijl, P.K., Pross, J., Bohaty, S.M., Passchier, S., Stickley, C.E., Rohl, U., Sugisaki, S., Tauxe, L.,
van de Flierdt, T., Olney, M., Sangiorgi, F., Sluijs, A., Escutia, C., Brinkhuis, H., 2013. Reorganization of
Southern Ocean Plankton Ecosystem at the Onset of Antarctic Glaciation. *Science* (80-). 340, 341–344.
- Huber, M., Sloan, L.C., 2001. Heat transport, deep waters, and thermal gradients: Coupled simulation of an
Eocene greenhouse climate. *Geophys. Res. Lett.* 28, 3481–3484.

- 115 Huck, C.E., van de Flierdt, T., Bohaty, S.M., Hammond, S.J., 2017. Antarctic climate, Southern Ocean
circulation patterns, and deep water formation during the Eocene. *Paleoceanography* 32, 674–691.
- Jaccard, S.L., Galbraith, E.D., Martínez-García, A., Anderson, R.F., 2016. Covariation of deep Southern Ocean
oxygenation and atmospheric CO₂ through the last ice age. *Nature* 530, 207–10.
- 120 Johnson, G.C., 2008. Quantifying Antarctic Bottom Water and North Atlantic Deep Water volumes. *J. Geophys.
Res. Ocean.* 113, 1–13.
- Kemp, E.M., Barrett, P.J., 1975. Antarctic glaciation and early Tertiary vegetation. *Nature* 258, 507–508.
- Kemp, E.M., Grigorov, I., Pearce, R.B., Naveira Garabato, A.C., 2010. Migration of the Antarctic Polar Front
through the mid-Pleistocene transition: evidence and climatic implications. *Quat. Sci. Rev.* 29, 1993–2009.
- Kominz, M.A., Pekar, S.F., 2001. Oligocene eustasy from two-dimensional sequence stratigraphic backstripping.
125 *Geol. Soc. Am. Bull.* 113, 291–304.
- Korff, L., von Dobeneck, T., Frederichs, T., Kasten, S., Kuhn, G., Gersonde, R., Diekmann, B., 2016. Cyclic
magnetite dissolution in Pleistocene sediments of the abyssal northwest Pacific Ocean: Evidence for glacial
oxygen depletion and carbon trapping. *Paleoceanography* 31, 600–624.
- Kuhn, G., Diekmann, B., 2002. Late Quaternary variability of ocean circulation in the southeastern South
130 Atlantic inferred from the terrigenous sediment record of a drift deposit in the southern Cape Basin (ODP
Site 1089). *Palaeogeogr. Palaeoclimatol. Palaeoecol.* 182, 287–303.
- Laskar, J., Robutel, P., Joutel, F., Gastineau, M., Correia, a. C.M., Levrard, B., 2004. A long-term numerical
solution for the insolation quantities of the Earth. *Astron. Astrophys.* 428, 261–285.
- Lear, C.H., Rosenthal, Y., Coxall, H.K., Wilson, P.A., 2004. Late Eocene to early Miocene ice sheet dynamics
135 and the global carbon cycle. *Paleoceanography* 19, n/a-n/a.
- Leckie, R., Webb, P., 1983. Late Oligocene–early Miocene glacial record of the Ross Sea, Antarctica: Evidence
from DSDP site 270. *Geology*.
- Levy, R., Harwood, D., Florindo, F., Sangiorgi, F., Tripathi, R., von Eynatten, H., Gasson, E., Kuhn, G., Tripathi,
A., DeConto, R., Fielding, C., Field, B., Golledge, N., McKay, R., Naish, T., Olney, M., Pollard, D.,
140 Schouten, S., Talarico, F., Warny, S., Willmott, V., Acton, G., Panter, K., Paulsen, T., Taviani, M., 2016.
Antarctic ice sheet sensitivity to atmospheric CO₂ variations in the early to mid-Miocene. *Proc. Natl. Acad.
Sci.* 201516030.
- Liebrand, D., Lourens, L.J., Hodell, D. a., de Boer, B., van de Wal, R.S.W., Pälike, H., 2011. Antarctic ice sheet
and oceanographic response to eccentricity forcing during the early Miocene. *Clim. Past* 7, 869–880.
- 145 Liebrand, D., Beddow, H.M., Lourens, L.J., Pälike, H., Raffi, I., Bohaty, S.M., Hilgen, F.J., Saes, M.J.M.,
Wilson, P.A., van Dijk, A.E., Hodell, D.A., Kroon, D., Huck, C.E., Batenburg, S.J., 2016. Cyclostratigraphy
and eccentricity tuning of the early Oligocene through early Miocene (30.1–17.1 Ma): *Cibicides mundulus*
stable oxygen and carbon isotope records from Walvis Ridge Site 1264. *Earth Planet. Sci. Lett.* 450, 392–
405.
- 150 Liebrand, D., de Bakker, A.T.M., Beddow, H.M., Wilson, P.A., Bohaty, S.M., Ruessink, G., Pälike, H.,
Batenburg, S.J., Hilgen, F.J., Hodell, D.A., Huck, C.E., Kroon, D., Raffi, I., Saes, M.J.M., van Dijk, A.E.,
Lourens, L.J., 2017. Evolution of the early Antarctic ice ages. *Proc. Natl. Acad. Sci.* 114, 3867–3872.
- Lisiecki, L.E., Raymo, M.E., Curry, W.B., 2008. Atlantic overturning responses to Late Pleistocene climate
forcings. *Nature* 456, 85–88.
- 155 Lucchi, R.G., Rebesco, M., 2007. Glacial contourites on the Antarctic Peninsula margin: insight for
palaeoenvironmental and palaeoclimatic conditions. *Geol. Soc. London, Spec. Publ.* 276, 111–127.
- Mackensen, A., Grobe, H., Hubberten, H., Spiess, V., 1989. Stable isotope stratigraphy from the Antarctic
continental margin during the last one million years. *Mar. Geol.*
- Mann, M.E., Lees, J.M., 1996. Robust estimation of background noise and signal detection in climatic time
160 series. *Clim. Change* 33, 409–445.
- Martín-Chivelet, J., Fregenal-Martínez, M.A., Chacón, B., 2008. Chapter 10 Traction Structures in Contourites,
in: *Contourites*. pp. 157–182.
- McKay, R., Naish, T., Carter, L., Riesselman, C., Dunbar, R., Sjunneskog, C., Winter, D., Sangiorgi, F., Warren,
C., Pagani, M., Schouten, S., Willmott, V., Levy, R., DeConto, R., Powell, R.D., 2012. Antarctic and
165 Southern Ocean influences on Late Pliocene global cooling. *Proc. Natl. Acad. Sci.* 109, 6423–6428.
- McKay, R., Browne, G., Carter, L., Cowan, E., Dunbar, G., Krissek, L., Naish, T., Powell, R., Reed, J., Talarico,
F., Wilch, T., 2009. The stratigraphic signature of the late Cenozoic Antarctic Ice Sheets in the Ross
Embayment. *Geol. Soc. Am. Bull.* 121, 1537–1561.
- Meyers, S.R., Sageman, B.B., Hinnov, L.A., 2001. Integrated quantitative stratigraphy of the Cenomanian-
170 Turonian Bridge Creek Limestone Member using evolutive harmonic analysis and stratigraphic modeling. *J.
Sediment. Res.* 71, 628–644.
- Meyers, S.R., 2014. *Astrochron: An R Package for Astrochronology*. [http://cran.r-
project.org/package=astrochron](http://cran.r-project.org/package=astrochron).

- 175 Meyers, S.R., Sageman, B.B., Arthur, M.A., 2012. Obliquity forcing of organic matter accumulation during Oceanic Anoxic Event 2. *Paleoceanography* 27.
- Moore, W.S., Dymond, J., 1991. Fluxes of ²²⁶Ra and barium in the Pacific Ocean: The importance of boundary processes. *Earth Planet. Sci. Lett.* 107, 55–68.
- Mudelsee, M., Bickert, T., Lear, C.H., Lohmann, G., 2014. Cenozoic climate changes: A review based on time series analysis of marine benthic $\delta^{18}\text{O}$ records. *Rev. Geophys.* 52, 333–374.
- 180 Naish, T., Powell, R., Levy, R., Wilson, G., Scherer, R., Talarico, F., Krissek, L., Niessen, F., Pompilio, M., Wilson, T., Carter, L., Deconto, R., Huybers, P., McKay, R., Pollard, D., Ross, J., Winter, D., Barrett, P., Browne, G., Cody, R., Cowan, E., Crampton, J., Dunbar, G., Dunbar, N., Florindo, F., Gebhardt, C., Graham, I., Hannah, M., Hansaraj, D., Harwood, D., Helling, D., Henrys, S., Hinnov, L., Kuhn, G., Kyle, P., Läufer, a, Maffioli, P., Magens, D., Mandernack, K., McIntosh, W., Millan, C., Morin, R., Ohneiser, C.,
- 185 Paulsen, T., Persico, D., Raine, I., Reed, J., Riesselman, C., Sagnotti, L., Schmitt, D., Sjunneskog, C., Strong, P., Taviani, M., Vogel, S., Wilch, T., Williams, T., 2009. Obliquity-paced Pliocene West Antarctic ice sheet oscillations. *Nature* 458, 322–8.
- Naish, T.R., Woolfe, K.J., Barrett, P.J., Wilson, G.S., Atkins, C., Bohaty, S.M., B?cker, C.J., Claps, M., Davey, F.J., Dunbar, G.B., Dunn, A.G., Fielding, C.R., Florindo, F., Hannah, M.J., Harwood, D.M., Henrys, S. a, Krissek, L. a, Lavelle, M., van der Meer, J., McIntosh, W.C., Niessen, F., Passchier, S., Powell, R.D.,
- 190 Roberts, A.P., Sagnotti, L., Scherer, R.P., Strong, C.P., Talarico, F., Verosub, K.L., Villa, G., Watkins, D.K., Webb, P.-N., Wonik, T., 2001. Orbitally induced oscillations in the East Antarctic ice sheet at the Oligocene/Miocene boundary. *Nature* 413, 719–723.
- Nelson, C.S., Cooke, P.J., 2001. History of oceanic front development in the New Zealand sector of the Southern Ocean during the Cenozoic—a synthesis. *New Zeal. J. Geol. Geophys.* 44, 535–553.
- 195 O’Regan, M., John, K. St., Moran, K., Backman, J., King, J., Haley, B.A., Jakobsson, M., Frank, M., Röhl, U., 2010. Plio-Pleistocene trends in ice rafted debris on the Lomonosov Ridge. *Quat. Int.* 219, 168–176.
- Orsi, A.H., Johnson, G.C., Bullister, J.L., 1999. Circulation, mixing, and production of Antarctic Bottom Water. *Prog. Oceanogr.* 43, 55–109.
- 200 Orsi, A.H., Whitworth, T., Nowlin, W.D., 1995. On the meridional extent and fronts of the Antarctic Circumpolar Current. *Deep Sea Res. Part I Oceanogr. Res. Pap.* 42, 641–673.
- Otto-Bliesner, B.L., Brady, E.C., Shields, C., 2002. Late Cretaceous ocean: Coupled simulations with the National Center for Atmospheric Research Climate System Model. *J. Geophys. Res.* 107, ACL-11.
- Pagani, M., Zachos, J.C., Freeman, K.H., Tiplle, B., Bohaty, S., 2005. Marked Decline in Atmospheric Carbon Dioxide Concentrations During the Paleogene. *Science* (80-). 309, 600–603.
- 205 P?liike, H., Norris, R.D., Herrle, J.O., Wilson, P. a, Coxall, H.K., Lear, C.H., Shackleton, N.J., Tripathi, A.K., Wade, B.S., 2006. The Heartbeat of the Oligocene Climate System. *Science* (80-). 314, 1894–1898.
- Patterson, M.O., McKay, R., Naish, T., Escutia, C., Jimenez-Espejo, F.J., Raymo, M.E., Meyers, S.R., Tauxe, L., Brinkhuis, H., Klaus, a, Fehr, a, Bendle, J. a. P., Bijl, P.K., Bohaty, S.M., Carr, S. a, Dunbar, R.B., Flores, J. a, Gonzalez, J.J., Hayden, T.G., Iwai, M., Katsuki, K., Kong, G.S., Nakai, M., Olney, M.P., Passchier, S.,
- 210 Pekar, S.F., Pross, J., Riesselman, C.R., Röhl, U., Sakai, T., Shrivastava, P.K., Stickley, C.E., Sugasaki, S., Tuo, S., van de Flierdt, T., Welsh, K., Williams, T., Yamane, M., 2014. Orbital forcing of the East Antarctic ice sheet during the Pliocene and Early Pleistocene. *Nat. Geosci.* 7, 841–847.
- Payne, R.R., Conolly, J.R., Aabbott, W.H., 1972. Turbidite Muds within Diatom Ooze off Antarctica: Pleistocene Sediment Variation Defined by Closely Spaced Piston Cores. *GSA Bull.* 83, 481–486.
- 215 Pekar, S.F., DeConto, R.M., Harwood, D.M., 2006. Resolving a late Oligocene conundrum: Deep-sea warming and Antarctic glaciation. *Palaeogeogr. Palaeoclimatol. Palaeoecol.* 231, 29–40.
- Pollard, D., DeConto, R.M., 2009. Modelling West Antarctic ice sheet growth and collapse through the past five million years. *Nature* 458, 329–32.
- 220 Prebble, J.G., Raine, J.I., Barrett, P.J., Hannah, M.J., 2006. Vegetation and climate from two Oligocene glacioeustatic sedimentary cycles (31 and 24 Ma) cored by the Cape Roberts Project, Victoria Land Basin, Antarctica. *Palaeogeogr. Palaeoclimatol. Palaeoecol.* 231, 41–57.
- Pritchard, H.D., Ligtenberg, S.R.M., Fricker, H.A., Vaughan, D.G., van den Broeke, M.R., Padman, L., 2012. Antarctic ice-sheet loss driven by basal melting of ice shelves. *Nature* 484, 502–505.
- 225 Pudsey, C.J., 2000. Sedimentation on the continental rise west of the Antarctic Peninsula over the last three glacial cycles. *Mar. Geol.* 167, 313–338.
- Pudsey, C.J., 1992. Late Quaternary changes in Antarctic Bottom Water velocity inferred from sediment grain size in the northern Weddell Sea. *Mar. Geol.*
- Pudsey, C.J., Camerlenghi, A., 1998. Glacial–interglacial deposition on a sediment drift on the Pacific margin of
- 230 the Antarctic Peninsula. *Antarct. Sci.* 10.
- Pudsey, C.J., Howe, J. a, 1998. Quaternary history of the Antarctic Circumpolar Current: evidence from the Scotia Sea. *Mar. Geol.* 148, 83–112.

- Raine, J., Askin, R., 2001. Terrestrial palynology of Cape Roberts Project Drillhole CRP-3, Victoria Land Basin, Antarctica. *Terra Antart.*
- 235 Rebesco, M. (Michele), Camerlenghi, A. (Angelo), 2008. *Contourites*. Elsevier Science.
- Rebesco, M., Hernández-Molina, F.J., Van Rooij, D., Wåhlin, A., 2014. Contourites and associated sediments controlled by deep-water circulation processes: State-of-the-art and future considerations. *Mar. Geol.* 352, 111–154.
- 240 Reinardy, B.T.I., Escutia, C., Iwai, M., Jimenez-Espejo, F.J., Cook, C., van de Flierdt, T., Brinkhuis, H., 2015. Repeated advance and retreat of the East Antarctic Ice Sheet on the continental shelf during the early Pliocene warm period. *Palaeogeogr. Palaeoclimatol. Palaeoecol.* 422, 65–84.
- Richter, T.O., van der Gaast, S., Koster, B., Vaars, A., Gieles, R., de Stigter, H.C., De Haas, H., van Weering, T.C.E., 2006. The Avaatech XRF Core Scanner: technical description and applications to NE Atlantic sediments. *Geol. Soc. London, Spec. Publ.* 267, 39–50.
- 245 Rignot, E., Jacobs, S., Mouginot, J., Scheuchl, B., 2013. Ice-shelf melting around Antarctica. *Science* (80-.). 341, 266–70.
- Rodriguez, A.B., Anderson, J.B., 2004. Contourite origin for shelf and upper slope sand sheet, offshore Antarctica. *Sedimentology* 51, 699–711.
- Roeske, T., 2011. Dissolved Barium and Particulate Rare Earth Elements as Tracers for Shelf-Basin Interaction in the Arctic Ocean, Ph.D. Thesis. Alfred-Wegener Institute for Polar and Marine Research.
- 250 Rothwell, R.G., Croudace, I.W., 2015. Micro-XRF studies of sediment cores: a perspective on capability and application in the environmental sciences, in: *Micro-XRF Studies of Sediiment Cores*. pp. 1–24.
- Salzmann, U., Strother, S., Sangiorgi, F., Bijl, P., Pross, J., Woodward, J., Escutia, C., Brinkhuis, H., 2016. Oligocene to Miocene terrestrial climate change and the demise of forests on Wilkes Land, East Antarctica, in: *EGU General Assembly Conference Abstracts, EGU General Assembly Conference Abstracts*. p. EPSC2016-2717.
- 255 Sangiorgi, F., Bijl, P.K., Passchier, S., Salzmann, U., Schouten, S., McKay, R., Cody, R.D., Pross, J., van de Flierdt, T., Bohaty, S.M., Levy, R., Williams, T., Escutia, C., Brinkhuis, H., 2018. Southern Ocean warming and Wilkes Land ice sheet retreat during the mid-Miocene. *Nat. Commun.* 9, 317.
- 260 Scher, H.D., Martin, E.E., 2008. Oligocene deep water export from the North Atlantic and the development of the Antarctic Circumpolar Current examined with neodymium isotopes. *Paleoceanography* 23.
- Scher, H.D., Whittaker, J.M., Williams, S.E., Latimer, J.C., Kordesch, W.E.C., Delaney, M.L., 2015. Onset of Antarctic Circumpolar Current 30 million years ago as Tasmanian Gateway aligned with westerlies. *Nature* 523, 580–583.
- 265 Schneider, R.R., Price, B., Müller, P.J., Kroon, D., Alexander, I., 1997. Monsoon related variations in Zaire (Congo) sediment load and influence of fluvial silicate supply on marine productivity in the east equatorial Atlantic during the last 200,000 years. *Paleoceanography* 12, 463–481.
- Shanmugam, G., 2008. Deep - Water Bottom Currents and Their Deposits. *Dev. Sedimentol.* 60, 59–81.
- Shanmugam, G., Spalding, T.D., Rofheart, D.H., 1993. Traction structures in deep-marine, bottom-current-reworked sands in the Pliocene and Pleistocene, Gulf of Mexico. *Geology* 21, 929–932.
- 270 Shen, Q., Wang, H., Shum, C.K., Jiang, L., Hsu, H.T., 2018. Recent high-resolution Antarctic ice velocity maps reveal increased mass loss in Wilkes Land, East. *Sci. Rep.* 1–8.
- Solomon, S., D. Qin, M. Manning, Z. Chen, M. Marquis, K.B. Averyt, M.T. and H.L.M., 2007. IPCC, 2007: Climate Change 2007: The Physical Science Basis. Contribution of Working Group I to the Fourth Assessment Report of the Intergovernmental Panel on Climate Change, Cambridge University Press. Cambridge University Press, Cambridge, United Kingdom and New York, NY, USA.
- 275 Strother, S., Salzmann, U., Sangiorgi, F., Bijl, P., Pross, Escutia, C., Salabarnada A., Pound M.J., Voss, P., Woodward, J. 2017. A new quantitative approach to identify reworking in Eocene to Miocene pollen records from offshore Antarctica using red fluorescence and digital imaging. *Biogeosciences* 14, 2089–2100.
- 280 St-Onge, G., Long, B.F., 2009. CAT-scan analysis of sedimentary sequences: An ultrahigh-resolution paleoclimatic tool. *Eng. Geol.* 103, 127–133.
- Stow, D., 2002. Deep-water contourite systems : modern drifts and ancient series, seismic and sedimentary characteristics. Geological Society.
- 285 Stow, D., Faugères, J.-C., 2008. Chapter 13 Contourite Facies and the Facies Model. pp. 223–256.
- Taxe, L., Stickley, C.E., Sugisaki, S., Bijl, P.K., Bohaty, S.M., Brinkhuis, H., Escutia, C., Flores, J. a., Houben, a. J.P., Iwai, M., Jimenez-Espejo, F., McKay, R., Passchier, S., Pross, J., Riesselman, C.R., R?hl, U., Sangiorgi, F., Welsh, K., Klaus, A., Fehr, A., Bendle, J. a. P., Dunbar, R., Gonz?lez, J., Hayden, T., Katsuki, K., Olney, M.P., Pekar, S.F., Shrivastava, P.K., van de Flierdt, T., Williams, T., Yamane, M.,
- 290 2012. Chronostratigraphic framework for the IODP Expedition 318 cores from the Wilkes Land Margin: Constraints for paleoceanographic reconstruction. *Paleoceanography* 27, 19.

- Thorn, V., 2001. Oligocene and early Miocene phytoliths from CRP-2/2A and CRP-3, Victoria Land Basin, Antarctica. *Terra Antart.*
- 295 Tjallingii, R., Röhl, U., Kölling, M., Bickert, T., 2007. Influence of the water content on X-ray fluorescence core-scanning measurements in soft marine sediments. *Geochemistry, Geophys. Geosystems* 8.
- Toggweiler, J.R., Russell, J., 2008. Ocean circulation in a warming climate. *Nature* 451, 286–288.
- Tribovillard, N., Algeo, T.J., Lyons, T., Riboulleau, A., 2006. Trace metals as paleoredox and paleoproductivity proxies: An update. *Chem. Geol.* 232, 12–32.
- 300 Van Daele, M., Cnudde, V., Duyck, P., Pino, M., Urrutia, R., De Batist, M., 2014. Multidirectional, synchronously-triggered seismo-turbidites and debrites revealed by X-ray computed tomography (CT). *Sedimentology* 61, 861–880.
- van Hinsbergen, D.J.J., de Groot, L. V., van Schaik, S.J., Spakman, W., Bijl, P.K., Sluijs, A., Langereis, C.G., Brinkhuis, H., 2015. A Paleolatitude Calculator for Paleoclimate Studies. *PLoS One* 10, e0126946.
- 305 van Wijk, E.M., Rintoul, S.R., 2014. Freshening drives contraction of Antarctic Bottom Water in the Australian Antarctic Basin. *Geophys. Res. Lett.* 41, 1657–1664.
- Vandenberghe, N., Hilgen, F.J., Speijer, R.P., Ogg, J.G., Gradstein, F.M., Hammer, O., Hollis, C.J., Hooker, J.J., 2012. The Paleogene Period, in: *The Geologic Time Scale*. Elsevier, pp. 855–921.
- Veldkamp, A., Kroonenberg, S.B., 1993. Application of bulk sand geochemistry in mineral exploration and Quaternary research: a methodological study of the Allier and Dore terrace sands, Limagne rift valley, France. *Appl. Geochemistry* 8, 177–187.
- 310 Villa, G., Persico, D., 2006. Late Oligocene climatic changes: Evidence from calcareous nannofossils at Kerguelen Plateau Site 748 (Southern Ocean). *Palaeogeogr. Palaeoclimatol. Palaeoecol.* 231, 110–119.
- Villa, G., Persico, D., Wise, S.W., Gadaleta, A., 2012. Calcareous nannofossil evidence for Marine Isotope Stage 31 (1Ma) in Core AND-1B, ANDRILL McMurdo Ice Shelf Project (Antarctica). *Glob. Planet. Change* 96–97, 75–86.
- 315 Wanlu Fu, Jiang, D., Montañez, I.P., Meyers, S.R., Motani, R., Tintori, A., 2016. Eccentricity and obliquity paced carbon cycling in the Early Triassic and implications for post-extinction ecosystem recovery. *Sci. Rep.* 6, 27793.
- Weertman, J., 1974. Stability of the Junction of an Ice Sheet and an Ice Shelf. *J. Glaciol.* 13, 3–11.
- 320 Whitehead, J.M., Wotherspoon, S., Bohaty, S.M., 2005. Minimal Antarctic sea ice during the Pliocene. *Geology* 33, 137.
- Whitehead, J.M., Bohaty, S.M., 2003. Pliocene summer sea surface temperature reconstruction using silicoflagellates from Southern Ocean ODP Site 1165. *Paleoceanography* 18.
- 325 Wilhelms-Dick, D., Westerhold, T., Röhl, U., Wilhelms, F., Vogt, C., Hanebuth, T.J.J., Römmermann, H., Kriews, M., Kasten, S., 2012. A comparison of mm scale resolution techniques for element analysis in sediment cores. *J. Anal. At. Spectrom.* 27, 1574.
- Williams, T., Handwerger, D., 2005. A high-resolution record of early Miocene Antarctic glacial history from ODP Site 1165, Prydz Bay. *Paleoceanography* 20.
- 330 Wilson, G.S., Levy, R.H., Naish, T.R., Powell, R.D., Florindo, F., Ohneiser, C., Sagnotti, L., Winter, D.M., Cody, R., Henrys, S., Ross, J., Krissek, L., Niessen, F., Pompillio, M., Scherer, R., Alloway, B. V., Barrett, P.J., Brachfeld, S., Browne, G., Carter, L., Cowan, E., Crampton, J., DeConto, R.M., Dunbar, G., Dunbar, N., Dunbar, R., von Eynatten, H., Gebhardt, C., Giorgetti, G., Graham, I., Hannah, M., Hansaraj, D., Harwood, D.M., Hinnov, L., Jarrard, R.D., Joseph, L., Kominz, M., Kuhn, G., Kyle, P., Läufer, A., McIntosh, W.C., McKay, R., Maffioli, P., Magens, D., Millan, C., Monien, D., Morin, R., Paulsen, T., Persico, D., Pollard, D., Raine, J.I., Riesselman, C., Sandroni, S., Schmitt, D., Sjunneskog, C., Strong, C.P., Talarico, F., Taviani, M., Villa, G., Vogel, S., Wilch, T., Williams, T., Wilson, T.J., Wise, S., 2012. Neogene tectonic and climatic evolution of the Western Ross Sea, Antarctica — Chronology of events from the AND-1B drill hole. *Glob. Planet. Change* 96–97, 189–203.
- 335 Zachos, J., 2001. Climate Response to Orbital Forcing Across the Oligocene-Miocene Boundary. *Science* (80-). 292, 274–278.
- 340 Zachos, J., 2001. Trends, Rhythms, and Aberrations in Global Climate 65 Ma to Present. *Science* (80-). 292, 686–693.
- Zachos, J., Kroon, D., Bloom, P., Et, A., 2004. Initial Reports Leg 208. *Proc. Ocean Drill. Progr.* 208.
- 345 Zhang, Y.G., Pagani, M., Liu, Z., Bohaty, S.M., DeConto, R., 2013. A 40-million-year history of atmospheric CO₂. *Philos. Trans. R. Soc. A Math. Phys. Eng. Sci.* 371, 20130096–20130096.
- Ziegler, M., Jilbert, T., de Lange, G.J., Lourens, L.J., Reichert, G.-J., 2008. Bromine counts from XRF scanning as an estimate of the marine organic carbon content of sediment cores. *Geochemistry, Geophys. Geosystems* 9.

Tables 1-3:

Table 1: Age model by Tauxe et al., (2012) and transformed ages to GPTS 2012

Core Section Site U1356 Exp. 318	Top depth (mbsf)	Bottom depth (mbsf)	Depth used (m)	GPTS 2004 (Myr) (Tauxe et al., 2012)	GPTS 2012 (Myr)	Chron
68R-2	643.10	643.65	643.37	25.444	25.260	C8n.1n (o)
69R-2	652.55	652.60	652.57	25.492	25.300	C8n.2n (y)
71R-6	678.06	679.90	678.98	26.154	25.990	C8n.2n (o)

Table 2: Types of facies differentiated by physical, geochemical, and biological character and their interpretation in terms of sedimentary processes and paleoclimate.

		Facies 1 (F1)	Facies 2 (F2)
Lithological description		Bioturbated green claystones with thin silt laminae with planar and cross-bedded laminations	Highly bioturbated, thicker pale-brown, silty-claystones
Contacts	Top	Gradual, bioturbated	Sharp
	Bottom	Sharp	Gradual, bioturbated
Bioturbation		Sparse bioturbation. Primary structures preserved	Strong bioturbated. Massive. No primary structures preserved
Nannos		Barren to rare	Barren to variable abundance and preservation
IRD		No	No
Magnetic susceptibility (MS)		Low in claystones and high in silty laminations	High
XRF-Scanner elements concentration	Zr	Low in claystones and high in silty laminations	High, (max. values on top)
	Ba	High, (max. values on bottom)	Low
	Ca	No	Variable, low to high
Formation process		Bottom currents of fluctuating intensities	Bottom currents with higher velocity and constant flux
Facies interpretation		Cold periods. Supply of terrigenous by density current flows, reworked by bottom currents.	Well-oxygenated deep-sea sedimentation. Warm periods with reworking of sediments by bottom currents

365

Table 3: R Pearson Linear correlation between XRF-scanner elements.

	MS	S	Ca	Ti	Mn	Fe	Br	Rb	Zr	Sr
S	-0.214									
Ca	0.226	-0.122								
Ti	-0.212	0.620	-0.290							
Mn	0.151	-0.121	0.858	-0.246						
Fe	0.0419	0.0449	-0.396	0.510	-0.324					
Br	-0.297	0.111	-0.438	0.118	-0.363	0.056				
Rb	-0.282	0.036	-0.576	0.286	-0.489	0.455	0.493			
Zr	0.480	-0.164	-0.036	-0.099	-0.058	-0.055	0.102	0.067		
Sr	0.186	0.006	0.871	-0.074	0.677	-0.345	-0.303	-0.515	0.040	
Ba	-0.290	0.339	-0.234	0.662	-0.210	0.354	0.343	0.402	0.018	0.039

370

375

380

385

390

395

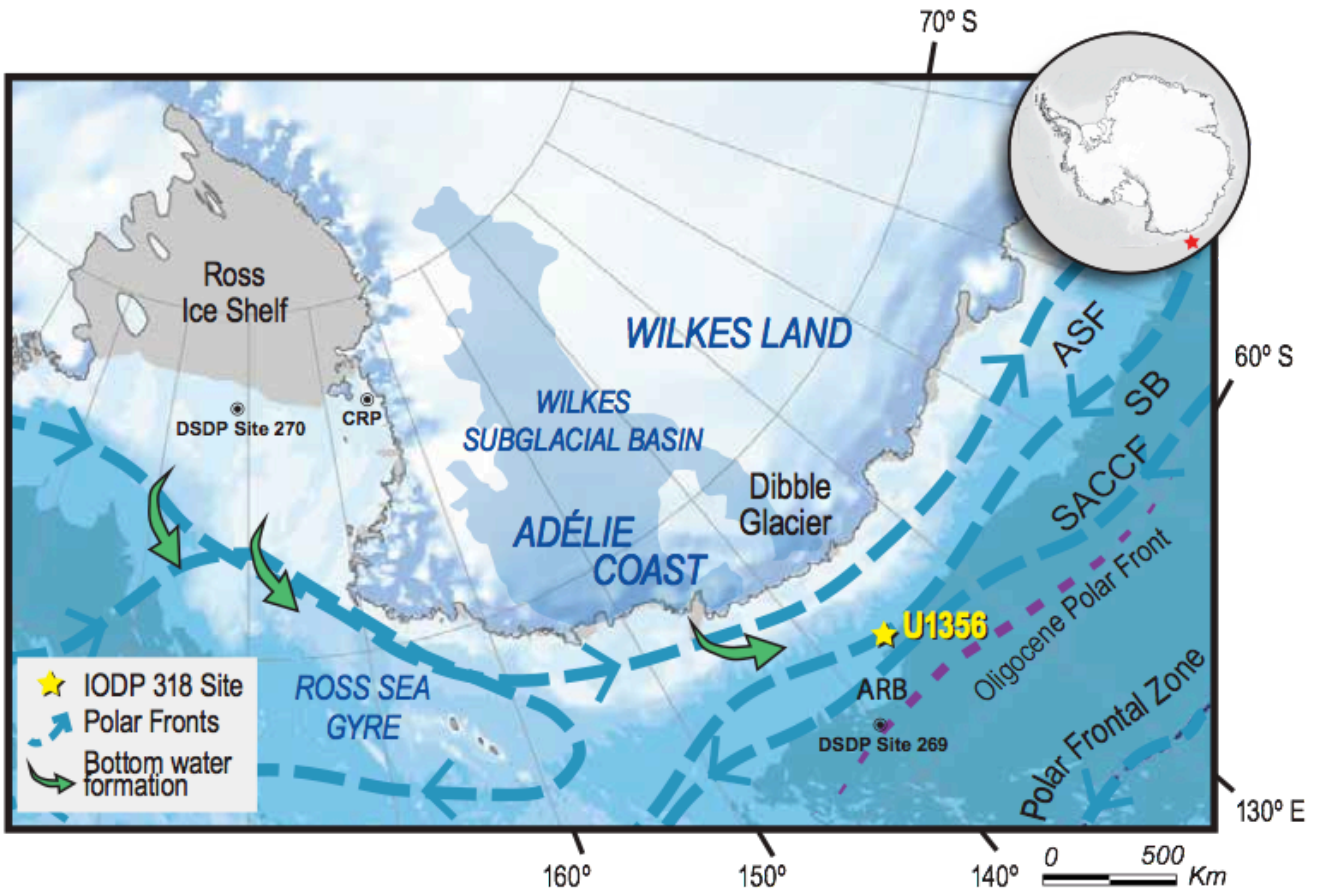
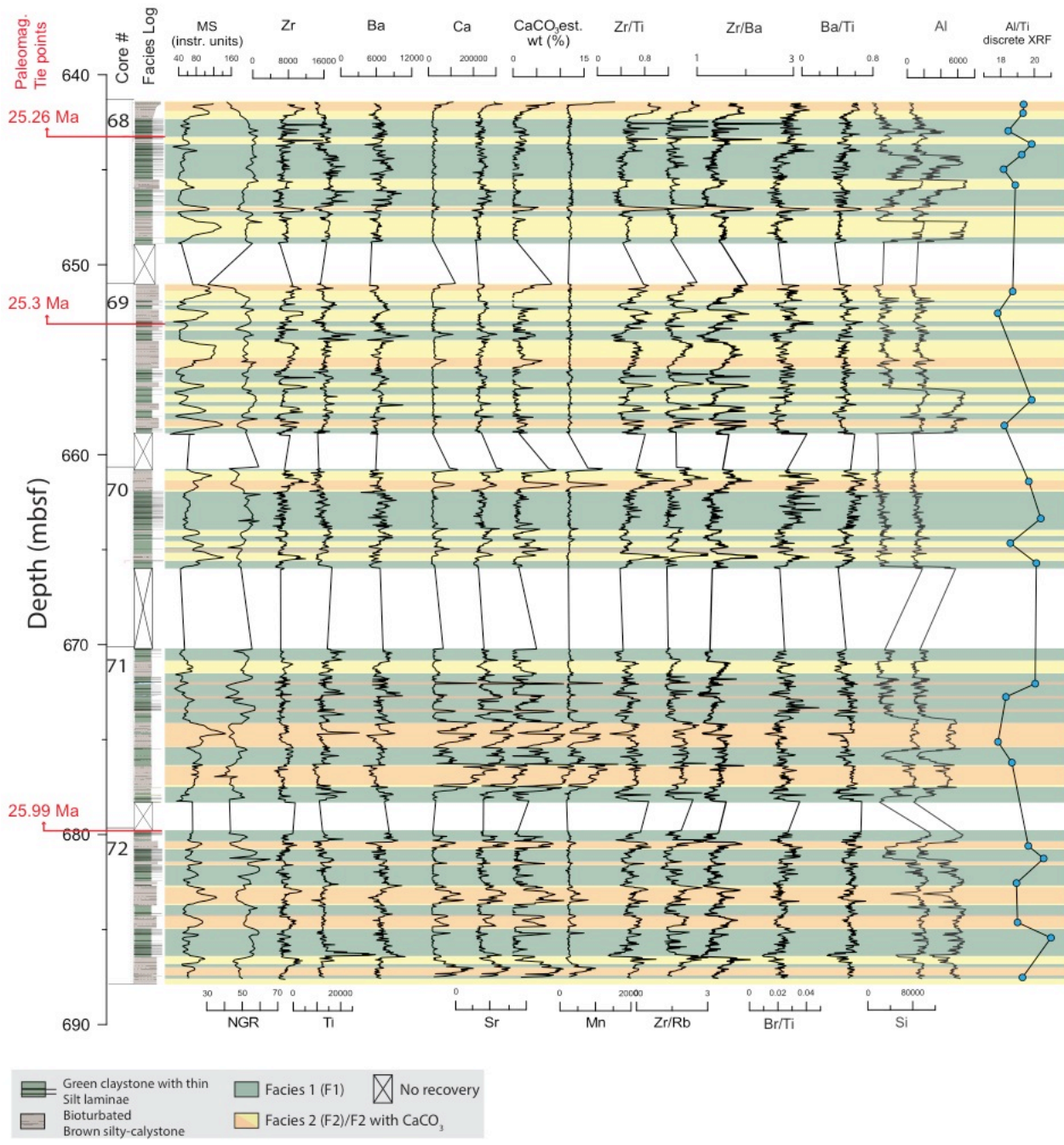


Fig. 1: Location of IODP 318 Site U1356 (Escutia et al., 2010) on the Adélie coast continental rise. Bed topography from IBSCO2 (Arndt, JE et al., 2013). Schematic position of the different water masses at present and locations of Antarctic Bottom Water formation (Orsi, 1995) are indicated. The position of the Oligocene Polar Front (Scher et al., 2015) is also shown. ASF: Antarctic Slope Front; SB: Southern Boundary; SACCF: Southern Antarctic Counter Current Front; ARB: Adélie Rift Block.

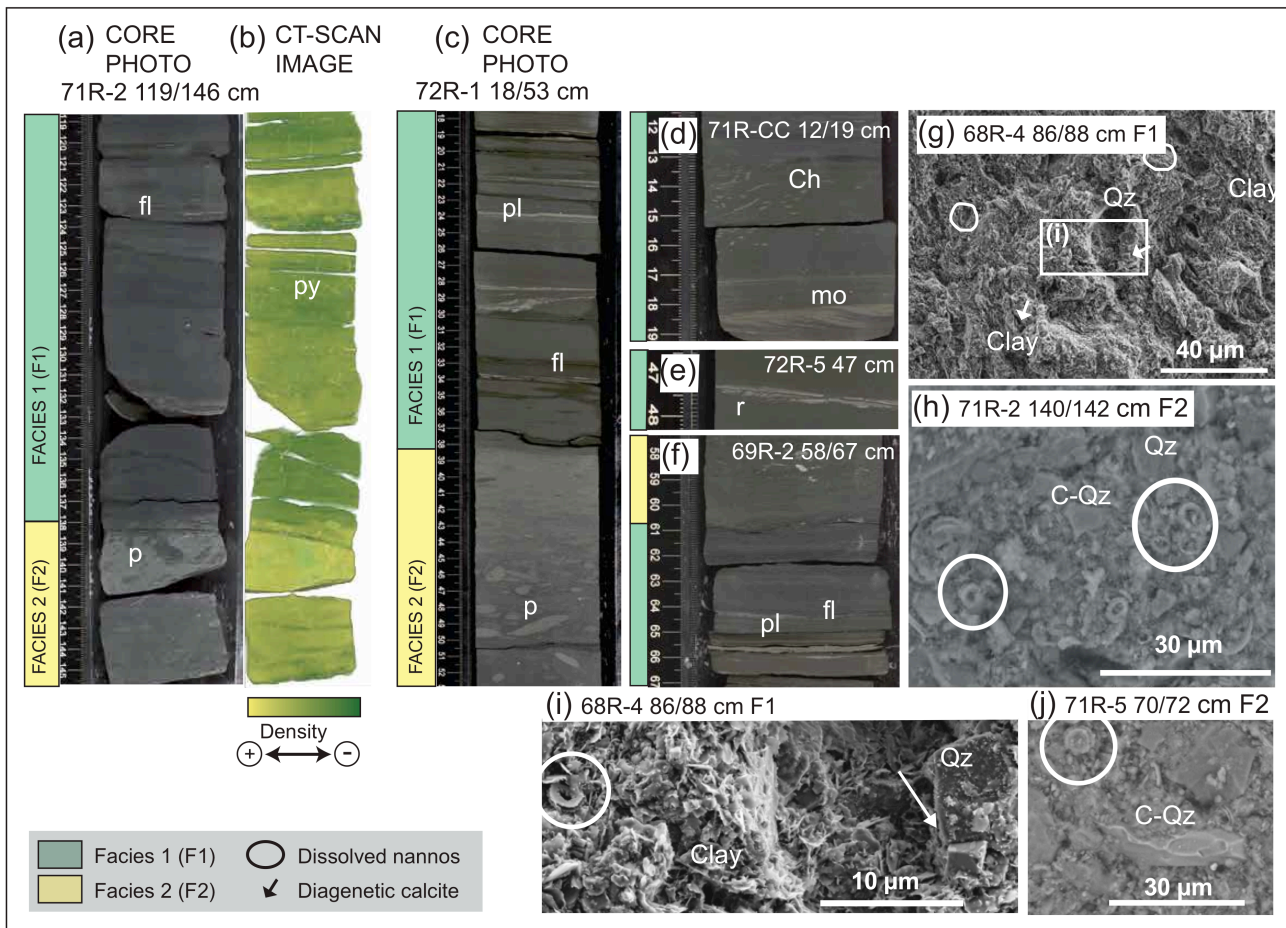


420

425

Fig. 2: Magnetic susceptibility (MS) and natural gamma radiation (NGR) physical properties, and selected X-Ray Fluorescence (XRF) data (in total counts) and elemental ratios plotted against the new detailed U1356 facies log between 689.4 and 641.4 mbsf.

430



435

Fig. 3: Detailed images, CT-scans and HRSEM from Facies 1 (F1) and Facies 2 (F2). (a) Example of F1 taken from Core 71R-2 119/146 cm, showing faint laminations (fl) and bioturbation by *Planolites* (p) (b) CT-scan 3D image of the same core interval, note the pyritized burrows (py). (c) Example of F2 taken from core 72R-1 18/53 cm). (d-f) Close-ups of laminations from F1: ripples (r), planar lamination (pl), and faint laminations (fl), with mud offshoots (mo). (d) *Chondrites* (Ch) bioturbation inside F1. (g) HRSEM image of F1 (68R-4-86/88 cm) with detritic aspect and a mudstone clay matrix, Quartz grains (Qz), diagenetic calcite (arrows), and dissolved coccoliths (circles); (h) HRSEM image of F2 (71R-2 140/142 cm) silt sized matrix and reworked calcareous nanofossils, and conchoidal quartz grain (C-Qz); (i) Detail of dissolved coccoliths and diagenetic calcite mineral; (j) Detail of a dissolved and reworked calcareous nanofossils and a fractured conchoidal quartz (C-Qz).

450

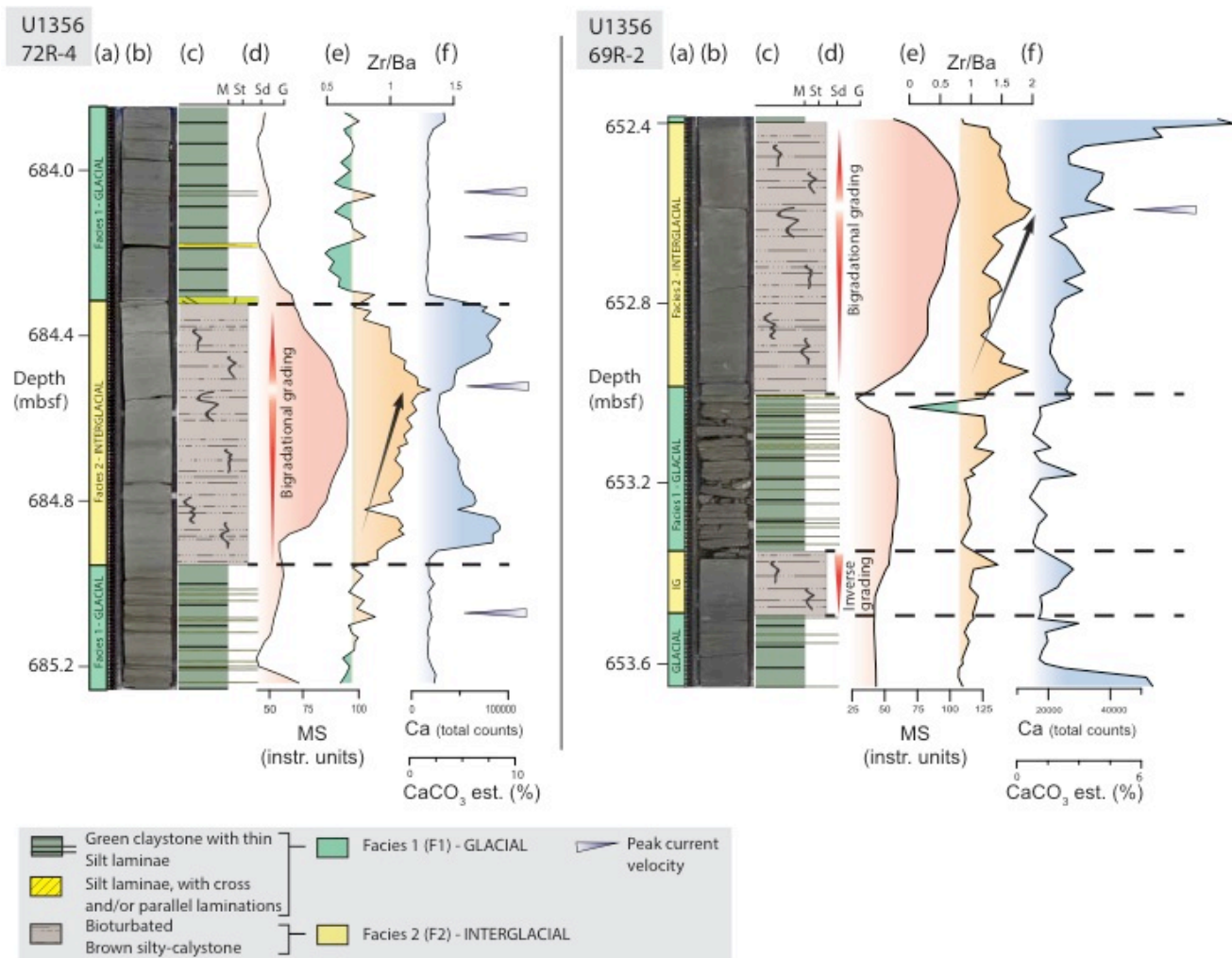


Fig. 4: Detailed facies characterization of two representative sections using: (a) Interpreted facies F1 and F2; a high-resolution digital image of the core sections (b), facies log (c), Magnetic susceptibility (MS) (d), XRF Zr/Ba ratio (e), and XRF calcium counts (f).

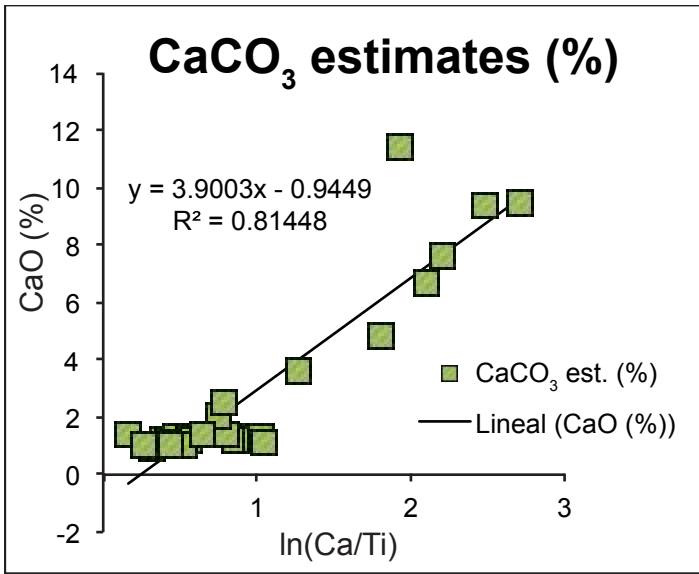
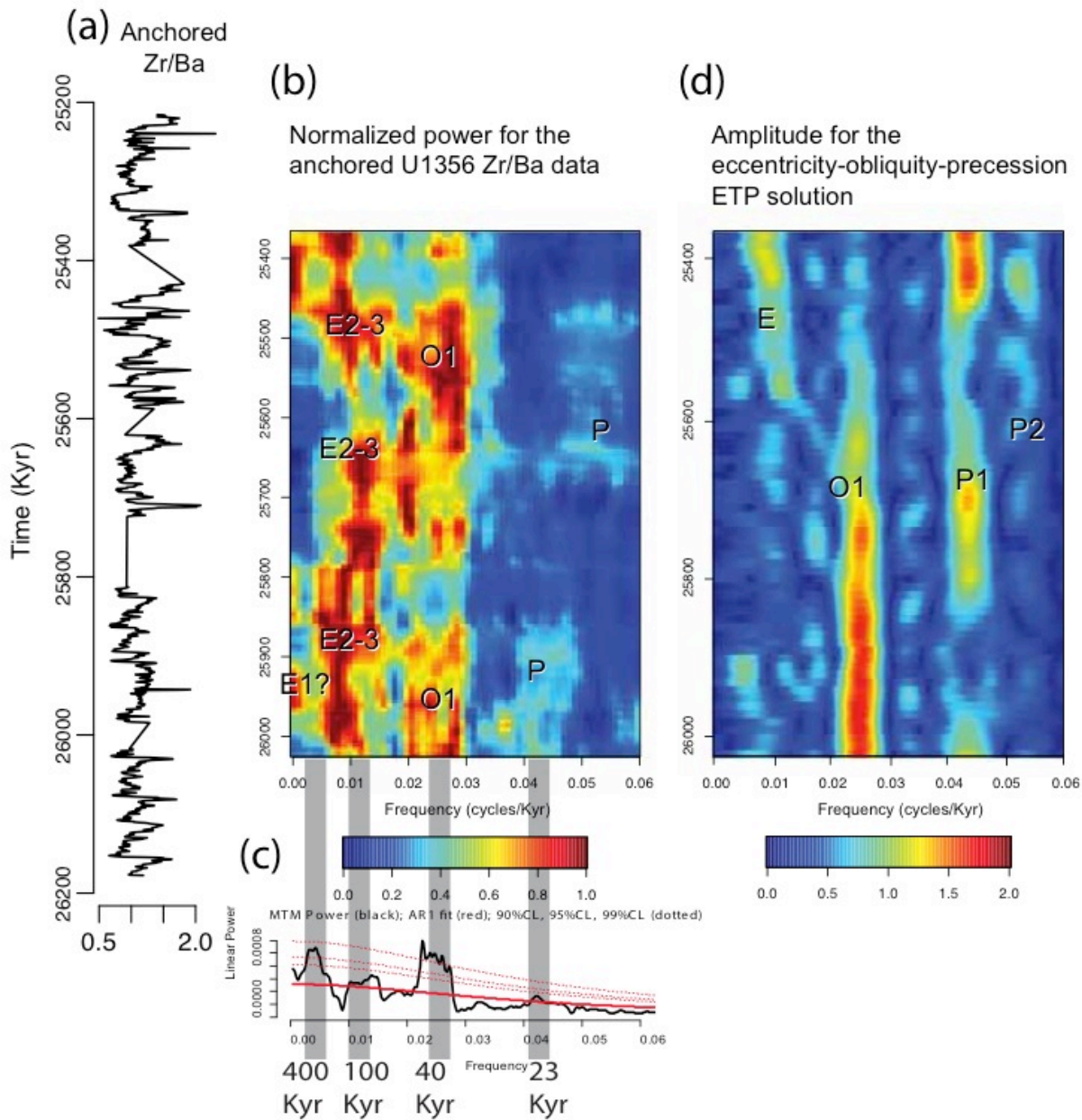


Fig. 5: Linear correlation between CaO% (discrete XRF) and ln(Ca/Ti) (XRF scanner) values in order to estimate carbonate contents (CaCO₃ est. %).



505

Fig. 6: Spectral analysis results of the Zr/Ba obliquity tuned and anchored data. (a) Zr/Ba ratio tuned with Astrochron (Meyers, 2014) and anchored to the top of the C8n.2n (o) chron. (b) EHA and (c) MTM spectral analysis on Zr/Ba tuned data. EHA normalized power with 300-kyr window with 3DPSS tapers. (d) EHA amplitude for the eccentricity-obliquity-precession ETP solution (Laskar et al., 2004) calculated for the same period of time with with 3DPSS tapers and 200-kyr window.

510

Paleoceanographic configuration of Wilkes Land region during the Late Warm Oligocene (~26-25 Ma)

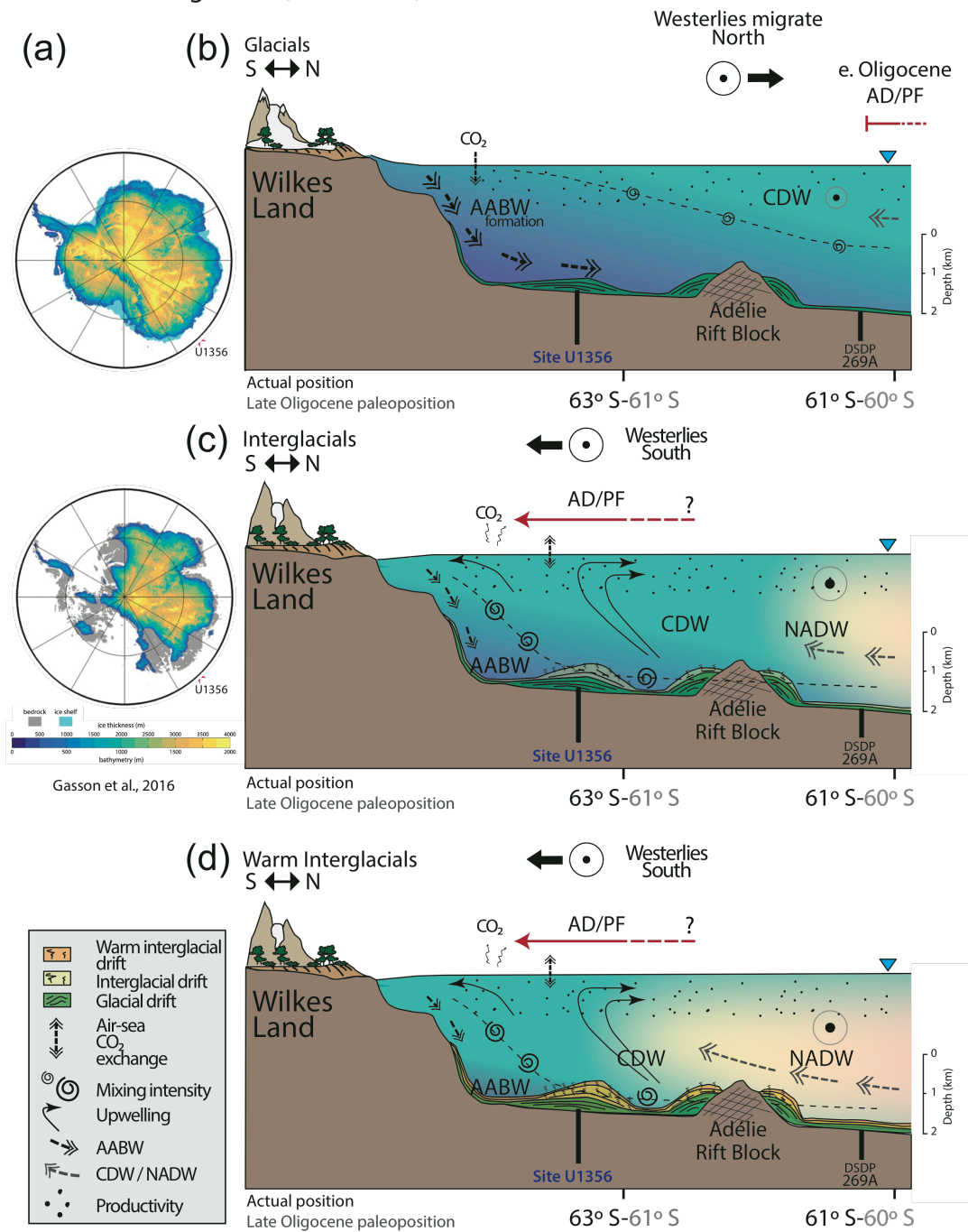


Fig. 7: Paleoceanographic reconstructions based on our interpretations for Facies 1 and 2. (a) Modelled ice thickness for the mid-Miocene ice sheet by Gasson et al., (2016). (b) Glacial periods with low obliquity configuration. Westerlies and Polar Front (PF) move northwards. There is enhanced proto-AABW formation. Low ventilation conditions occur at the ocean/sediment interface and mixing of waters masses is diminished. Bottom currents are weak and fluctuating, producing laminated sediments. (b) Interglacials occur during high obliquity configuration. Westerlies and the PF move southwards, close to the Site U1356. Proto-AABW formation is reduced. Intrusions of proto-CDW/NADW-like reach southernmost positions. (c) During warm Interglacials, NADW-like is enhanced and CaCO₃ sedimentation is more abundant. (b,c) Bottom water ventilation and upwelling are more vigorous, with stronger bottom currents that result in fully bioturbated and silty-sized sediments.

Supplementary materials

This file includes:

S.1 Lithostratigraphy

Figures S1, S2

S.2 Astrochronologic analysis

Figures S3-S10

R_analysis

References

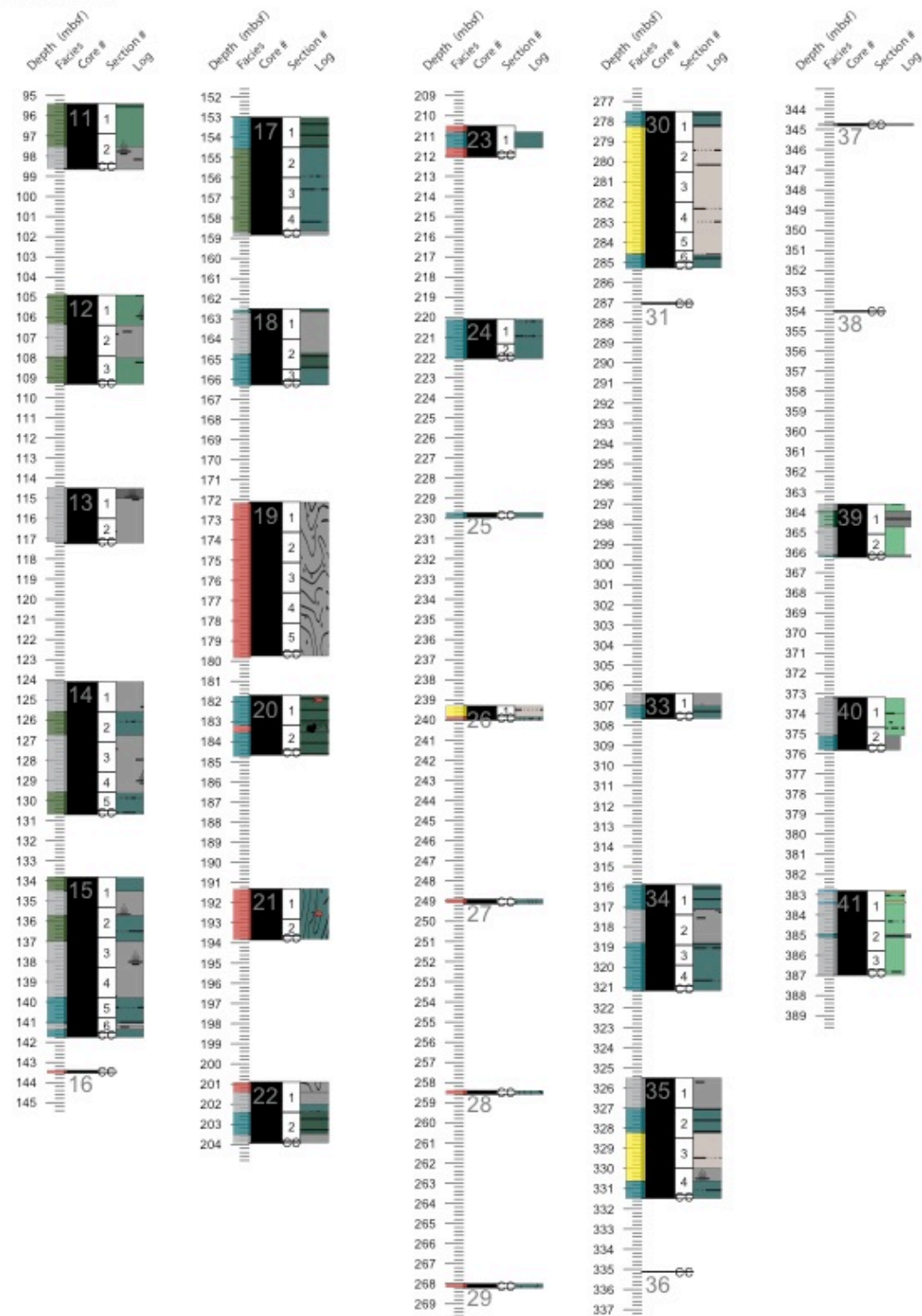
S1. Lithostratigraphy

Site U1356 from 392–95.4 to 896 mbsf (Cores 42R–11R to 95R) comprises lithostratigraphic Units IH to IX described on shipboard during IODP Expedition 318 (Escutia et al., 2011). Here we present a revised and more detailed lithostratigraphic log (Fig. S1) and a schematic facies interpretation (Fig. S2). Facies are interpreted based on a detailed visual description of the cores during a visit to the IODP-Gulf Coast Repository (GCR) following IODP Proceedings methods in Escutia et al. (2011). We aided our interpretations with shipboard magnetic susceptibility data and high-resolution digital-images of the cores, both available from <http://web.iodp.tamu.edu>. In addition, the XRF core scanner data results obtained from the interval between 641.4 and 689.4 mbsf, which is the main focus of this paper, have been interpolated to other intervals down-core where sediments are “in situ.” The facies interpretation column in Fig. S1S2, contains information on whether the sediments are deposited “in situ” or are deposited from allochthonous older materials.

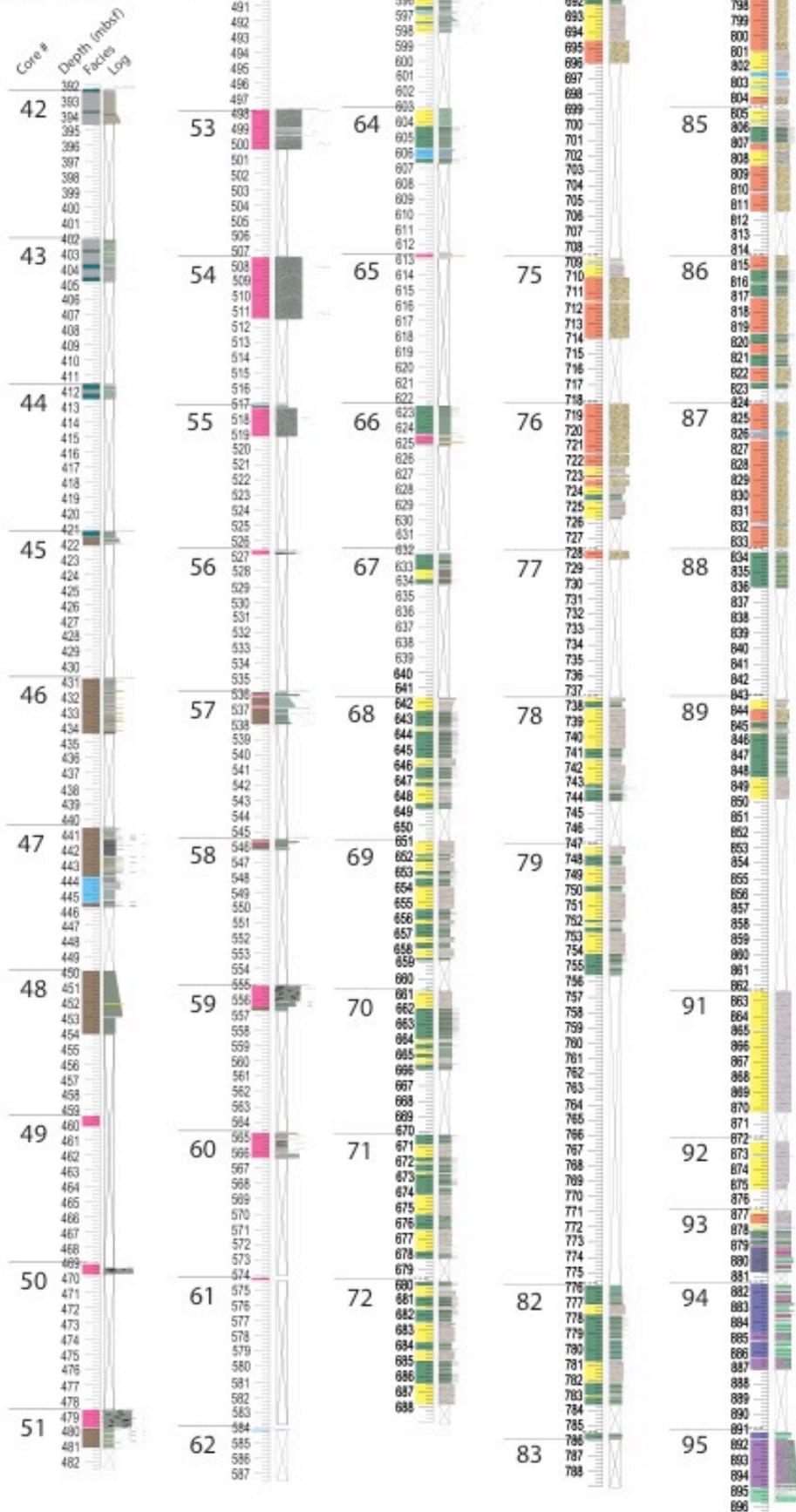
Facies are here described briefly from top to bottom (Fig. S1-2). Early and middle Miocene section is recovered between 95.4 and 430.8 mbsf, Cores U1356-11R to U1356-45R. Sediments are comprised by an alternation between glacial laminated green silty clay and interglacial grey clay-rich diatom oozes. In addition, there are some intervals with Mass Transport deposits (likely i.e., debris flows). Miocene facies are dominated by mix sedimentary processes between turbidites, contourites and hemipelagites and are included within shipboard lithostratigraphic units I and II (Escutia et al., 2011). The Oligocene section is recovered between 430.8 and 895 mbsf, Cores U1356-46R to U1356-95R-3 83 cm. Middle Miocene Facies, are dominated by turbidites and hemipelagites. From 392 to 413 mbsf facies are characterized by an intercalation of bioturbated green and grey claystones, slightly laminated. From 413–430.8 to 455 mbsf, turbidite facies dominate, with an alternation between dark grey claystones with *Nereites* *Nereites* ichnofacies and green claystones with silt laminae. Silt laminae have scours at the base, with cross lamination and planar laminations. These facies are included in shipboard lithostratigraphic Unit III. From 455 to 575 mbsf, sediments mostly comprise debris flow (DF) Facies, characterized by clast-rich/clast-poor contorted and chaotic intervals-sediments with a claystone to sandstone matrix. DF deposits exhibit with scours at the base. DF events are locally separated by claystones with silt laminations that present cross and/or planar laminations. Shipboard this corresponded with lithostratigraphic Unit IV, which extended from 459.4–593.8 mbsf. [1]The interval from 575 to 785 mbsf (which includes shipboard lithostratigraphic units V, VI and VII) is characterized by an alternation of two facies (F1 and F2). These facies are explained in detail in the main text of the article, and are composed of an alternation of glacial

green claystones with thin silt laminae with planar and cross-bedded laminations presenting different traction and suspension structures (F1). These are interbedded with interglacial highly bioturbated, thicker pale-brown, silty-claystones (F2). This alternation is disrupted from 710 to 730 mbsf by a MTD ~~s-slump~~ facies (i.e., slumps). From 785 to 879 mbsf (within shipboard lithostratigraphic unit VIII) slump facies prevail. Slump facies consist predominantly of allochthonous stratified and chaotic sediments of similar lithology to F1 and F2. The interval from 879 to 895 corresponds with lithostratigraphic unit IX described on shipboard. This unit comprises sediments from the middle Eocene and the earliest Oligocene consisting of bioturbated purple silty claystones with some laminations. Erosion/non-deposition surfaces are present within this facies. They are intercalated with coarser green micaceous (very shiny) (sandy) silty-claystone. Laminations with ripples and pinstripe and cross-lamination are also observed. This facies are intercalated with MTD facies composed of these same sediments. The interval between 895 and 896 mbsf is within shipboard lithostratigraphic unit X and is characterized by a lithological change to Eocene green sands Facies.

Site U1356
IODP Exp. 318
Cores 11-41R



Site U1356
IODP Exp. 318
Cores 42-95R



LEGEND U1356 CORES 42R-95R



Fig. S1: Detailed sedimentary log from IODP U1356 Site U1356 exp. 318 from 11R to 95R (95.4 to 896 mbsf).

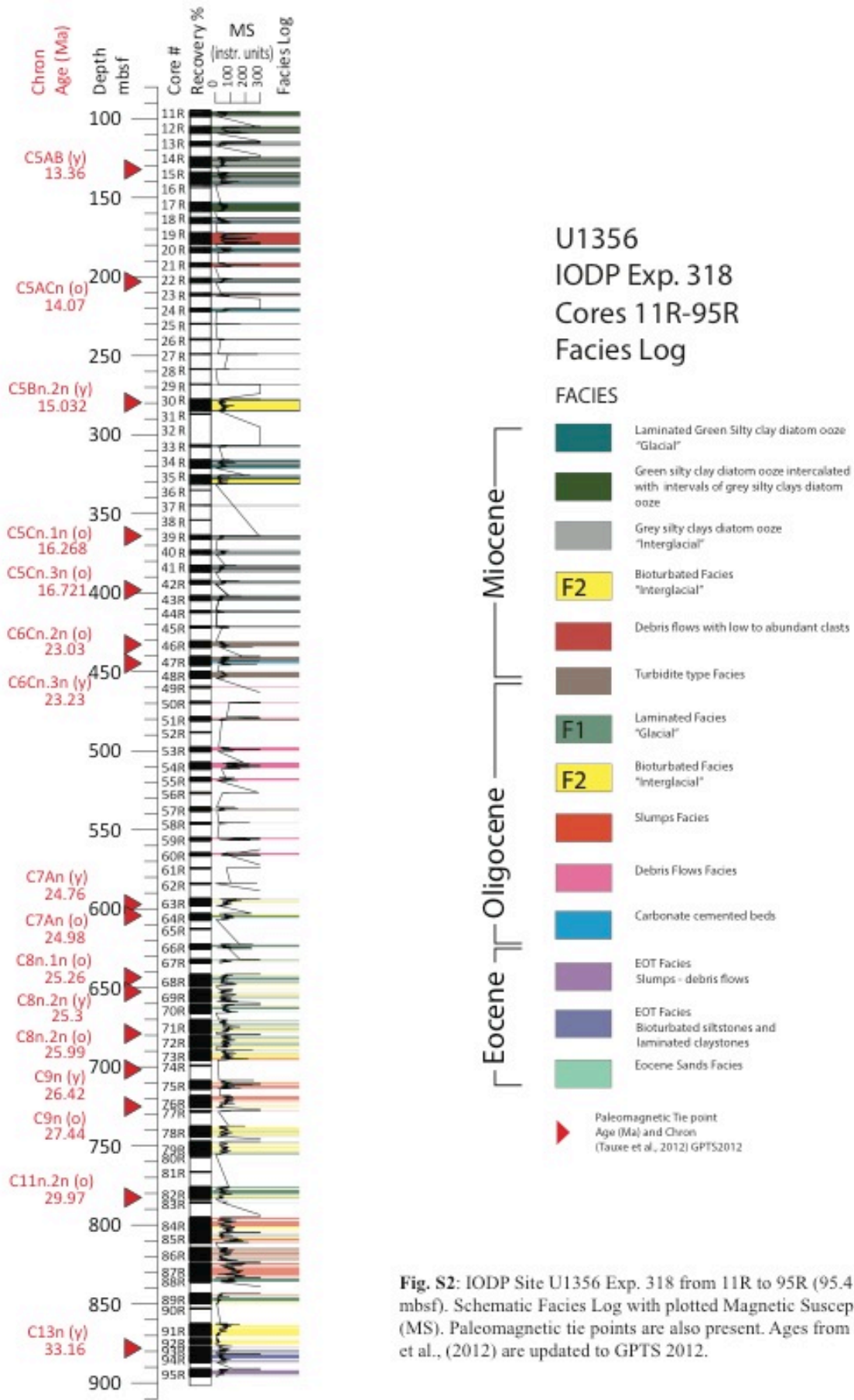


Fig. S2: IODP Site U1356 Exp. 318 from 11R to 95R (95.4 to 896 mbsf). Schematic Facies Log with plotted Magnetic Susceptibility (MS). Paleomagnetic tie points are also present. Ages from Tauxe et al., (2012) are updated to GPTS 2012.

S.2 Astrochronologic analysis

Materials and methods

We followed the procedures published by Meyers et al. (2012) and Wanlu Fu et al. (2016) in order to generate spectral analysis on our data.

We selected Zr/Ba ratio as we consider this ratio to integrate and summarize the processes shaping our facies model, showing clearly the marked cyclicity present.

Data preparation:

In order to remove the long-term trend data series were detrended, outliers were removed, and sampling interval was linearly interpolated in order to resample the dataset to an even spacing of 2cm. Average sedimentation rates between the two paleomagnetic tie end points were linearly interpolated and is 5cm/kyr for the investigated interval. Age model is calibrated to the Geologic Timescale 2012 (GPTS 2012, Table 1).

For initial cyclostratigraphic analyses, we used Anlyseries software (Paillard et al., 1996). We used B-Tukey method in order to preliminary assess the cyclicity on the record on a depth scale. A clear and statistically significant cyclicity is observed in Ba, Zr and Zr/Ti every 2m (0.5 cycles/m), and less significant ones but also reliable at 4.67m (0.21 cycles/m), and 1m (0.94 cycles/m) (Fig. S3). On the basis of the calculated sedimentation rate, the cycles above (0.5 cycles/m) account for 40 Kyr. After determining the significant frequency, we filtered the Zr/Ba dataset (at depth domain) at 0.5 frequency in order to extract the wavelet and compare it with the obliquity solution for that time-period (Laskar et al., 2004). Cycles can be correlated one to one with a total of 23 cycles of obliquity (Fig. S3). After initial analysis we proceed with Astrochron Evolutive Average Spectral Misfit method (Meyers et al., 2012). Astrochron package is prepared to resolve unevenly sampled series, and changing sedimentation rates.

Time-frequency analysis:

Evolutive Harmonic Analysis (EHA; Fig. S4) of the prepared Zr/Ba (in depth scale) data provides an evaluation of changes in the spectral features through depth/time. EHA employs five 3π DPSS tapers, and a moving window of 15 m. Significant frequencies are retrieved for further study.

Astrochronologic testing:

The Evolutive Average Spectral Misfit method (Meyers, 2014) (E-ASM; five 3π tapers; searching to the mean Nyquist frequency of 1.504221 cycles/m) was used to test a range of plausible timescales and simultaneously evaluate the reliability of the presence of astronomical cycles. The ETP (eccentricity, obliquity and precession) target periods were determined from La04 (Laskar et al., 2004) using the interval from 25.0e – 26.4 Ma: 400.00 kyr (E1), 131.58 kyr (E2), 99.01 kyr (E3), 40.49 kyr (O1), 32.79 kyr (O2), 20.70 kyr (P1), 19.69 kyr (P2) and 17.06 kyr (P3).

The Zr/Ba MTM Harmonic F-test results of the EHA (Fig. 6) are evaluated using a grid of 100 sedimentation rates spanning 3 cm/Kyr to 10 cm/Kyr. This range of sedimentation rates encompasses the long-term average sedimentation rate for the section based on available paleomagnetic constraints with a total duration of 0.71 Ma and a total stratigraphic thickness between 30 – 40 m given the range of plausible correlation horizons for the section. We interpolate an average sedimentation rate of 5 cm/Kyr.

All spectral peaks above 90% F-test confidence level were evaluated using E-ASM, and Monte Carlo significance testing utilizing 10,000 simulations. Results with Null Hypothesis Significance Levels (Ho-SL) less than or equal to 0.1% were identified (Fig. S5).

Astronomical tuning:

Frequency domain minimal tuning (Meyers et al., 2001) is used for tracking obliquity in EHA harmonic F-test for the calibrated periods and sedimentation rates. Spatial frequencies are afterwards converted to sedimentation rates using average period of 41 Kyr (Fig. S6) and a time-space map is created with a new calibrated time series. Time series is afterwards anchored to our paleomagnetic tie points (Fig. S7).

MTM and EHA results on the tuned data provide further evidence of the presence of precession, obliquity and eccentricity cycles, supporting the obliquity tuning (Fig. S8).

Significant Harmonic F-test peaks that achieve 95% CL are: 102.77 Kyr, 69.26 Kyr, 40.84 Kyr, 30.05 Kyr, 22.27 Kyr, 20.68 Kyr (Fig. S8).

The new time-scale is used to tune the other records (Zr/Ti; Ca/Ti; MS; Ba). EHA is then applied to tuned records in order to see the frequencies that appear (Fig. S9).

Orbital frequencies were tested in each core section individually in the Zr/Ba dataset in the depth scale in order to assure that cyclicity is not an artefact related to the gaps in the series (Fig. S10).

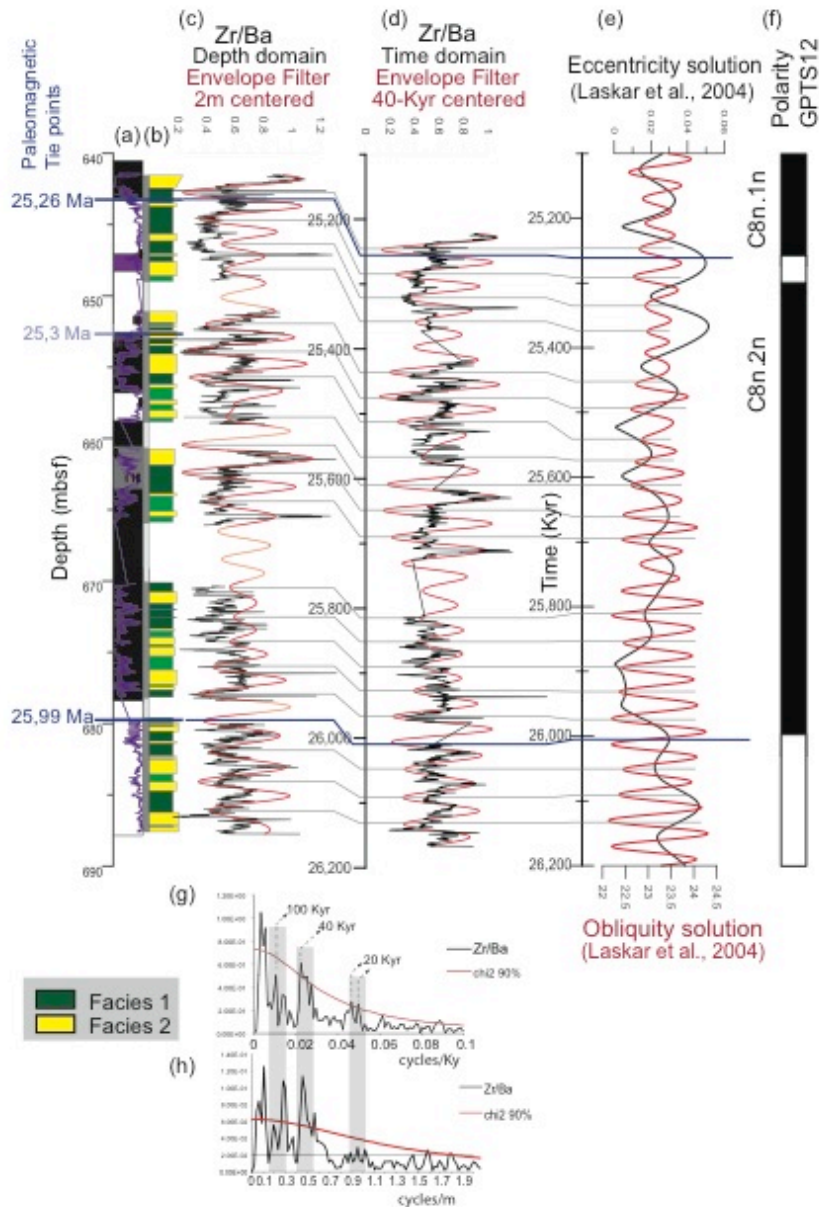


Fig. S3: Tuning of Zr/Ba to the obliquity solution. Zr/Ba (in the depth domain) is tuned to the obliquity solution cycle by cycle. Tuning of Zr/Ba record (in depth scale) and bandpass filtering were done in Analyseries (Paillard et al., 1996). (a) Magnetostratigraphic chrons (Tauxe et al., 2012); (b) schematic stratigraphic log; (c) Zr/Ba data in depth scale with the envelope filter centred at 2m (in red); (d) Zr/Ba data in time scale using paleomagnetic tie points and a linear sedimentation rate, with the envelope filter centred at 40 Kyr (in red); (e) Eccentricity and obliquity solutions (Laskar et al., 2004); (f) Polarity

chrons from the GPTS2012; (g) Blakmann-Tukey in the Zr/Ba data in time domain (not tuned), with statistical (>90%) periodic peaks in the 40 Kyr and 20 Kyr periodicities; g) Blakmann-Tukey in the Zr/Ba data in depth domain, with statistical (>90%) periodic peaks.

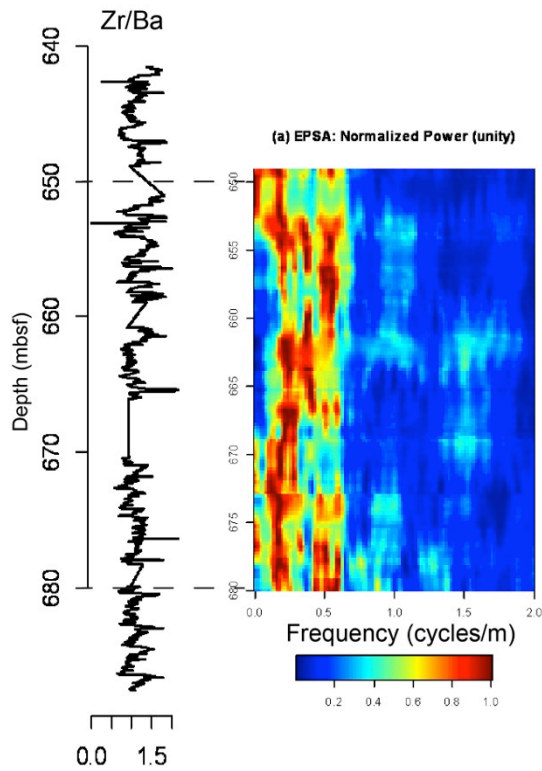


Fig. S4: Evolutive Harmonic Analysis (EHA) in depth scale Zr/Ba data. The detrended Zr/Ba data is linearly interpolated to a constant sample spacing of 2 cm prior to analysis. EHA employs with 3DSDP tapers and a 15 window.

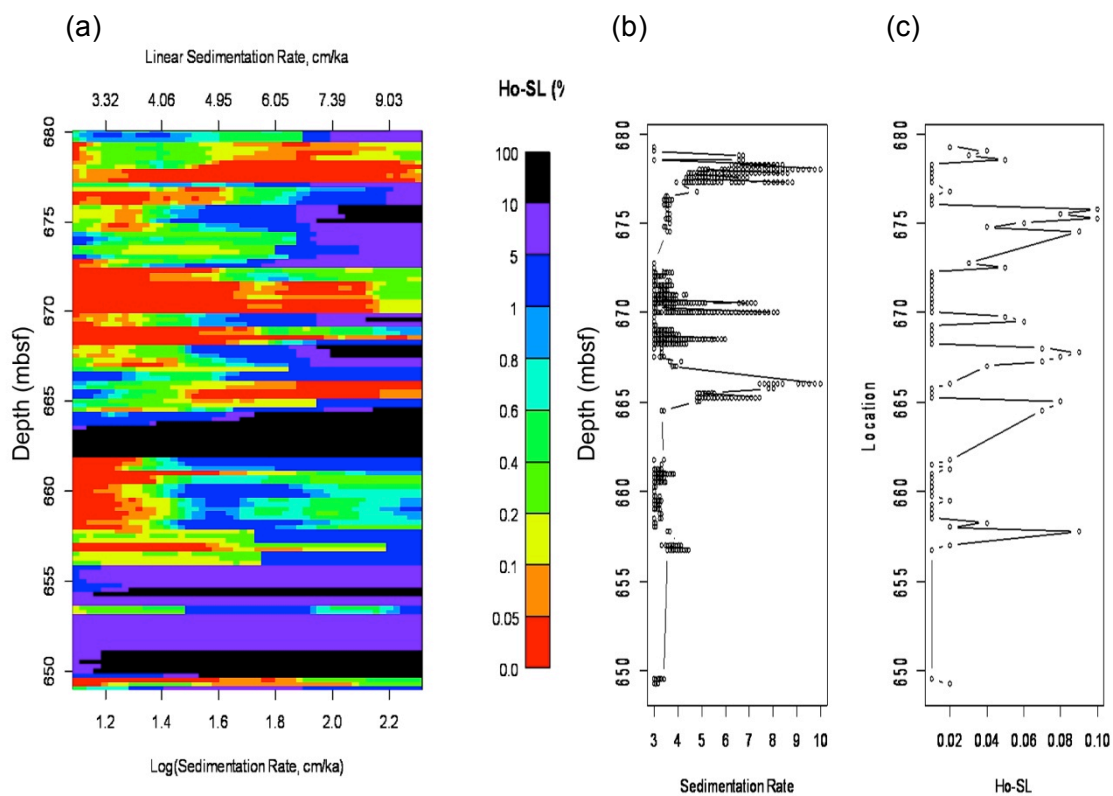


Fig. S5: Astrochronologic testing using evolutive ASM analysis. (a) Evolutive ASM plot, displaying Ho-SL values (90% confidence level), across sedimentation rates spanning 3 to 10 cm/kyr. (b-c) Summary of evolutive ASM results, using a threshold Ho-SL value of 0.1 to identify optimal sedimentation rates. (b) displays each sedimentation rate, and (c) displays the associated Ho-SL.

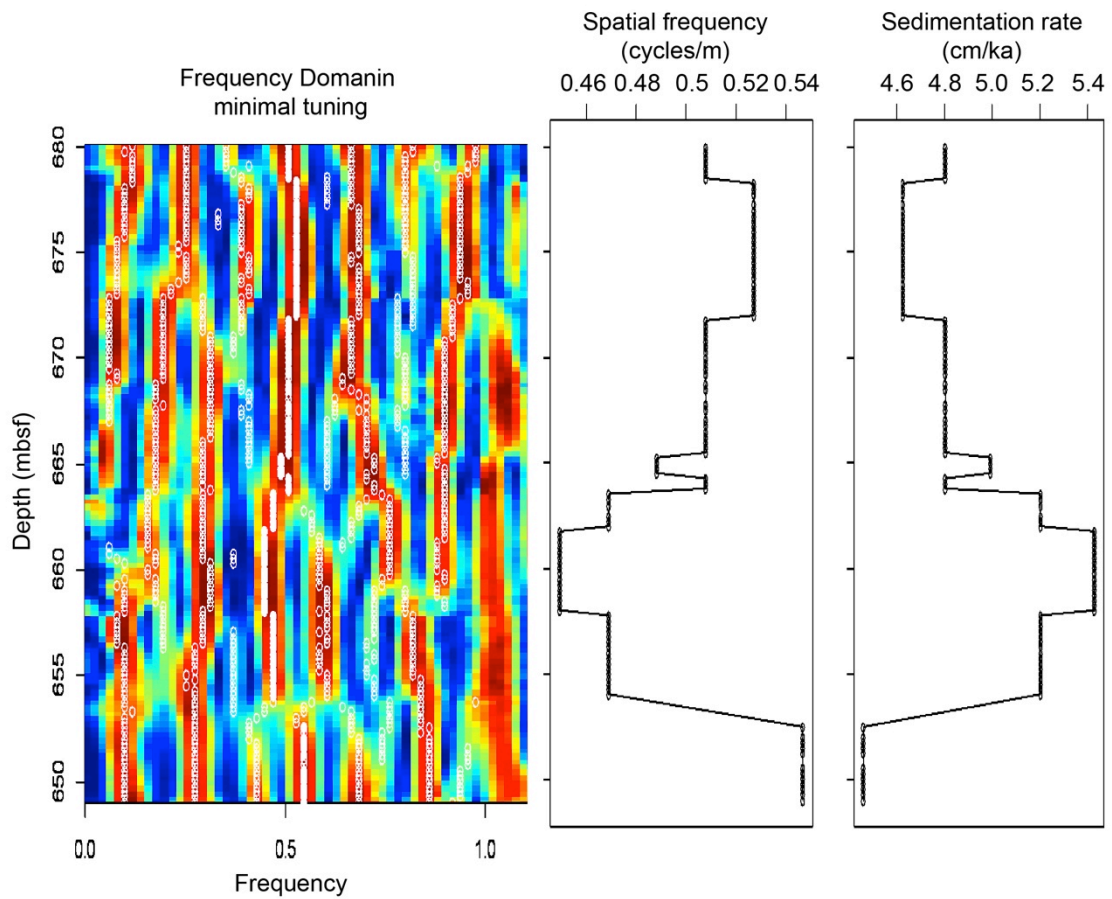


Fig. S6: Frequency tracking for minimal tuning. The obliquity cyclicity (41 Kyr) can be tracked in the EHA harmonic F-test confidence level results by setting the $f_{min}=0.01$ and $f_{max}=0.4$ based on the spatial frequencies calculated by EASM results. Calculated sedimentation rates based on spatial frequency tracking.

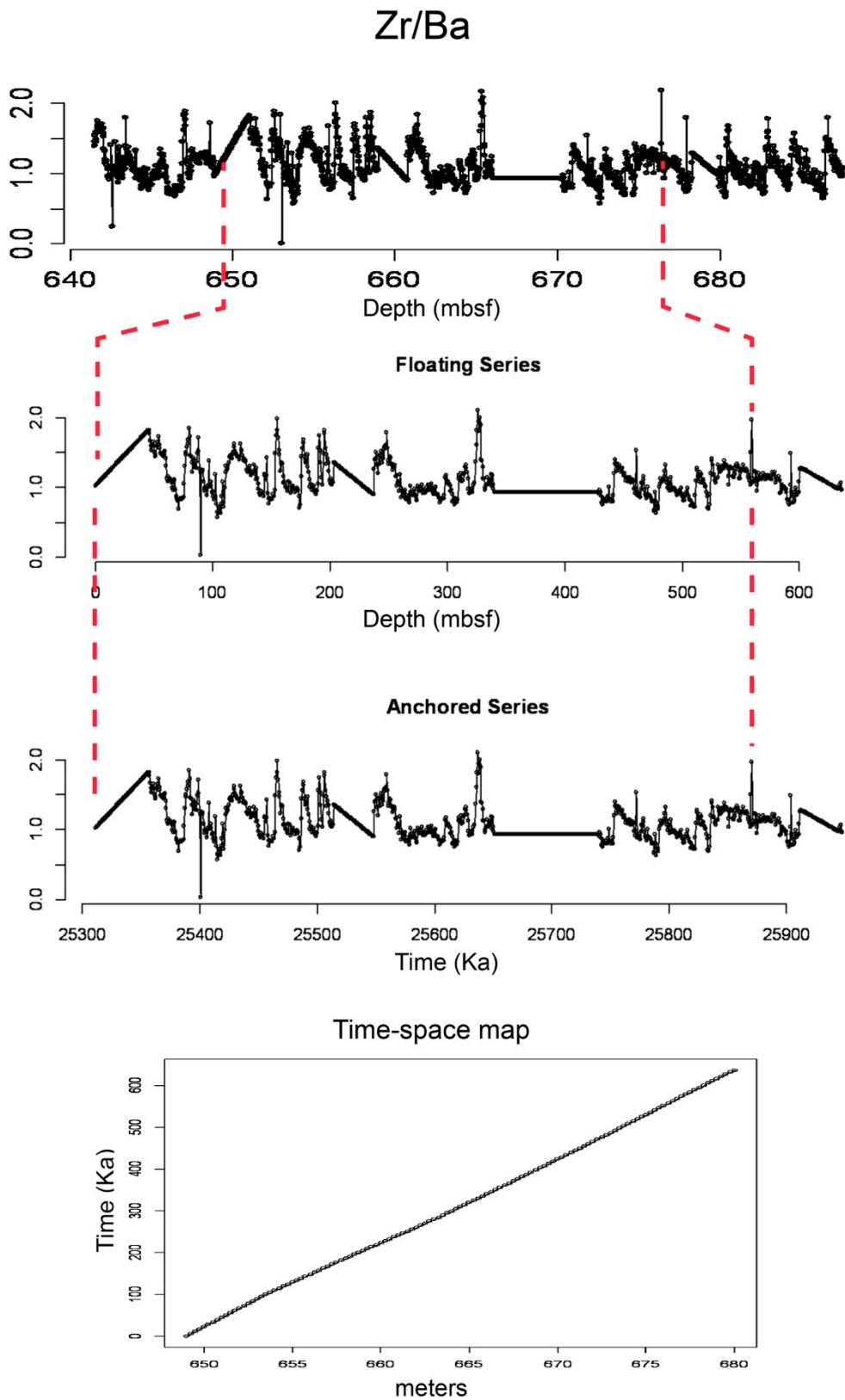


Fig. S7: Tuned record and depth-time plot derived by frequency domain minimal tuning to the obliquity cycle. The red dotted lines show the correlated depth and time.

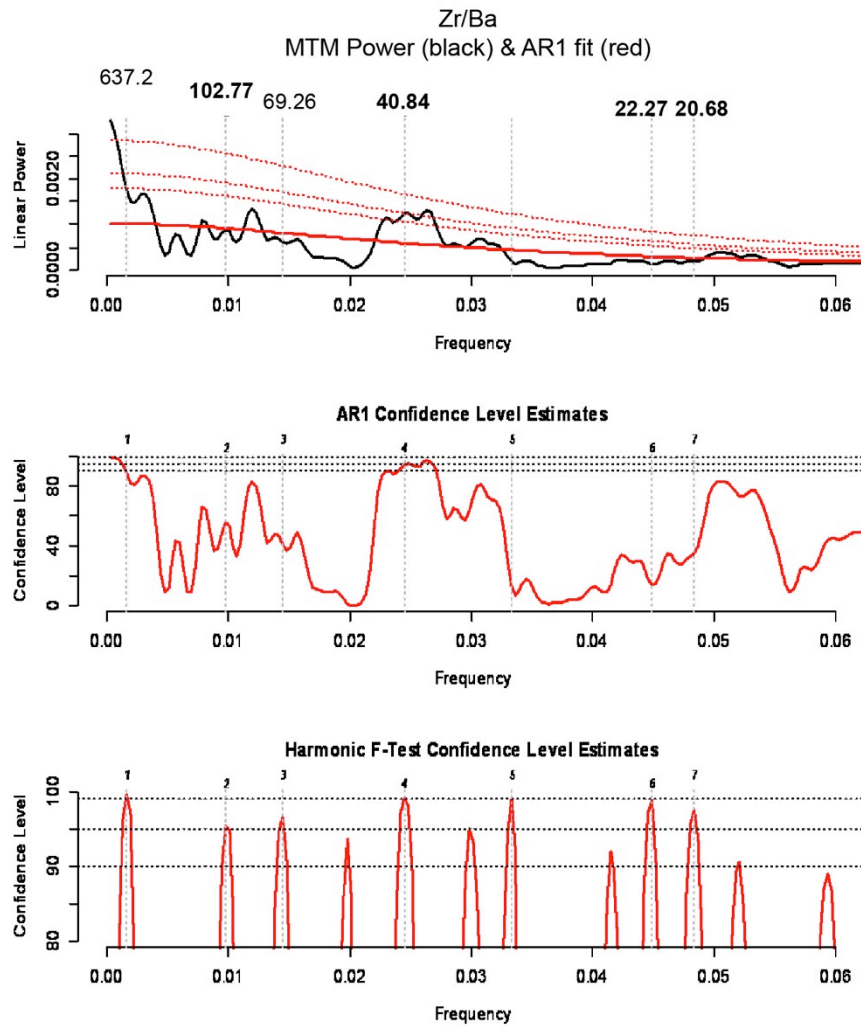
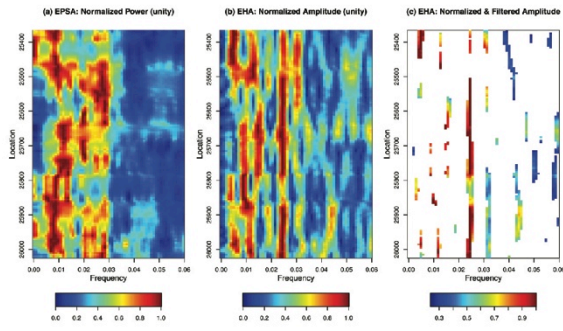
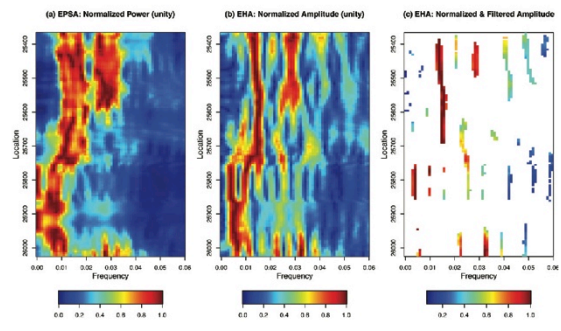


Fig. S8: MTM results of the tuned data with the major periods in kyr. These peaks achieve the 95% confidence level for both the MTM harmonic F-test and the AR1 red noise model or the AR1 noise model only.

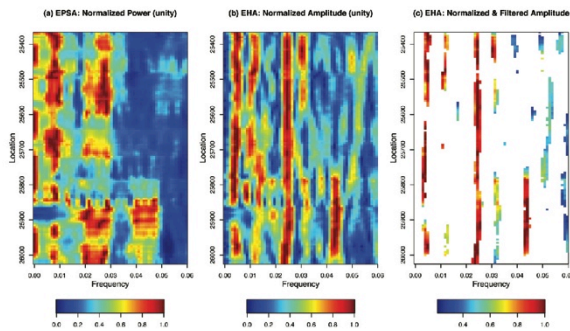
Zr/Ba Tuned
EHA with 300win



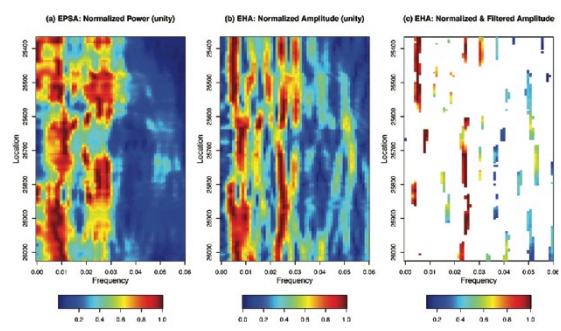
MS Tuned
EHA with 300win



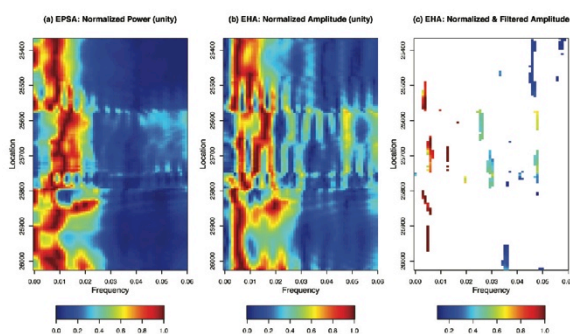
Zr/Ti Tuned
EHA with 300win



Ba Tuned
EHA with 300win



Ca/Ti Tuned
EHA with 300win



ETP Solution
EHA with 200win

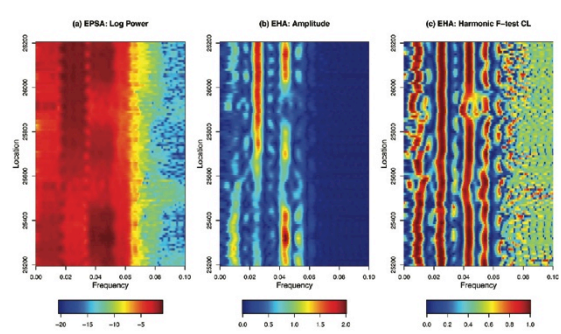


Fig. S9: Following Zr/Ba tuning (a), MS (b), Zr/Ti (c), Ba (d), and Ca/Ti (e) have been tuned. EHA analysis was applied in order to depict the frequencies. EHA on the ETP solution is also added in order to compare the resulting frequencies (f).

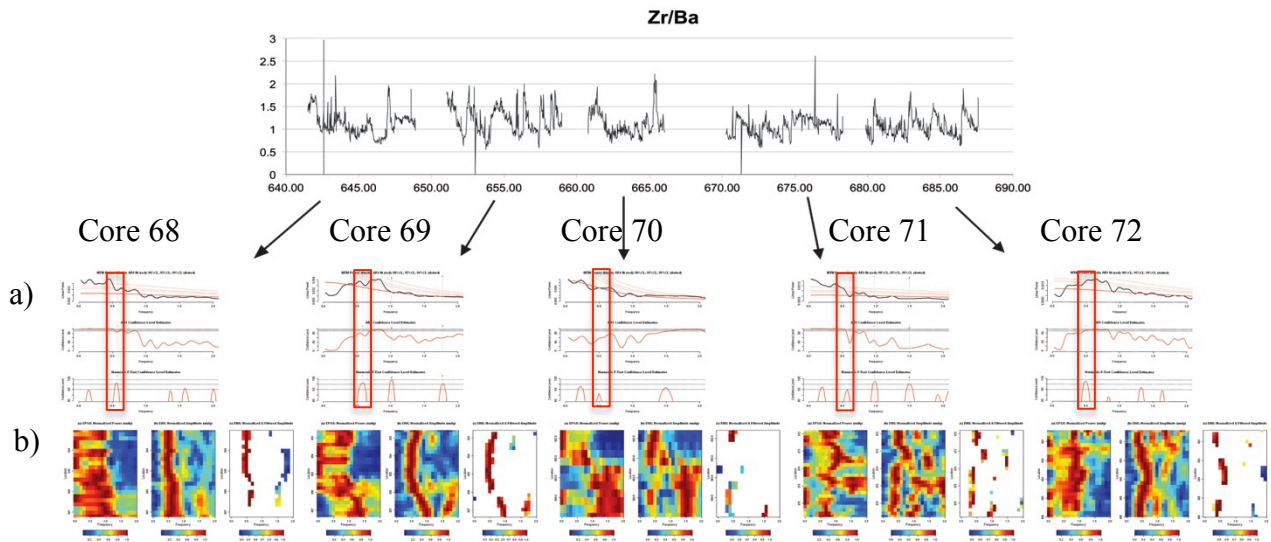


Fig. S10: Spectral analysis over individual core sections for the Zr/Ba dataset on the depth scale. The 0.5 cycle/m (that counts for obliquity) achieve >90% significance in all cores except for core 70 where smaller frequencies seem to dominate. Changes in peak frequency seem to be dominated by slightly changes in sedimentation rate. Each core was analysed by a) MTM and b) EHA with a 5 m window.

R_analysis

```
#####  
# (1) LOAD THE R-PACKAGE 'ASTROCHRON'  
#####  
library(astrochron)  
  
#####  
# (2) READ DATA FILE  
#####  
# Read the carbon isotope data from file 'CarbonIso.csv'  
dat<-read(d=0)  
  
#####  
# (3) PREPARE TIME SERIES  
#####  
# The median sampling interval of the prepared data is 0.02 m, and the mean  
# sampling interval is 0.023 m  
# Resample Zr/Ba data to 2.5 cm sampling grid, using piecewise linear  
# interpolation  
ZrBa<- linterp(dat,dt=0.025)  
  
#####  
# (4) PERFORM EVOLUTIVE HARMONIC ANALYSIS  
#####  
mtmML96(ZrBa,xmax=2,pl=2,siglevel=.90,sigID=T)  
mtm(ZrBa,xmax=2,pl=2,sigID=T)  
# Use a 12 meter window, with five 3pi DPSS tapers.  
# * Search up to the mean Nyquist frequency of 1.504221 cycle/m  
# * Output F-test confidence level estimates for evolutive average spectral misfit (ASM)  
# analysis.  
prob=eha(ZrBa,fmax=2,output=4,genplot=4,pl=2,ydir=-1,win=15)  
  
#####  
# (5) IDENTIFY TARGET PERIODS FOR AVERAGE SPECTRAL MISFIT ANALYSIS  
#####  
# Obliquity and precession terms from Laskar et al. (2004)  
model=etp(tmin=25000,tmax=26400)  
eha(model,win=200,fmax=0.1,sigID=T,pad=10000)  
mtm(model,xmax=0.1,pl=2,sigID=T)  
  
#####  
# (6) EVOLUTIVE AVERAGE SPECTRAL MISFIT ANALYSIS  
#####  
# Set up analysis parameters:  
# * Astronomical target frequencies are determined from Laskar et al. (2004)  
target=c(1/404,1/124,1/95,1/54,1/41,1/29,1/23,1/19)  
#Ray=(1/N*Ax) on N= number of points in data series and Ax= sampling resolution of data  
# series  
# * Use average sampling interval to estimate the Nyquist frequency (for 1/(0.025m sampling *  
# 2) Fnyq=(1/2*Ax)  
rayleigh=0.0217  
nyquist=20  
# * Average sedimentation rates is around 5cm/Kyr  
# The total duration between the youngest and oldest age is 0.71 Ma +/- ? Ma.
```

```

# Given the range of plausible correlation horizons into the LO section,
# the total stratigraphic thickness can range from 30 m to 40 m.
# Execute evolutive ASM analysis. This will take 10-20 minutes to complete.
res1=eAsm(prob,target=target,rayleigh=rayleigh,nyquist=nyquist,sedmin=3,sedmax=10,numsed
=100,siglevel=0.95,iter=10000,output=4)
# Track Ho-SL minima from evolutive ASM results
# * Identify those results with Ho-SL less than or equal to 0.1%
pl(1); eAsmTrack(res1[1],threshold=0.1,ydir=1)

#####
# (7) EXAMINE SELECTED SPECTRA AND ASM-CALIBRATED PERIODS
#####
# F-test CL spectrum from 43.965 m
# Calculate calibrated periods in kyr (observed)

prob_674.53=extract(prob,get=674.53)
1/(peak(prob_674.53,level=0.9)[2]*0.025)

prob_670.03=extract(prob,get=670.03)
1/(peak(prob_670.03,level=0.9)[2]*0.025)

prob_656.03=extract(prob,get=656.03)
1/(peak(prob_656.03,level=0.9)[2]*0.025)

prob_661.03=extract(prob,get=661.03)
1/(peak(prob_661.03,level=0.9)[2]*0.025)

#####
# (8) ASTRONOMICALLY-TUNE Zr/Ba DATA USING
# FREQUENCY-DOMAIN MINIMAL TUNING (Meyers et al., 2001)
#####
# Track obliquity in EHA harmonic F-test confidence level given the ASM-calibrated periods
# Track obl term on the basis of the ASM calibrated sedimentation rates
# Note that the Rayleigh frequency is 0.0217 cycles/m
freqs=trackFreq(prob,fmin=0.023,fmax=1,threshold=0.9)
# convert spatial frequencies to sedimentation rates using average period of 41 kyr
sedrate=freq2sedrate(freqs,period=41,ydir=-1)
sedrate
# View the calibrated sedimentation rates on depth sedrate
# Integrate the sedimentation rate curve to create a time-space map
time=sedrate2time(sedrate)
# View the calibrated time series
time

# The duration of specific interval can be calculated by the output of sedrate and time
# Tune the ZRBA series using the time-space map
tuned=tune(ZrBa,time)
#####
# (9) PREPARE TUNED SERIES AND EVALUATE SPECTRA
#####
# Interpolate the tuned series. Median sampling interval is 0.5 kyr and mean is 0.55 kyr.
# Will use AR1 test; use a conservative interpolation to avoid introducing serial correlation.
datatuned=linterp(tuned,dt=0.6)
# Perform MTM analysis on the tuned series
spec=mtm(datatuned,tbw=2,pl=2,siglevel=0.95,xmax=0.06,output=1,sigID=T)

```

```

# identify periods of AR1 CL peaks that acheive the 90% AR1 CL
1/peak(cb(spec,c(1,4)),level=95)[2]
# Perform EHA on the tuned series
ZrBa_final<-read(d=0)
pwr=eha(datatuned,fmax=0.06,output=2,ydir=-1,win=250)
plotEha(pwr,pl=1,ydir=-1)

#####
# (10) BANDPASS FILTERING AND ECCENTRICITY AMPLITUDE
MODULATION ANALYSIS
#####
# Perform bandpass-filtering on the tuned series to extract short eccentricity (E2+E3)
e23_data=bandpass(datatuned,flow=0.006,fhigh=0.011,xmax=0.02)
# Perform bandpass-filtering on the eccentricity terms from Laskar et al. (2011)
model=getLaskar("la10d")
model=iso(model,xmin=25000,xmax=26400)
e23_model=bandpass(model,flow=0.006,fhigh=0.011,xmax=0.02) #short-term
eccentricity
# Evaluate the alignment between the amplitude envelope of the filtered short-term eccentricity
and the filtered long-term eccentricity
am_data=hilbert(bandpass(datatuned,flow=0.006,fhigh=0.011))
pl(1)
plot(s(am_data),type="l",ylim=c(-3,3))
lines(s(e1_data),col="red")

#Anchor the tuned data to a tie point from the time scale where 606.226 is equivalent to 678.78
ZrBa_tuned2=anchorTime(datatuned,606.2262,25990,flipOut=T,timeDir=2)

write.csv(ZrBa_tuned2,file="ZrBa_tuned_at_606.226to25990.csv") #Save data

Tune other data series and analyse with EHA:

Ba<-read(d=0)
Ba_tuned=tune(Ba,time)
eha(linterp(Ba_tuned,dt=0.5),fmax=0.06,output=2,ydir=-1,win=150)
Ba_tuned=anchorTime(datatuned,678.9,25990,flipOut=T,timeDir=2)

MS<-read(d=0)
MS_tuned=tune(MS,time)
eha(linterp(MS_tuned,dt=0.5),fmax=0.06,output=2,ydir=-1,win=150)
MS_tuned=anchorTime(datatuned,678.9,25990,flipOut=T,timeDir=2)

```

References:

- Escutia, C., Brinkhuis, H., Klaus, A., Scientists, I.E. 318, 2011. Expedition 318 summary, in: Proceedings of the Integrated Ocean Drilling Program, Volume 318.
- Fu, W., Jiang, D., Montañez, I.P., Meyers, S.R., Motani, R., Tintori, A., 2016. Eccentricity and obliquity paced carbon cycling in the Early Triassic and implications for post-extinction ecosystem recovery. *Sci. Rep.* 6, 27793.
- Laskar, J., Robutel, P., Joutel, F., Gastineau, M., Correia, a. C.M., Levrard, B., 2004. A long-term numerical solution for the insolation quantities of the Earth. *Astron. Astrophys.* 428, 261–285.
- Meyers, S.R., Sageman, B.B., Hinnov, L.A., 2001. Integrated quantitative stratigraphy of the Cenomanian-Turonian Bridge Creek Limestone Member using evolutive harmonic analysis and stratigraphic modeling. *J. Sediment. Res.* 71, 628–644.
- Meyers, S.R., Sageman, B.B., Arthur, M.A., 2012. Obliquity forcing of organic matter accumulation during Oceanic Anoxic Event 2. *Paleoceanography* 27.
- Paillard, D., Labeyrie, L., Yiou, P., 1996. Macintosh Program performs time-series analysis. *Eos, Trans. Am. Geophys. Union* 77, 379–379.
- Tauxe, L., Stickley, C.E., Sugisaki, S., Bijl, P.K., Bohaty, S.M., Brinkhuis, H., Escutia, C., Flores, J. a., Houben, a. J.P., Iwai, M., Jiménez-Espejo, F., McKay, R., Passchier, S., Pross, J., Riesselman, C.R., Röhl, U., Sangiorgi, F., Welsh, K., Klaus, A., Fehr, A., Bendle, J. a. P., Dunbar, R., González, J., Hayden, T., Katsuki, K., Olney, M.P., Pekar, S.F., Shrivastava, P.K., van de Flierdt, T., Williams, T., Yamane, M., 2012. Chronostratigraphic framework for the IODP Expedition 318 cores from the Wilkes Land Margin: Constraints for paleoceanographic reconstruction. *Paleoceanography* 27, 19.